UNIVERSIDAD MIGUEL HERNÁNDEZ DE ELCHE
Programa de Doctorado en
Medioambiente y Sostenibilidad

APLICACIÓN DE TELEDETECCIÓN Y GESTIÓN INTEGRADA DEL AGUA EN ZONAS SEMIÁRIDAS

GEMA MARCO DOS SANTOS

DIRECTOR: JOSE NAVARRO PEDREÑO
CODIRECTOR: IGNACIO MELÉNDEZ PASTOR

2022

Embalse de Guadalest, Alicante.
Fotografía: Gema Marco Dos Santos

UNIVERSIDAD MIGUEL HERNÁNDEZ DE ELCHE
Programa de Doctorado en
Medioambiente y Sostenibilidad

APLICACIÓN DE TELEDETECCIÓN Y GESTIÓN INTEGRADA DEL AGUA EN ZONAS SEMIÁRIDAS

GEMA MARCO DOS SANTOS

DIRECTOR: JOSE NAVARRO PEDREÑO
CODIRECTOR: IGNACIO MELÉNDEZ PASTOR

2022

La presente tesis titulada **"Aplicación de teledetección y gestión integrada del agua en zonas semiáridas",** se presenta bajo la modalidad de **tesis por compendio** de las siguientes **publicaciones:**

- Marco Dos Santos, G. Meléndez-Pastor, I., Navarro-Pedreño, J., Gómez Lucas, I. (2018). Water management in irrigation systems by using satellite information. Satellite Information Classification and Interpretation. IntechOpen. Chapter 6, 89-101. https://doi.org/10.5772/intechopen.82368
- Marco Dos Santos, G., Meléndez-Pastor, I., Navarro-Pedreño, J. Gómez Lucas, G. (2019). A review of Landsat TM/ETM based vegetation indices as applied to wetland ecosystems. *Journal of Geographical Research*, 2*(1)*, 499. https://doi.org/10.30564/jgr.v2i1.499
- Marco Dos Santos, G., Meléndez-Pastor, I., Navarro-Pedreño, J., Koch, M. (2019). Assessing water availability in Mediterranean regions affected by water conflicts through MODIS data time series analysis. *Remote sensing*, 11*(11)*, 1355. https://doi.org/10.3390/rs11111355 **Q1 (JCR - SJR)**
- Marco Dos Santos, G., Meléndez-Pastor, I., Navarro-Pedreño, J. Gómez Lucas, G. (2021). Using Landsat images to determine water storing capacity in Mediterranean environments. *Journal of Geographical Research*, 4*(4)*, 3780. https://doi.org/10.30564/jgr.v4i4.3780
- Marco Dos Santos, G., Navarro-Pedreño, J., Meléndez-Pastor, I., Gómez Lucas, I., Almendro Candel, M.A., Zorpas, A.A. (2021). Agricultural drainage water characterization to determine the desalination possibilities for irrigation in a semiarid environment. *Desalination and Water Treatment*, 227*(2021)*, 34-41. https://doi.org/10.5004/dwt.2021.27301 **Q3 (JCR - SJR)**

Informe CAPD

El Dr. D. Jose Navarro Pedreño, Coordinador del Programa de Doctorado en Medio Ambiente y Sostenibilidad

INFORMA:

Que *Dña. Gema Marco Dos Santos* ha realizado bajo la supervisión de nuestro Programa de Doctorado el trabajo titulado **"Aplicación de teledetección y gestión integrada del agua en zonas semiáridas"** conforme a los términos y condiciones definidos en su Plan de Investigación y de acuerdo al Código de Buenas Prácticas de la Universidad Miguel Hernández de Elche, cumpliendo los objetivos previstos de forma satisfactoria para su defensa pública como tesis doctoral.

Lo que firmo para los efectos oportunos, en Elche a 29 de julio de 2022.

Prof. Dr. D Jose Navarro Pedreño

Coordinador del Programa de Doctorado en Medio Ambiente y Sostenibilidad

Informe Directores

El Dr. D. Jose Navarro Pedreño, director, y el Dr. D. Ignacio Meléndez Pastor, codirector de la tesis titulada **"Aplicación de teledetección y gestión integrada del agua en zonas semiáridas"**

INFORMAN:

Que *Dña. Gema Marco Dos Santos* ha realizado bajo nuestra supervisión el trabajo titulado **"Aplicación de teledetección y gestión integrada del agua en zonas semiáridas"** conforme a los términos y condiciones definidos en su Plan de Investigación y de acuerdo al Código de Buenas Prácticas de la Universidad Miguel Hernández de Elche, cumpliendo los objetivos previstos de forma satisfactoria para su defensa pública como tesis doctoral.

Lo que firmamos para los efectos oportunos, en Elche a 29 de julio de 2022.

Director de la tesis	Codirector de la tesis
Dr. D. Jose Navarro Pedreño	***Dr. D. Ignacio Meléndez Pastor***

Sayonara baby

INDICE

Embalse del Negratín, Granada.
Fotografía: Gema Marco Dos Santos

1. Resumen

El agua es un recurso esencial para el mantenimiento de los ecosistemas naturales, la regulación del clima y el desarrollo de la humanidad. La creciente presión sobre este recurso en las últimas décadas y los cambios en el clima hacen prioritario evaluar y proteger nuestros recursos naturales de manera cooperativa, hacia unos mismos objetivos. Por ello, la legislación y el impulso de la administración resultan fundamentales para llevar a cabo diferentes estrategias para poner en marcha proyectos que favorecen el uso coordinado, equitativo y sostenible de los recursos hídricos y alcanzar los objetivos de la planificación hidrológica.

Algunos de los planes propuestos por las administraciones consisten en realizar el seguimiento del estado cuantitativo y cualitativo del agua, tanto subterránea como superficial, medidas de adaptación y mitigación de los efectos del cambio climático, recuperación de los ecosistemas fluviales y mejoras en su estado ecológico, adaptaciones y gestión de los riesgos de inundación, planes para minimizar los efectos de situaciones de sequía, gestión de la seguridad de presas y embalses, así como nuevas propuestas y medidas para potenciar la depuración, saneamiento y la reutilización del agua. Con estas estrategias se pretende desarrollar una metodología que permita lograr el cumplimiento de los objetivos sociales, ambientales y económicos planteados por las políticas de gestión comunitarias y nacionales. Junto a ello, la desalinización, es uno de los principales objetivos de la administración.

Sobre esta base, la finalidad de esta tesis es destacar la capacidad de la teledetección y los Sistemas de Información Geográfica (SIG) en la planificación hidrológica, no solo como herramienta de diagnóstico del estado actual de los recursos, sino también para incorporarlo al proceso de toma de decisiones en los sistemas de control en tiempo real. La teledetección nos proporciona una gran cantidad de información complementaria a la obtenida *in situ* a la que, además, se pueden incluir otro tipo de parámetros ambientales como indicadores de los efectos producidos por el cambio climático.

En los artículos que comprenden esta tesis se realiza una evaluación de los recursos hídricos a partir de metodologías sencillas con imágenes de satélite y formulación de modelos que permitan prever la disponibilidad de agua bajo diversos escenarios de escasez hídrica. Al mismo tiempo, se apunta hacia una de las estrategias de reutilización y de obtención de recursos como es la desalinización.

Para evaluar los cambios de usos del suelo y su relación con el consumo de agua, se realizó un análisis mediante imágenes aéreas a escala de cuenca hidrográfica, en una zona que, a pesar de estar afectada por condiciones de aridez, se ha producido un gran

crecimiento poblacional e intensificación de la actividad agrícola. En la primera publicación, ***"Water Management in Irrigation Systems by Using Satellite Information"***, se estimaron las pérdidas de agua por evaporación en relación con el incremento del número de balsas para el riego comparando dos periodos de estudio, entre 1973-1986 y en 2016. En este estudio, se ha determinado un aumento por cuatro del número de balsas, que se traduce en un ascenso de las pérdidas por evaporación anual de alrededor de 15,62 hm^3/año.

La utilización de imágenes de satélite y el cálculo de índices espectrales para obtener información sobre la evolución, estado y disponibilidad de los recursos hídricos se ha convertido en los últimos años en una herramienta habitual principalmente para en el sector agrícola y el estudio de los ecosistemas naturales.

En la segunda publicación, ***"A review of Landsat TM/ETM based vegetation indices as applied to wetland ecosystems"*** se utilizó información de Landsat 5 del área localizada entre las Salinas de Santa Pola y el Parque Natural de El Hondo en Elche y Crevillente, con el objetivo de evaluar el ajuste de varios índices de vegetación en zonas de humedales. Entre los índices de estimación de la biomasa, se encontró una relación directa y una elevada correlación. En cambio, para los índices de contenido de humedad, no se consiguieron buenas correlaciones. Estos resultados muestran que la selección de los diferentes índices debe realizarse de acuerdo con las características de la zona, teniendo en cuenta que, por ejemplo, en áreas con baja densidad vegetal y mayor exposición, se deberían elegir aquellos que corrigen las distorsiones producidas por la reflectividad del suelo.

En el caso de la tercera publicación, ***"Assessing water availability in Mediterranean regions affected by water conflicts through MODIS data time series analysis",*** se utilizaron series temporales de imágenes MODIS desde 2001 a 2014 del Índice de Diferencia Normalizada (NDVI) y de Temperatura de la Superficie Terrestre (LST) localizadas en las cuencas hidrográficas de los ríos Amadorio y Guadalest. También se utilizaron datos diarios de precipitación, volumen anual almacenado en los dos embalses de la zona y proyecciones de modelos climáticos para 2050 del IPCC. Con el cálculo de las anomalías de esta serie de datos, se pudieron visualizar patrones espacio-temporales de cambio para poder analizar la relación entre el volumen de agua almacenado en los embalses y el resto de variables (NDVI, LST y precipitación), encontrándose una correlación significativa entre el NDVI y los datos de volumen de agua almacenado. Además, se evaluó la capacidad de predicción de almacenamiento de agua, NDVI y LST teniendo en cuenta los escenarios de cambio climático, en el que se muestra una relación significativa inversa con LST.

El objetivo de la cuarta publicación, ***"Using Landsat images to determine water storing capacity in Mediterranean environments",*** fue estimar y modelizar la capacidad de almacenamiento de agua con la posibilidad de incorporarlo a un sistema de control y gestión automatizado. Para ello, se utilizó la clasificación supervisada de una serie temporal de imágenes Landsat para extraer una estimación de la superficie de lámina de agua y generar modelos de predicción. En la validación se obtuvieron valores que indicaban un buen ajuste y una buena capacidad de predictiva.

Para una gestión sostenible de los recursos es necesario la implantación de medidas que permitan el máximo aprovechamiento del agua y reducir la presión actual. Una de las propuestas que define las políticas nacionales y comunitarias es la reutilización y depuración de las aguas como estrategia clave en la consecución de los objetivos planteados.

En la quinta publicación, ***"Agricultural drainage water characterization to determine the desalination possibilities for irrigation in a semiarid environment",*** se evaluó la calidad de las aguas de drenajes agrícolas relacionadas con las áreas estudiadas en la segunda publicación, para determinar la posibilidad de implantar un sistema de desalinización para su reutilización como recursos no convencionales. Se realizaron diferentes muestreos en los que se estimó el caudal y se analizó el pH, la conductividad eléctrica, sales disueltas y sólidos en suspensión. Aunque en algunos de los canales de drenaje se obtuvo un caudal demasiado variable y elevados valores de salinidad y sólidos disueltos, en otros casos, los datos indicaron la posibilidad de instalar una pequeña planta de ósmosis inversa para la desalinización y reutilización de esas aguas.

A modo de conclusión, el agua debe de tratarse con una visión de conjunto, gestión integrada, de manera que los recursos y su obtención estén bajo un sistema de control en el que la teledetección ofrece una serie de posibilidades y se combine con otras estrategias y procesos. Sin lugar a dudas, y centrándonos en el entorno inmediato, la escasez de recursos aboga a la necesidad de reutilizar al máximo las aguas, incluidas aquellas sobrantes y la desalación, no solo de agua marina, existen muchas posibilidades, como se ha puesto de manifiesto.

1. Abstract

Water is an essential resource for the maintenance of natural ecosystems, climate regulation and the development of humanity. The growing pressure on this resource in recent decades and changes in the climate make a priority to evaluate and protect our natural resources in a cooperative manner, towards the same objectives. Therefore, legislation and the administration management are essential to carry out different strategies to implement projects that favor the coordinated, equitable and sustainable use of water resources and achieve the objectives of hydrological planning.

Some of the plans proposed by the administrations consist of monitoring the quantitative and qualitative status of both groundwater and surface water, adaptation measures and mitigation of the effects of climate change, recovery of river ecosystems and improvements in their ecological status, adaptations and management of flood risks, plans to minimize the effects of drought situations, safety management of dams and reservoirs, as well as new proposals and measures to promote the purification, sanitation and reuse of water. With these strategies, it is intended to develop a methodology that allows achieving the fulfillment of the social, environmental and economic objectives set out by the community and national management policies. Beside these strategies, desalination is one of the major targets of the administration.

On this basis, the purpose of this thesis is to highlight the capacity of remote sensing and Geographic Information Systems (GIS) in hydrological planning, not only as a tool for diagnosing the current state of resources but also to incorporate it into the decision-making process. Remote sensing provides us with a large amount of complementary information to that obtained *in situ*, to which, in addition, other types of environmental parameters can be included as indicators of the effects produced by climate change.

In the articles that comprise this thesis, an evaluation of water resources was carried out based on simple methodologies with satellite images and the formulation of models that allow predicting the availability of water under various scenarios of water scarcity. At the same time, one of the strategies for reuse and obtaining resources such as desalination is added.

To evaluate the changes in land use and its relationship with water consumption, an analysis was carried out using aerial images at a hydrographic basin scale, in an area that, despite being affected by arid conditions, has produced a large population growth and intensification of agricultural activity. In the first publication, ***"Water Management in Irrigation Systems by Using Satellite Information"***, water losses due to evaporation were estimated in relation to with the increase in the number of ponds for irrigation

comparing two study periods, between 1973-1986 and in 2016. In this study period, an increase by four in the number of ponds has been estimated, which means an increase in losses by annual evaporation of around 15.62 hm^3/year.

The use of satellite images and the calculation of spectral indices to obtain information on the evolution, state and availability of water resources has become in recent years a common tool mainly for the agricultural sector and the study of natural ecosystems.

In the second publication, ***"A review of Landsat TM/ETM based vegetation indices as applied to wetland ecosystems"***, information from Landsat 5 of the area located between the Salinas de Santa Pola and the Natural Park of El Hondo in Elche and Crevillente was used, with the aim of evaluate the fit of various vegetation indices in wetland areas. A direct relationship and a high correlation were found between biomass estimation indices. On the other hand, for the moisture content indices, they did not indicate a good correlation. These results show that the selection of the different indices must be made according to the characteristics of the area, considering that, for example, in areas with low plant density and greater exposure, those that correct the distortions produced by ground reflectivity should be chosen.

In the case of the third publication, ***"Assessing water availability in Mediterranean regions affected by water conflicts through MODIS data time series analysis"***, time series of MODIS images from 2001 to 2014 of the Normalized Difference Index (NDVI) and Land Surface Temperature (LST) located in the hydrographic basins of the Amadorio and Guadalest rivers. Daily precipitation data, annual volume stored in both reservoirs, and climate model projections for 2050 were also used. With the calculation of the anomalies of this data series, it was possible to visualize spatio-temporal patterns of change in order to analyze the relationship between the volume of water stored in the reservoirs and the rest of the variables (NDVI, LST and precipitation), finding a significant correlation between the NDVI and the data on the volume of water stored. In addition, the prediction capacity of water storage, NDVI and LST was evaluated considering climate change scenarios, in which a significant inverse relationship with LST is shown.

The objective of the fourth publication, ***"Using Landsat images to determine water storing capacity in Mediterranean environments",*** was to estimate and model the water storage capacity with the possibility of incorporating it into an automated control and management system. To do this, the supervised classification of a time series of Landsat images was used to extract an estimate of the surface of the water table and generate prediction models. In the validation, values were obtained that indicated a good fit and a good predictive capacity.

For sustainable resources management it is necessary to implement methods that guarantee the maximum water exploitation while reducing the current pressure. One of the proposals that defines national and community policies is water reuse and depuration as a key strategy in achieving the objectives. In the fifth publication, ***"Agricultural drainage water characterization to determine the desalination possibilities for irrigation in a semiarid environment",*** the quality of agricultural drainage water was evaluated to determine the possibility of implementing a desalination system for its reuse as unconventional water resources. Flow rate, pH, electrical conductivity, chloride and sodium, and total dissolved solids were analyzed in different samplings. Although in some of drainage canals a highly variable flow and high salinity and dissolved solids values were obtained, in other cases, data indicated the possibility of installing a small reverse osmosis plant for the desalination and reuse of water.

In conclusion, water must be treated with an overall vision, integrated management, so that the resources and their collection are under a control system in which remote sensing offers a series of possibilities and would be combined with other strategies and processes. Without any doubt, and focusing on the immediate environment, the scarcity of resources calls for the need to reuse water as much as possible, including surplus water, and desalination, not only of seawater, many possibilities existing, as has been shown.

2. Introducción

2.1. La gestión de los recursos hídricos

El sistema de gobernanza del agua en España está basado en una gestión integrada del recurso a nivel de cuenca hidrográfica como una unidad territorial superpuesta a otras, como pueden ser las Comunidades Autónomas (1). El concepto de Gestión Integrada de los Recursos Hídricos (GIRH), según la definición de la Asociación Mundial para el Agua (Global Water Partnership-GWP) (2), aceptado a nivel internacional y sobre el que se apoya nuestro sistema, se plantea como *"un proceso que promueve la gestión y el desarrollo coordinados del agua, el suelo y los otros recursos relacionados, con el fin de maximizar los resultados económicos y el bienestar social de forma equitativa sin comprometer la sostenibilidad de los ecosistemas vitales"*. Por lo tanto, para aplicar este enfoque, los aspectos fundamentales son el seguimiento, la planificación y el control de la cantidad y calidad de los recursos (3).

La gestión del agua y las medidas para su seguimiento y control nacen de la incertidumbre histórica sobre la disponibilidad del agua, sobre todo en regiones mediterráneas, asociada principalmente a una distribución irregular en el espacio y en el tiempo de las precipitaciones (4). El crecimiento económico, de la población, y la expansión agrícola y ganadera, conlleva un incremento de la demanda hídrica y, por tanto, se produce la necesidad de encontrar estrategias para el aprovechamiento de los recursos disponibles y garantizar el abastecimiento de la población (5). En numerosas ocasiones, estas estrategias desembocan en un conflicto entre su uso para abastecimiento y para la conservación de los ecosistemas y sus funciones.

En la planificación, se incorporan datos sobre las demandas y presiones ejercidas sobre el recurso hídrico, así como toda la información recogida a través de diferentes herramientas, el estudio de los recursos disponibles y la incorporación de otros nuevos, y se programan todas las medidas y acciones encaminadas a garantizar el suministro de los recursos hídricos y protección de los ecosistemas asociados. Se trata de una hoja de ruta específica para cada territorio (cuenca hidrográfica), teniendo en cuenta los efectos del cambio climático (6), en la que se establecen además las actuaciones de mejora que deben llevarse a cabo para minimizar los impactos asociados a las alteraciones producidas por nuestras actividades (7) o incluso, para desarrollar estrategias para la gestión de los fenómenos meteorológicos extremos.

En el caso de España, la mayor parte de la demanda hídrica se satisface con los recursos superficiales (1), aunque en muchos lugares es necesario recurrir a las aguas subterráneas, cada día más explotadas.

Este es el caso del sureste de la Península Ibérica, donde hay una de las mayores presiones por el uso y disminución de los recursos existentes en las masas de aguas subterráneas (8,9).

Según los datos del sistema de Planes Hidrológicos y Programas de Medidas del segundo ciclo (2015-2021) (7), hay afectadas en las demarcaciones españolas, sin incluir las islas, un total de 4.428 masas de agua con presiones significativas (puntuales, difusas, extracciones, alteraciones hidrológicas entre otras) de las 5.593 presentes, incluyendo ríos, lagos, aguas subterráneas, aguas costeras y de transición. En el caso de las extracciones, se encuentran afectadas alrededor del 30% de las masas de agua superficiales y un 36% de las subterráneas.

El consumo urbano medio de agua, según los datos publicados por el Instituto Nacional de Estadística (INE) para el año 2018, fue de 133 litros por habitante y día, un volumen aproximado de 4.236 hm^3. La estimación de las pérdidas de agua en la red de abastecimiento fue de alrededor de 653 hm^3 , un 15,4% del agua suministrada (10).

En el caso del sector agrario, los datos para el mismo periodo indican un aumento del consumo de agua del 3,7% de 2016 a 2018, unos 15.495 hm^3 (11). El agua suministrada procede en un 74,3% de aguas superficiales, un 23,9% de origen subterráneo, y un 1,8% de otros recursos hídricos (agua desalada o regenerada). En España se producen unos 400 hm^3/año de agua desalada, de los cuales más del 50% se destina al abastecimiento del riego agrícola (12,13). De hecho, hay instaladas 765 plantas desaladoras de más de 100 m^3/d de producción, con una capacidad total de 950 hm^3 (14).

Las propuestas y los proyectos que se pretenden instaurar en los últimos años para cubrir las demandas en zonas deficitarias apuntan, tanto a la implementación de mejoras de la eficiencia de las plantas ya instaladas, como al incremento de la cantidad de agua producida con nuevas plantas desaladoras (Plan DSEAR), siendo una estrategia clave para la gestión y planificación, no solo como complemento y recurso para la agricultura, sino también para potenciar el abastecimiento urbano o industrial (12).

La superficie de regadío en España, según el último análisis de la Encuesta sobre Superficies y Rendimientos de Cultivos (ESYRCE 2020), se calcula en 3.831.181 hectáreas. El porcentaje de superficie regada respecto la superficie cultivada supone, en las comunidades autónomas del Levante un 45.7% en la Comunidad Valencia, un 38.5% en la Región de Murcia, 32.8% en Cataluña y 31.6% en Andalucía, siendo el riego localizado el más ampliamente utilizado (15).

Aunque la tradición en la construcción de presas se remonta a la época romana, debido precisamente a la necesidad de abastecer a una población y sectores económicos crecientes, se promueve a mediados del siglo XX como estrategia prioritaria, la construcción de grandes infraestructuras para embalsar agua. Se pasa de unas 450 existentes hasta la década de los 60 del siglo XX, a alcanzar más de 1.200 presas con una capacidad de 56.000 hm^3 en la actualidad según la Sociedad Española de Presas y Embalses (SEPREM) (16). Estas infraestructuras aportan unos beneficios que van desde la retención del agua y el almacenamiento para su control, la regulación y distribución a través de miles de kilómetros de canalizaciones, la generación de energía hidroeléctrica y, en definitiva, el de garantizar la disponibilidad de este recurso en los periodos de mayor escasez.

2.2. La planificación hidrológica como herramienta fundamental para la gestión

El agua es un recurso escaso e indispensable para el desarrollo de la vida y de nuestras actividades económicas y culturales. Es por ello que, para garantizar el suministro necesario para nuestro desarrollo socioeconómico y para la conservación de los ecosistemas, la planificación hidrológica ha sido y es de interés general. Muestra de ello es la evolución de la legislación específica y planes de cuenca que se han propuesto a lo largo del tiempo, buscando adaptarse al constante cambio de las circunstancias a nivel político, económico y cultural, así como la ordenación territorial y los grandes avances técnicos o incluso, dar respuesta a los requerimientos de una creciente conciencia por el medio ambiente.

La Ley de Aguas de 13 de junio de 1879, fue una gran novedad legislativa, desarrollada sobre una base científica y tecnológica. Aunque estuvo vigente más de 100 años, fue rápidamente insuficiente para dar solución a los nuevos requerimientos de la sociedad en el siglo XX (17). Por ello, se creó la Ley 29/1985, de 2 de agosto, de Aguas (18), modificada por la Ley 46/1999, de 13 de diciembre (19), para resolver algunas insuficiencias y lagunas legales y crear *"instrumentos eficaces para afrontar las nuevas demandas"*. Esta ley, en el artículo 38, estableció que la planificación hidrológica debe realizarse a través del Plan Hidrológico Nacional y los planes de cuenca. Actualmente, la elaboración de la planificación hidrológica queda definida en el Título III del Real Decreto Legislativo 1/2001, de 20 de julio (20) y el Real Decreto 907/207, de 6 de julio (21), por el que se aprueba el Reglamento de la Planificación Hidrológica, modificado por el Real Decreto 1159/2021, de 28 de diciembre (22).

Sin embargo, la aprobación de los planes hidrológicos (PH) de cuencas no comenzó hasta 1998 con el Real Decreto 1664/1998, de 24 de julio (23). Posteriormente, se desarrolló el Libro Blanco del Agua (24), que reflejaba la situación de los recursos hídricos de España, recopilando, evaluando y unificando la información procedente de los diferentes planes de cuenca, y bajo una perspectiva multidisciplinar.

A nivel europeo, la Directiva Marco del Agua (DMA) también nació como respuesta a esa necesidad de unificar la política de aguas y establecer un marco común de actuación, de forma que se garantice la calidad y cantidad de agua suficientes a pesar de la presión creciente que ha venido sucediendo desde entonces (25). El Plan Hidrológico Nacional, se aprobó con la Ley 10/2001, del 5 de julio (26), el cual englobaba los principios de la DMA.

Por lo tanto, todo el entramado legislativo que ha ido desarrollándose a lo largo de los años, refleja la prioridad en el proceso de planificación, siguiendo unos criterios técnicos, interdisciplinares, consensuados y unificados.

De acuerdo con lo establecido en el artículo 1 del Reglamento de la Planificación Hidrológica (21), *"La planificación hidrológica tendrá por objetivos generales conseguir el buen estado y la adecuada protección del dominio público hidráulico y de las aguas […], la satisfacción de las demandas de agua, el equilibrio y armonización del desarrollo regional y sectorial, incrementando las disponibilidades del recurso, protegiendo su calidad, economizando su empleo y racionalizando sus usos en armonía con el medio ambiente y los demás recursos naturales."*

Los planes hidrológicos (PH) proporcionan una visión global del estado de los recursos hídricos actuales (inventario y localización, caudales ecológicos, resumen de presiones e incidencias y control, usos y demandas, identificación de zonas protegidas), y establecen criterios de seguimiento, medidas de protección adoptadas y acciones de mejora del estado de las aguas y de las zonas protegidas (27).

Las actuaciones para la gestión de los recursos hídricos que vienen definidas en los PH, se basan en la integración de medidas estructurales (presas, embalses, trasvases, desaladoras) y no estructurales (políticas, sistemas de información y comunicación), de manera que se consigan los objetivos previstos en la planificación. La complejidad y la integración de muy diversas estrategias hace que los planes y la gestión sean complejos, destacando sin lugar a dudas, la obligatoria participación y atención que se debe prestar a los usuarios para determinar las actuaciones.

Dentro de las herramientas que se emplean en planificación, se ha incrementado el interés en modelos informáticos, en los que es posible integrar gran cantidad de información acerca del estado los recursos e infraestructuras existentes, así como la demanda de toda la cuenca. De esta forma, se simulan diferentes alternativas o escenarios, y se puede evaluar la adecuación de las diferentes propuestas de actuaciones, así como justificar las medidas adoptadas para la gestión de los recursos.

En la actualidad, disponemos de herramientas, como son las asociadas a la teledetección, que ayudan sustancialmente al estudio espacial de los diferentes componentes del ciclo del agua, y que son parte fundamental de todos los organismos gestores. Con toda la información recogida, es posible modelar escenarios climáticos e hidrológicos más ajustados, incorporando la variabilidad espacial y temporal, para poder evaluar los riesgos y la afección sobre los distintos usos del agua con el objetivo de desarrollar medidas de adaptación o minimización del impacto (28).

De hecho, con las mejoras introducidas en el Reglamento de la Planificación Hidrológica (RD 1159/2021, de 28 de diciembre), los organismos de cuenca deben mantener una infraestructura informática de datos espaciales con el registro de zonas protegidas y masas de agua asociadas, que permita el intercambio de información con las administraciones para la gestión y el seguimiento. Este hecho, no hace más que cumplir con la necesidad de acceso a la información en materia de medio ambiente (29).También, en el artículo 4 bis de este Real Decreto y con el artículo 19 de la Ley 7/2021, de 20 de mayo (30), los organismos de cuenca deben elaborar un estudio de adaptación a los riesgos del cambio climático en cada ciclo de planificación hidrológica.

Es por ello que, el estudio de los recursos hídricos a largo plazo mediante la teledetección y los SIG puede dar un enfoque más sostenible e integrado a la gestión, sobre todo con la creciente preocupación sobre los efectos que el cambio climático puede ocasionar sobre nuestros recursos y la amenaza que supone para nuestras actividades socioeconómicas, así como para la conservación de los ecosistemas.

2.3. Teledetección y Sistemas de Información Geográfica

La teledetección se basa en la obtención de datos de forma remota de las características de la superficie terrestre y atmósfera, a través de la radiación reflejada desde los diferentes elementos hasta los sensores instalados en plataformas espaciales (31,32).

Los datos obtenidos no solo contienen información espectral, sino también información geográfica que es transmitida a estaciones terrestres en las que se procesa de forma que se pueda obtener información interpretable (Figura 1).

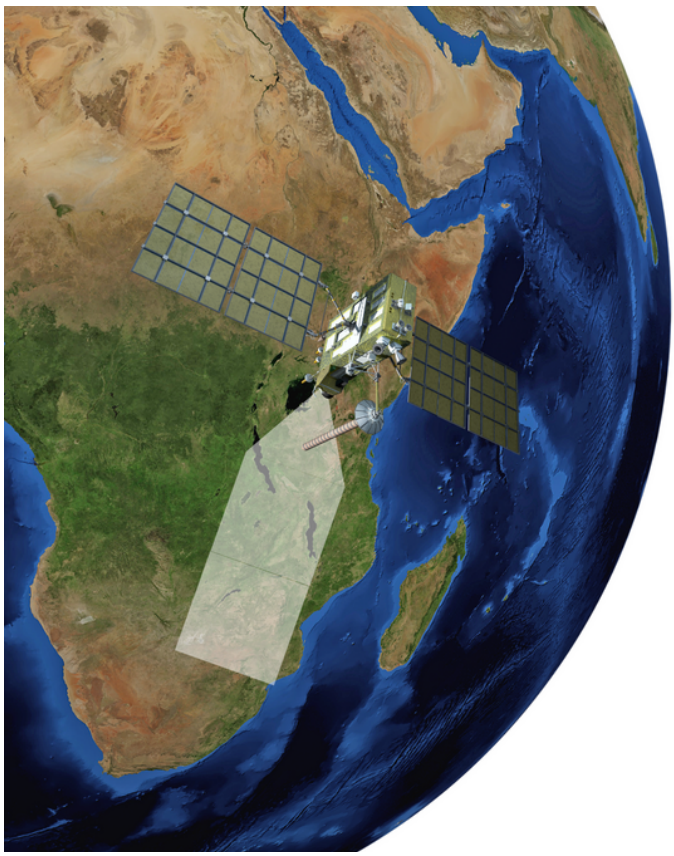

Figura 1. *Obtención de imágenes espectrales a partir de sensores instalados en satélites. Fuente: elaboración propia.*

Cada objeto o superficie posee un conjunto de valores característicos captados en las diferentes zonas del espectro que se conoce como “firma espectral” (Figura 2) (33). Esta firma, permite identificar los objetos en función de sus niveles de reflectancia y la longitud de onda en aquellas regiones del espectro en las que se produce una menor dispersión atmosférica. Por tanto, la transmisión de la radiación se produce más fácilmente. Son en estas zonas del espectro en las que se colocan las bandas o canales de los sensores. La combinación de algunas de esas bandas permite visualizar imágenes que revelan características de los diferentes elementos que configuran el paisaje y aportan información ambiental (34).

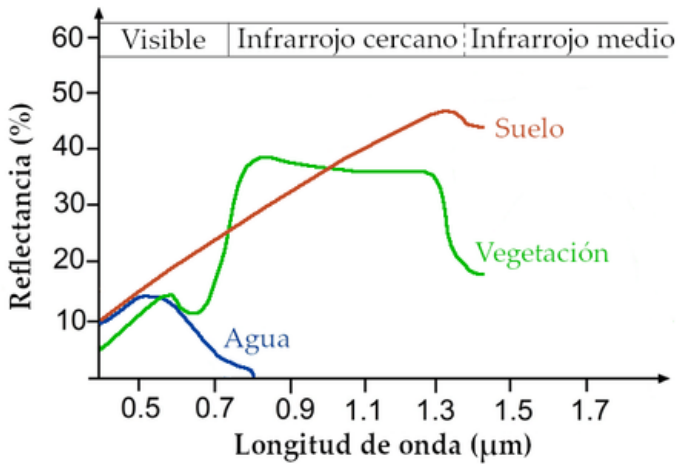

Figura 2. *Representación de las firmas espectrales del agua, suelo y vegetación. Modificado de: www.esa.int/SPECIALS/Eduspace_EN/.*

El sensor es un instrumento que es capaz de detectar y registrar la radiación electromagnética que emiten los diferentes objetos o superficies de la Tierra. Se distinguen dos tipos de sensores según si recogen la radiación que reflejan los objetos por sí mismos, como son los sensores pasivos, o, si emiten la radiación y la recogen cuando es reflejada por las superficies, como los activos (32). Los sensores pasivos generan una imagen a partir de la transformación de los valores de radiancia captados por cada banda, en valores numéricos. Estos valores se conocen como Niveles Digitales (ND). Para utilizar estas imágenes, se deben realizar diferentes tratamientos y correcciones dependiendo del análisis posterior a realizar.

Los sensores activos tienen una gran operatividad ya que son capaces de atravesar la atmósfera en casi cualquier condición, por lo que no se ven limitados por los elementos atmosféricos. Los dos ejemplos más comunes son el sensor RADAR *(Radio Detection and Ranging)* y el LIDAR *(Light Detection and Ranging)*. En estos casos, se genera una imagen formada por una nube de puntos que representan la distancia recorrida por la radiación o el tiempo que tarda el sensor el captar de vuelta la radiación emitida por las superficies (31).

La capacidad de los datos obtenidos por teledetección presenta algunas ventajas que pueden emplearse en multitud de áreas de estudio (geología, minería, edafología, cartografía, ordenación del territorio, hidrología, climatología, oceanografía…).

De hecho, una de las grandes ventajas es que pueden ser claves en la gestión del agua (35). Con esta técnica, se obtiene una visión global del objeto de estudio, incluso fuera de la región del espectro visible, permite la adquisición de imágenes con alta resolución temporal y espacial o realizar el seguimiento de la evolución de variables ambientales, incluso sin necesidad de datos recogidos en campo.

En las últimas décadas, se ha producido un rápido desarrollo de multitud de sensores y tecnologías de detección remota y programas espaciales para la observación de la Tierra, que permiten el estudio de los procesos naturales del planeta y monitorizar los cambios que se producen a lo largo del tiempo. Gracias a ello, se han creado grupos de investigación tanto a nivel nacional como internacional que centran sus esfuerzos en objetivos comunes sobre la gestión hídrica. Por ejemplo, los equipos de investigación de la Plataforma Temática Interdisciplinar TELEDETECT (36) coordinada por el CSIC, el grupo de investigación en recursos hídricos de la Universidad de Salamanca (37), el grupo *Integrated Water Resources Management* de la UNECE *(United Nations Economic Commission for Europe)* (38), la matriz de grupos de *Water Europe* (39), o incluso el portal WISE-Freshwater de la Comisión Europea (40) en el que proporciona información sobre el estado de las políticas de agua y legislación europeas y realiza el seguimiento de la consecución de los objetivos ambientales de los distintos países de la Unión Europea (UE), de acuerdo con la base de datos de la DMA.

Para el procesamiento de todos los datos obtenidos, se utilizan paquetes informáticos específicos, que combinan esta información y su uso con los SIG. Estos sistemas tienen la capacidad de almacenar, visualizar, analizar, editar y representar información espacial georreferenciada utilizando un sistema de coordenadas, que es el marco de referencia que posiciona un objeto en la superficie terrestre. Un sistema de coordenadas geográficas utiliza una superficie esférica tridimensional para definir la posición en la tierra, utilizando el Ecuador y los Polos Norte y Sur para trazar la red geográfica formada por paralelos (latitud) y meridianos (longitud), sobre la que se ubican los objetos representados en unidades angulares (grados, minutos, segundo). Para la representación bidimensional de la superficie de la Tierra, se utilizan los sistemas de coordenadas proyectadas, obtenidas de la transformación de las coordenadas geográficas mediante proyecciones cartográficas a un plano cartesiano X,Y (Figura 3) (33).

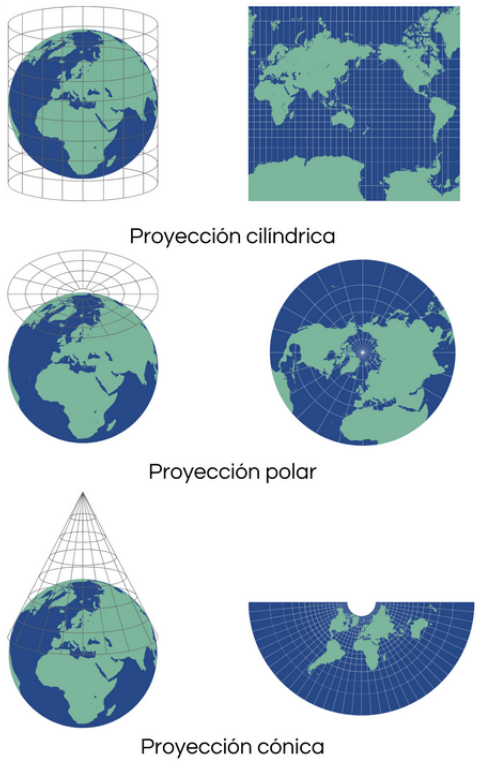

Figura 3. *Proyecciones en función de la figura geométrica sobre la que se proyecta. Fuente: elaboración propia.*

Los SIG permiten tanto el almacenamiento, como la visualización y tratamiento espacial de gran cantidad de información, ordenada en capas (ver Figura 4). Por ello, desempeñan un papel fundamental en la búsqueda de soluciones eficaces para la gestión hídrica facilitando la manipulación, actualización y análisis de datos, con lo que comprender patrones espaciales de cambio sobre los que poder generar y parametrizar modelos en los que basar la toma de decisiones (41,42).

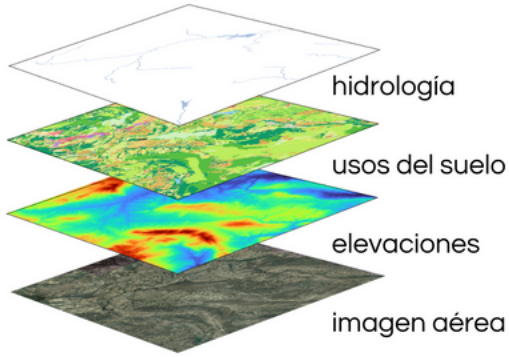

Figura 4. *Capas de información geoespacial que constituyen la base del funcionamiento de los Sistemas de Información Geográfica (SIG). Fuente: elaboración propia.*

2.4. La teledetección y SIG en la gestión de los recursos hídricos

En los últimos años, gracias al interés tanto público como privado, a las inversiones y el desarrollo tecnológico, se han conseguido grandes avances y mejoras no solo en los sensores y en las plataformas que los portan, habitualmente los satélites, sino también a nivel computacional, necesario para el procesamiento y tratamiento de los datos obtenidos. Conjuntamente a la democratización de estas tecnologías, la accesibilidad a datos globales sobre observaciones terrestres y la colaboración entre organizaciones, agencias y grupos de trabajo internacionales, se han podido llevar a cabo investigaciones realizadas con teledetección que han demostrado su enorme potencial para el estudio y modelización de los recursos hídricos (43,44). La precisión de las medidas nos da la oportunidad de lograr información cada vez más precisa e integrada en herramientas de gestión resolviendo, además, la limitación de la disponibilidad de datos a gran escala (45).

Algunos países operan actualmente con diferentes programas de observación terrestre que ofrecen a la comunidad científica una amplia variedad de mediciones y cobertura espacial y temporal, y que son de gran relevancia para el estudio del medio ambiente. Toda esta información disponible, nos sirve para mejorar el conocimiento de los cambios de variables hidrológicas, permitiendo la observación de las cuencas y el funcionamiento de todos sus elementos, necesario para desarrollar una planificación y políticas adecuadas para una gestión sostenible del agua (46,47).

Los SIG se convierten en una potente herramienta para la elaboración de modelos hidrológicos en la que se debe considerar la distribución espacial de los diferentes elementos y la posibilidad de controlar los parámetros que forman parte del ciclo hidrológico y su interacción con el entorno (48). Por lo tanto, la incorporación de los SIG al conjunto de mecanismos en los sistemas de gestión puede potenciar, por ejemplo, la capacidad de análisis de riesgos, la prevención y la anticipación a sequías o fenómenos extremos de precipitaciones, o la disposición de un sistema de alerta, así como para el estudio de las evidencias del cambio climático y medidas de adaptación de las actividades (49), los asentamientos y de los diferentes compartimentos ambientales.

En las diferentes Confederaciones Hidrográficas (CH) españolas, se realizan estudios y proyectos de colaboración técnica (50) que utilizan como parte de su metodología, las variables derivadas de la teledetección y los SIG. Por ejemplo, en las diferentes CH salen a contrato público para llevar a cabo estudios específicos para la planificación hidrológica mediante teledetección como estudios de cuantificación de la superficie regada o análisis de la información geográfica relacionada con los usos del suelo.

También publican contratos para la adquisición de productos LIDAR, escaneado y geolocalización de fotogramas procedentes de vuelos fotogramétricos históricos o incluso para el mantenimiento informático de sus SIG (51).

Además, siguiendo las recomendaciones y políticas de la Directiva Europea INSPIRE (52) y su transposición a la Ley 14/2010 de 5 de julio, sobre las infraestructuras y los servicios de información geográfica en España (53), las diferentes CH disponen de geoportales o Infraestructura de Datos Espaciales (IDE) de uso libre, en los que ofrecen gran cantidad de información cartográfica sobre los datos relativos al estado de las masas de agua de su demarcación, relativos al estado de los Planes Hidrológicos.

La Ley 14/2010 establece un marco común para desarrollar infraestructuras de información geográfica que permita la estandarización de la información y la interoperabilidad de la Infraestructura de Datos Espaciales de España (IDEE), de forma que, cada IDE de las diferentes Confederaciones Hidrográficas es un nodo dentro de la red nacional de proyectos, de acuerdo con la temática de la información que ofrecen. Algunos de los recursos que pueden consultarse, descargar y utilizar de las diferentes webs de las CH son: catálogos de datos cartográficos, mapas publicados, servicios web de mapas y visores cartográficos online con información básica para la consulta de series de datos hidrológicos a través de mapas interactivos.

Por ejemplo, el visor CHSIC de la Confederación Hidrográfica del Segura (54), SIA Júcar (55), el ideCHG de la Confederación Hidrográfica del Guadalquivir (56), o GeoGuadiana (57) (Figura 5).

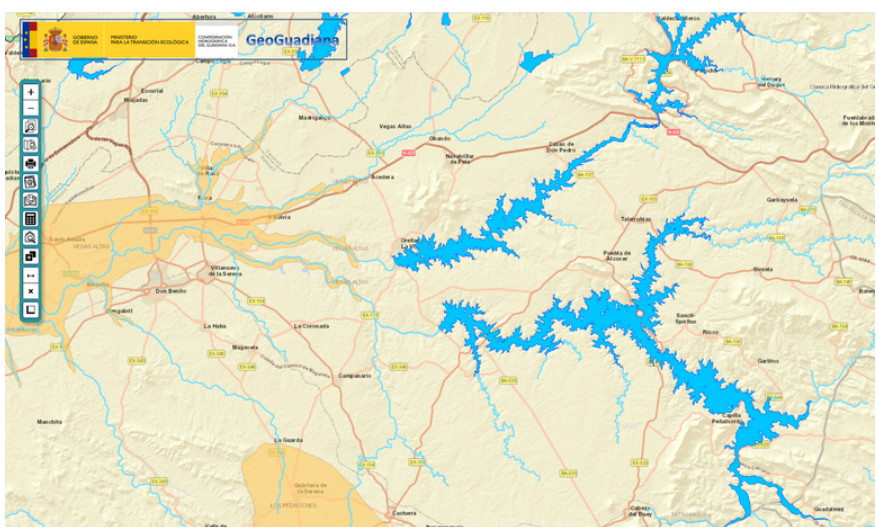

Figura 5. *Visor cartográfico GeoGuadiana. Fuente: Geoportal de la Confederación Hidrográfica del Guadiana.*

También a nivel nacional, el Área de Información Hidrológica del Ministerio para la Transición Ecológica y el Reto Demográfico, utiliza a través de la página web del MITECO, un cuadro de mandos (Figura 6) en el que se pueden visualizar en un mapa y gráficos, la información disponible del Boletín Hidrológico actualizada semanalmente (reserva hídrica, energía teórica producible, caudales medios semanales y pluviometría acumulada).

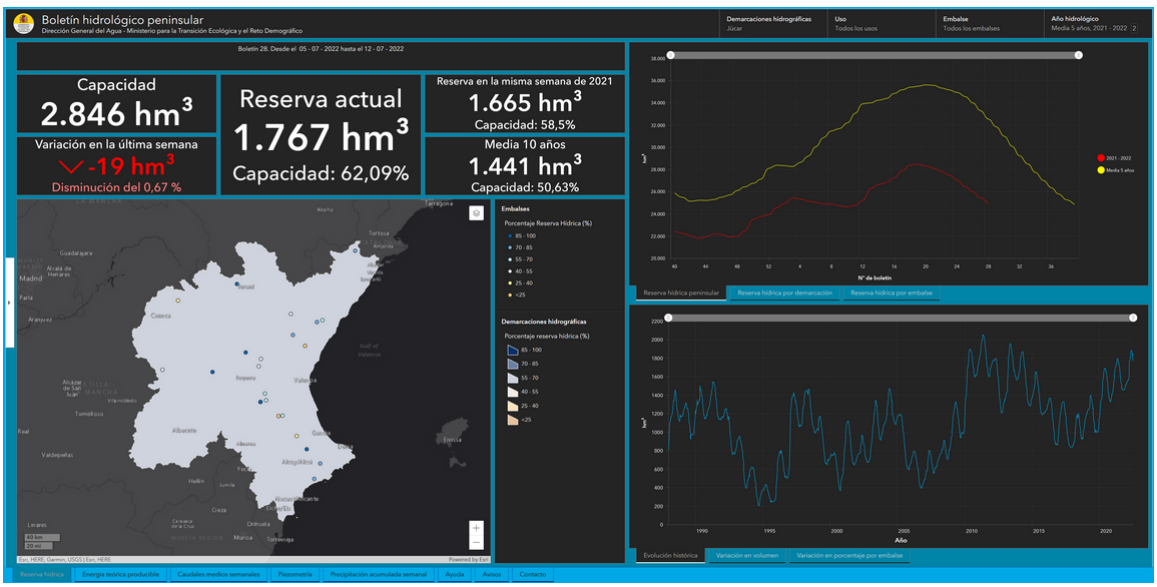

Figura 6. *Visor cartográfico del Boletín Hidrológico semanal. Fuente:* *https://miteco.maps.arcgis.com/apps/dashboards/912dfee767264e3884f7aea8eb1e0673*

Bajo esta perspectiva de nuevas estrategias de gobierno con programas de medidas e inversiones económicas y gracias al avance de nuevas tecnologías, la gestión de los recursos hídricos debe llevar implementada la aplicación de herramientas de teledetección y el uso de SIG. El objetivo es el de mejorar la visualización de la información, la interoperabilidad y, finalmente, establecer las líneas de actuación para alcanzar los objetivos ambientales, económicos y sociales planteados.

De hecho, para el cumplimiento de los objetivos de la planificación hidrológica, se han revisado algunos de los procedimientos de trabajo y hojas de ruta a seguir en los planes hidrológicos del tercer ciclo (2022-2027) (58,59), principalmente en referencia con el saneamiento, depuración y reutilización de las aguas residuales de forma que, queden alineadas con las políticas de los diferentes planes y estrategias (por ejemplo el Plan de Impulso al Medio Ambiente para la Adaptación al Cambio Climático en España, PIMA Adapta AGUA (60) o el Plan Nacional de Depuración, Saneamiento, Eficiencia, Ahorro y Reutilización, Plan DSEAR) (12).

Es por ello que, esta investigación trata de proponer y fomentar la integración de la teledetección y los SIG, para recabar información que sirva para aportar conocimientos de gran relevancia para la gestión hídrica y, sobre todo, para la toma de decisiones. Por lo tanto, los objetivos que persiguen y enmarcan esta tesis ahondan en la posibilidad de utilizar la combinación de series temporales de datos espaciales junto con variables climáticas e hidrológicas para la gestión eficiente de los recursos, principalmente en aquellas cuencas hidrográficas con mayor problema de disponibilidad frente a los futuros escenarios asociados a los cambios del clima con previsiones de escasez de agua. Es precisamente esta escasez que puede ser predicha con estos sistemas, la que nos lleva a apostillar la necesidad de garantizar otras fuentes de recursos basados en las propuestas de las administraciones, en este caso y en nuestro entorno inmediato, la desalación.

3. Objetivos

La teledetección y los SIG se han convertido en una herramienta que nos proporciona una gran cantidad de información complementaria a la obtenida *in situ* mediante las redes de seguimiento y estaciones de control y que permite, además, incluir otro tipo de parámetros ambientales que proporcionen información no solo como diagnóstico del estado de los recursos, sino también como indicadores de los efectos producidos por el cambio climático. Las imágenes obtenidas a partir de los sensores aportan un valor añadido al conocimiento sobre los procesos e interacciones entre las variables que componen el ciclo hidrológico y suponen un apoyo para la evaluación del estado de los recursos y proyección de las tendencias.

Se debe tener en cuenta diferentes aspectos fundamentales para el estudio y monitorización de las variables que conforman la gestión sostenible de los recursos hídricos (61). Para ello, es imprescindible incluir un enfoque social en el que es necesario la concienciación y participación conjunta de todos los agentes implicados para reducir los impactos asociados a nuestras actividades socioeconómicas que ponen en riesgo los recursos hídricos disponibles. Especialmente en regiones con una distribución natural del agua que parece insuficiente para abastecer las demandas de consumo actuales que causan estrés hídrico y el deterioro de los sistemas naturales.

Es por este motivo que, la planificación y regulación para un uso más racional del agua, juegan un papel fundamental en la mitigación de los efectos del cambio climático sobre el ciclo hidrológico (62). De hecho, se están adoptando políticas y estrategias que suponen una oportunidad de mejora para el modelo de gestión actual y una transformación de nuestro sistema económico, como es la reciente Ley 7/2021, de 20 de mayo, de cambio climático y Transición Energética (63) que, en su artículo 19 sobre la consideración del cambio climático en la planificación y gestión del agua, define como objetivos *"[…] conseguir la seguridad hídrica para las personas, para la protección de la biodiversidad y para las actividades socioeconómicas, de acuerdo con la jerarquía de usos, reduciendo la exposición y vulnerabilidad al cambio climático e incrementando la resiliencia."*

Por todo esto, la finalidad principal de esta tesis doctoral es la de aportar información acerca del potencial para el estudio y análisis del estado de los recursos hídricos a través de herramientas de teledetección y la integración de todos los datos en un SIG que permita visualizar los resultados, modelos o escenarios actuales y futuros.

Para desarrollar este fin, se han evaluado diferentes metodologías mediante imágenes de satélite, propiedades físicas de las superficies y variables climáticas, a partir de relaciones sencillas para la detección y medición de la disponibilidad de agua y la formulación de modelos que permiten prever su disponibilidad bajo diversos escenarios de cambio climático.

La gestión de los recursos hídricos está directamente relacionada con el uso que se hace de ellos para satisfacer las actividades antrópicas a la vez que se conservan los ecosistemas naturales asociados. Uno de los sectores que genera un mayor impacto sobre las masas de agua es la actividad agraria, no solo por la demanda hídrica, que supone alrededor del 80% de la demanda total sino también, como principal causa de degradación por contaminación puntual y difusa, canalizaciones, presas y otras alteraciones sobre el medio natural.

Debido a la expansión de la superficie dedicada al cultivo y el incremento del consumo de agua para satisfacer las necesidades agronómicas de los últimos años, se han desarrollado diferentes medidas que suponen una mejora en la gestión eficiente del agua, principalmente en aquellas regiones caracterizadas por un régimen de lluvias árido o semiárido.

Por ello, el primero de los objetivos específicos de esta tesis ha sido:

- *Estudiar los cambios en el uso del suelo y su relación con las actividades agrícolas y el riego.*

Para evaluar estos cambios, se realizó un análisis mediante imágenes aéreas a escala de cuenca hidrográfica, con una delimitación orográfica bien definida, como es la cuenca vertiente al Mar Menor, el mayor lago costero del Mediterráneo y que, además, ha experimentado importantes modificaciones en el uso del suelo, tanto por la expansión del sector agrícola como por el crecimiento de la población.

Comprobada la utilidad que tiene el uso de la fotografía aérea y ortofotografía, herramientas de teledetección en el rango del espectro visible, para el estudio de los cambios de las cubiertas y los usos del suelo, el trabajo se centró en la utilización de imágenes multiespectrales para analizar la reflectancia de las superficies (vegetación, suelo y agua). De esta forma, se puede obtener información sobre la evolución y el estado de los recursos hídricos, abordando el uso de plataformas satelitales con datos en abierto como son los procedentes del programa LANDSAT y del MODIS.

Así, los objetivos en este apartado fueron los siguientes:

- *Realizar una revisión del uso de índices de vegetación, ampliamente utilizados por su relación entre la respuesta espectral de la vegetación según diferentes propiedades biofísicas con la disponibilidad de agua, y su aplicación al estudio y modelización de zonas húmedas.*

- *Evaluar la disponibilidad de recursos hídricos en una zona semiárida con un elevado consumo de agua, a partir del estudio de índices espectrales y realizar una prospectiva del estado de estos recursos bajo escenarios de cambio climático.*

Modelizar y estimar de forma sencilla mediante imágenes LANDSAT la capacidad de almacenamiento de agua en embalses, pudiendo derivar a partir de este estudio un sistema de gestión aplicando inteligencia artificial que permitiera automatizar un sistema de control basado en las imágenes de satélite obtenidas periódicamente. Como parte de una política de uso eficiente del agua a través de metodologías enfocadas en reducir la presión sobre los recursos hídricos, la reutilización de las aguas y su reintroducción en el ciclo hidrológico es una de las propuestas de actuación con un elevado potencial para asegurar la calidad y disponibilidad del agua, y como estrategia de adaptación al cambio climático. Por ello, y para superar las barreras técnicas y culturales asociadas a la reutilización de agua, se ha desarrollado un marco de actuación que plantea oportunidades de mejora con la implantación de medidas para el uso de recursos no convencionales que permitan el máximo aprovechamiento para una gestión sostenible.

En este contexto, se planteó como objetivo:

- *Estudiar la calidad de las aguas de los drenajes agrícolas y la posibilidad de implantación de un sistema de desalinización que permita la reutilización de estos drenajes, como herramienta complementaria a la habitual reutilización de aguas depuradas de origen urbano en la agricultura, de la que el sureste español es un claro y significativo ejemplo.*

Este objetivo complementa a los anteriores, con la caracterización y la propuesta de reutilización de las aguas de drenaje agrícola del sur de la provincia de Alicante, Entronca directamente con las políticas de gestión que se proponen desde el Ministerio para la Transición Ecológica y el Reto Demográfico y ahonda en la necesidad de la utilización eficiente de los recursos disponibles a nivel local, en su reutilización y aprovechamiento máximo. Es el necesario cierre del círculo de la gestión y manejo de recursos, en este caso representado por una propuesta de sistema de aprovechamiento no convencional.

4. Materiales y métodos

A continuación, en este apartado se describe, de forma general, la metodología utilizada en las diferentes publicaciones que conforman esta tesis.

4.1. Instrumentos de observación de la superficie terrestre para la gestión de los recursos hídricos

Se podría decir que la técnica de teledetección más temprana es la fotografía aérea, en la que se utilizaban cometas, globos y posteriormente aviones con cámaras fotográficas a bordo para obtener imágenes de la superficie terrestre. Aunque en sus inicios, el principal uso era militar, posteriormente y debido entre otras cosas a las mejoras en las cámaras fotográficas y al desarrollo de la fotogrametría, una técnica con la que se pueden definir la posición y dimensiones de un objeto a partir de medidas sobre fotografías, se han realizado diferentes programas de vuelos fotogramétricos a nivel local y nacional, por encargo de diferentes organismos para estudios geológicos, gestión forestal, topografía, agricultura o urbanismo, entre otras muchas. La fotografía aérea presenta una gran ventaja para la evaluación ambiental y la ordenación del territorio ya que permite realizar estudios a una escala con mayor grado de detalle. Desde el Centro de Descargas del Instituto Geográfico Nacional, se pueden encontrar fotogramas desde principios de los años 20 escaneados y georreferenciados, disponibles para acceso público (Figura 7).

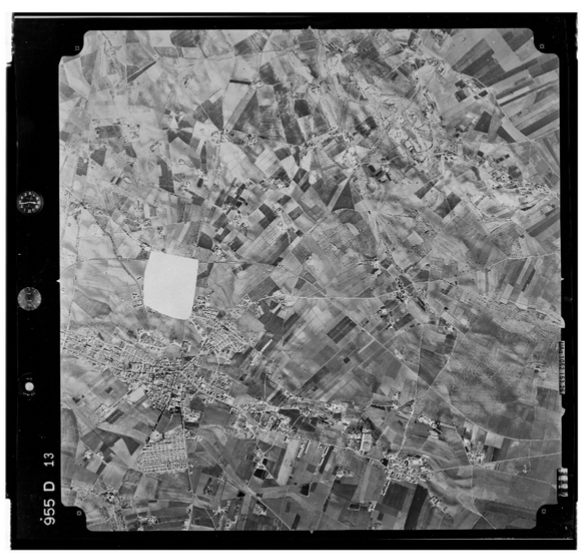

Figura 7. *Fotograma del vuelo fotogramético Interministerial de 1973-1986 en Torre Pacheco (Murcia). Escala 1:18.000. Tamaño de píxel (GSD) entre 25 cm y 50 cm, Sistema geodésico de referencia ETRS89. Fuente: FotoI 1973-1986 CC-BY 4.0 scne.es*

Para la representación fotográfica georreferenciada de la superficie terrestre, se aplica una rectificación en las imágenes aéreas y, posteriormente se corrigen las posibles deformaciones generadas por los desniveles del terreno o por la orientación de la cámara (64). Así se obtienen las ortofotografías, que se convierten de esta manera en un documento con características cartográficas (Figura 8).

A nivel nacional, se lleva realizando desde 2004, un proyecto coordinado entre administraciones públicas denominado el Plan Nacional de Ortofotografía Aérea (PNOA), que establece una Infraestructura de información espacial común, de acuerdo con la Directiva 2007/2/CE, de 14 de marzo de 2007 (Directiva INSPIRE), y que proporciona una base para obtener información geográfica general con una gran resolución.

Figura 8. *Ortofotografía aérea digital del Plan Nacional de Ortofotografía Aérea (PNOA) del año 2016 con resolución de 25 cm correspondiente a la hoja MTN50 0955 Torre-Pacheco Huso 30. Fuente: OrtoPNOA 2016 CC-BY 4.0 scne.es*

4.2. Teledetección espacial: evolución de los usos del suelo y el consumo de agua

Otra posibilidad que ofrece la fotogrametría aérea es la obtención de modelos de elevaciones del terreno en los que se representa la distribución espacial de la altitud (Figura 9).

Ya desde finales de los años 50, se comenzó a utilizar la estereoscopía que permite simular el efecto de relieve a partir de 2 fotogramas consecutivos con solapamiento deseable de al menos un 60% de la imagen. Actualmente, se obtienen modelos digitales de elevaciones con mayor precisión a partir, entre otros métodos, de tecnología LIDAR, en el que un sensor láser emite un haz sobre las superficies y mide el tiempo que tarda en llegar hasta la superficie u objeto reflectantes y regresar al sensor, obtenido así una nube de puntos del terreno situados a distintas alturas.

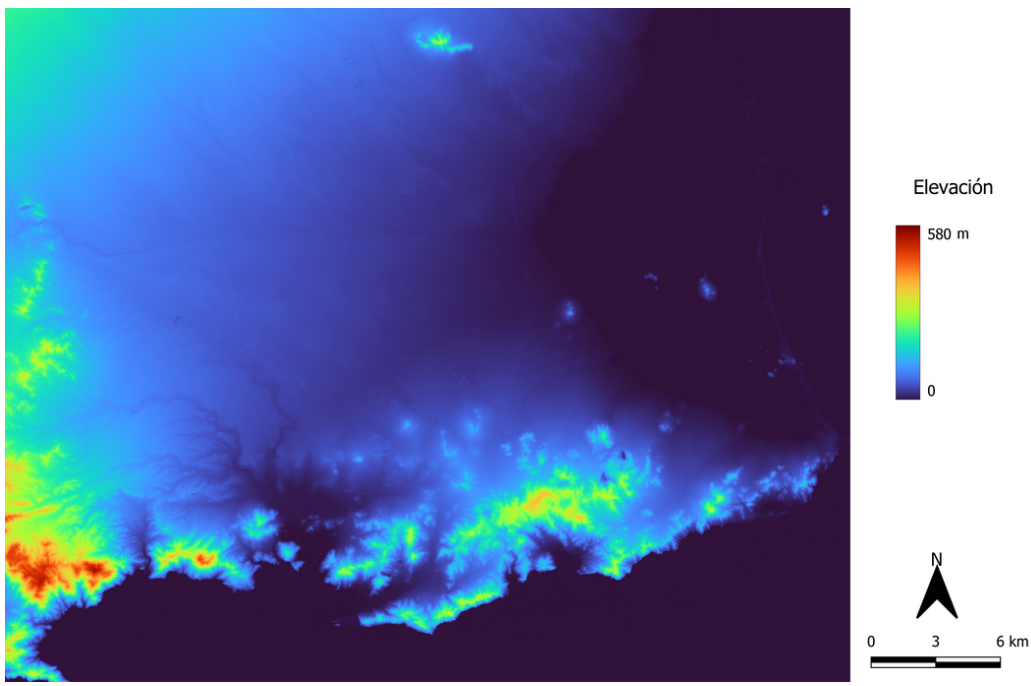

Figura 9. *Modelo Digital del Terreno con tamaño de píxel de 25 metros de la cuenca del Mar Menor. Fuente: elaboración propia a partir del MDT25 2015 CC-BY 4.0 ign.es*

En esta tesis, se ha utilizado este tipo de productos, como base para realizar un caso de estudio de la evolución de superficies de regadío y del consumo de agua asociado. En la publicación ***"Water management in irrigation systems by using satellite information"*** se delimitó el área de estudio, la cuenca del Mar Menor, utilizando el Modelo Digital de Elevaciones (MDT25 2015 CC-BY 4.0 ign.es).

Posteriormente, para la digitalización de las superficies agrícolas y urbanas se utilizaron de base, 298 fotogramas del vuelo interministerial de 1973-1986 y, por otro lado, ortofotografías del Plan Nacional de Ortofotografía Aérea (PNOA) máxima actualidad de 2016. Además, se localizaron las balsas de riego para ambos periodos de tiempo.

Con los resultados obtenidos, se estimaron las pérdidas de agua en relación con el incremento del número y superficie de las balsas de riego y comparar gráficamente su distribución en ambos periodos. Para ello se realizó un mapa de calor (*heatmap*) o de estimación de densidad de puntos a partir del número de localizaciones dentro de un radio de búsqueda, utilizando la estimación de densidad kernel (kernel density estimation). Cuanto mayor es el número de puntos localizados en una zona, mayor será la densidad.

El algoritmo de mapas de calor utiliza tres parámetros principalmente:

- El tamaño de píxel para la imagen ráster de salida,
- El ancho de banda o radio de búsqueda, que controla la expansión de la influencia alrededor de cada punto. Si el radio de búsqueda es grande, el resultado estará más suavizado al incorporar puntos más alejados, en cambio para valores más pequeños, se potenciará las pequeñas variaciones.
- El kernel o función que determina la proporción en la disminuye la influencia de un punto sobre el resto cuando aumenta la distancia dentro del radio de búsqueda.

Para el cálculo de la estimación anual de la pérdida de agua por evaporación, se utilizó la ecuación desarrollada por Martínez Alvarez et al. (2008), con la que estimaron la pérdida por evaporación en las balsas de riego localizadas en la cuenca del río Segura. Para ello utilizaron datos diarios de temperatura, precipitación, humedad relativa, velocidad y dirección del viento, y radiación solar obtenidos de 74 estaciones meteorológicas localizadas dentro de la cuenca en el periodo de 2000 a 2006. Además, utilizaron tanques evaporímetros clase A para estimar la evaporación.

El valor de evaporación anual obtenido de su estudio (0,014 hm^3 año/ha) es el que se utilizó de referencia para el cálculo de la evaporación media para ambos periodos en la cuenca del Mar Menor.

4.3. Obtención de información temática: índices espectrales y gestión del agua

Gracias a los resultados obtenidos de los primeros satélites meteorológicos y las diferentes misiones espaciales, se puso en órbita en 1972 el primer satélite dedicado a la observación de la superficie terrestre (ERTS/ Landsat 1), y que fue el inicio del desarrollo de programas espaciales específicos por parte de las diferentes Agencias Espaciales.

Algunos ejemplos de ello son el programa SPOT que lanzó en 1986 el Centro Nacional Francés de Estudios Espaciales en colaboración con la Agencia Espacial Europea (ESA) (65), el programa Copérnico Sentinel (66) o incluso los programas EOS (67) y CARTOSAT de la Agencia India de Investigación Espacial (68).

Una de las principales ventajas de la teledetección es la posibilidad de acceder a un repositorio de imágenes obtenidas durante décadas, que hace posible la extracción de series temporales de datos que permiten monitorizar y evaluar los cambios producidos sobre diferentes elementos utilizando multitud de técnicas de procesamiento de imágenes que han ido desarrollándose a lo largo de los años (69,70). Un ejemplo de estas técnicas son los índices de vegetación, que aportan conocimientos muy útiles en multitud de estudios (producción agrícola, evolución y estado de comunidades vegetales y gestión forestal, conservación de la biodiversidad, cambios de uso de suelo, …) y que se han implementado ampliamente dentro de las aplicaciones de teledetección en general para la evaluación de los recursos naturales (71,72). De hecho, desde 2004, se ha producido un incremento sustancial de las publicaciones en relación con la gestión hídrica a través de la teledetección, siendo el estudio de la vegetación a partir de índices espectrales una de las metodologías más ampliamente utilizadas (69).

Estos índices, son algoritmos relativamente sencillos que se obtienen operando con las diferentes bandas espectrales de las imágenes (73). El establecimiento de los valores de cada índice está relacionado con la reflectancia de las superficies de la planta que cambia según las características biológicas (pigmentos vegetales, morfología de las hojas, …) y estado fisiológico (como el contenido de humedad o estado nutricional) de la vegetación (71).

En la publicación incluida en esta tesis ***"A review of Landsat TM/ETM based vegetation indices as applied to wetland ecosystems",*** se utilizó una escena de Landsat 5 obtenida el 14/08/2005, localizada entre las Salinas de Santa Pola y el Parque Natural de El Hondo en Elche y Crevillente, para evaluar el ajuste de diferentes índices de vegetación y la redundancia de información en zonas próximas a humedales mediterráneos.

Para el pre-procesamiento de la imagen de Landsat-5 TM obtenida de la Agencia Espacial Europea (ESA) se realizó, en primer lugar, una corrección geométrica mediante una transformación polinómica de segundo grado y un método de remuestreo.

Este método está basado en el método del vecino más próximo, utilizando cartografía vectorial de ortofotografías aéreas con una resolución espacial de 1 metro, con un error RDCM (Raíz de la Desviación Cuadrática Media) de menos de medio píxel (13,84 m). Se realizó una calibración radiométrica para la conversión de niveles digitales a reflectancia. Para evitar las distorsiones causadas por la niebla, se utilizó el método de Sustracción del Objeto Oscuro (DOS), seleccionando los píxeles con menor valor de reflectancia del histograma.

Para facilitar el análisis de los índices de vegetación, y teniendo en cuenta la respuesta espectral de las superficies, se realizó una máscara para la extracción de las masas de agua utilizando el Índice Normalizado de Superficie de Cuerpos de Agua (NWBSI, en inglés) calculado como una ratio entre los valores de reflectancia de las bandas 1 (0.45 - 0.52 µm) y 5 (1.55 - 1.75 µm). De esta forma, en zonas de humedales en las que el contenido de humedad del suelo y la vegetación son elevados, se pretende reducir el efecto sobre los datos obtenidos y mejorar su análisis e interpretación.

Posteriormente, se calcularon los diferentes índices de vegetación (ver ejemplo de Figura 10), de los que se obtuvieron la media, valores máximos y mínimos, desviación estándar y el error, obtenidos del análisis píxel a píxel.

Se realizó un análisis de regresión lineal entre los índices comparando cada uno de ellos con el resto para evaluar el grado de correlación (74). Para ello se relacionaron aquellos dentro de un mismo grupo, categorizados según el tipo de parámetros biofísicos que aportan: los índices de estimación de la biomasa y los índices basados en el contenido de humedad de la vegetación. La pendiente y el coeficiente de correlación obtenidos se utilizaron para evaluar la información redundante; la pendiente indica el tipo de relación entre dos índices, y r^2 el grado de similitud entre el par de variables.

Desde el lanzamiento de los primeros satélites dedicados a la observación de la Tierra, se ha logrado recabar información temática de forma periódica y con carácter global así como diversificar las aplicaciones de las imágenes obtenidas por los sensores, y que han supuesto un gran impulso para promover la investigación en el desarrollo de instrumentos y técnicas de teledetección (75) que posibilitan un análisis complejo de variables ambientales.

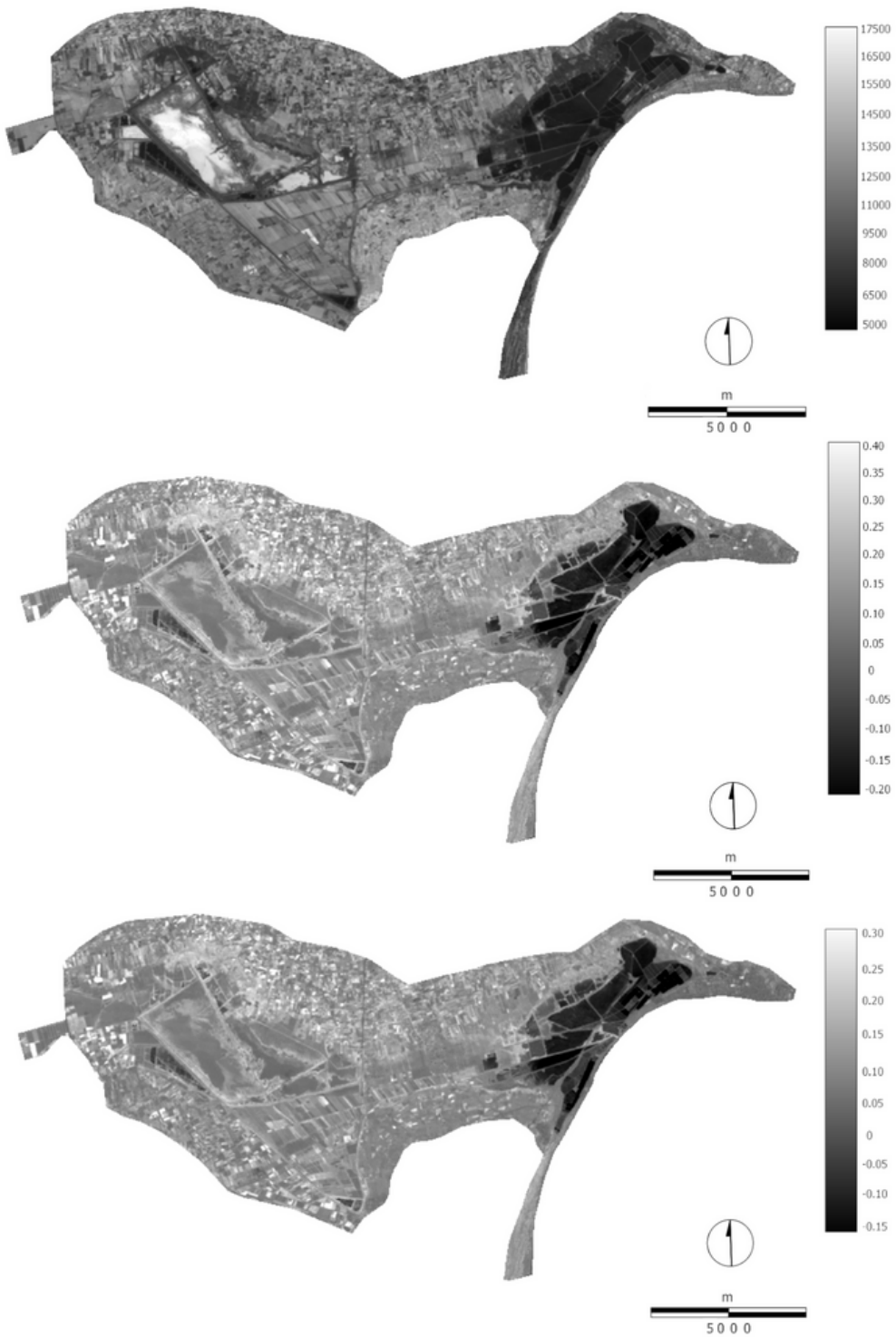

Figura 10. *Cálculo de diferentes índices de vegetación 1) Integral, 2) SAVI, 3) NDVI en el área de estudio a partir de imágenes Landsat 5. Fuente: Servicio Geológico de Estados Unidos (USGS).*

Uno de estos primeros grandes proyectos para la observación de la Tierra ha sido el lanzamiento del satélite Terra en 1999 por la NASA dentro del proyecto EOS (Earth Observing System). Este satélite incorpora 5 sensores que han recopilado una importante cantidad de datos a lo largo de los años que ha servido para la comprensión y el estudio de los procesos naturales de la Tierra, el cambio climático y evaluar el impacto de los desastres naturales o de la actividad humana.

Los cinco sensores que transporta el satélite son:

- **ASTER** *(Advanced Spaceborne Thermal Emission and Reflection Radiometer)*. Obtiene imágenes de alta resolución en 14 longitudes de onda diferentes del espectro electromagnético, desde la luz visible hasta el infrarrojo térmico. Las imágenes suelen emplearse en estudios para la detección de cambios y validación relacionados con la temperatura, la emisividad, la reflectancia o la elevación de la superficie terrestre.
- **CERES** *(Clouds and Earth's Radiant Energy System)*. Proporciona estimaciones de las propiedades y del papel de las nubes en los flujos radiativos desde la superficie hasta la parte superior de la atmósfera.
- **MISR** *(Multi-angle Imaging SpectroRadiometer).* Permite conocer la cantidad de luz solar que se dispersa en distintas direcciones de cada región de la superficie de la Tierra fotografiada con cámaras apuntadas en nueve ángulos diferentes.
- **MODIS** *(Moderate-resolution Imaging Spectroradiometer).* Opera en 36 bandas espectrales con una resolución temporal de 1-2 días, y es capaz de registrar la frecuencia y distribución de la cobertura de nubes, las propiedades de los aerosoles, distribución vertical de la temperatura y el vapor de agua, o la actividad fotosintética de la vegetación.
- **MOPITT** *(Measurements of Pollution in the Troposphere).* Mide la radiación emitida y reflejada desde la Tierra en tres bandas espectrales con la finalidad de estudiar la distribución, transporte, fuentes y sumideros de monóxido de carbono en la troposfera.

En la figura 11 se muestra un ejemplo de índice de vegetación derivado del sensor MODIS que se produce a intervalos de 16 días con una resolución espacial de 500 metros.

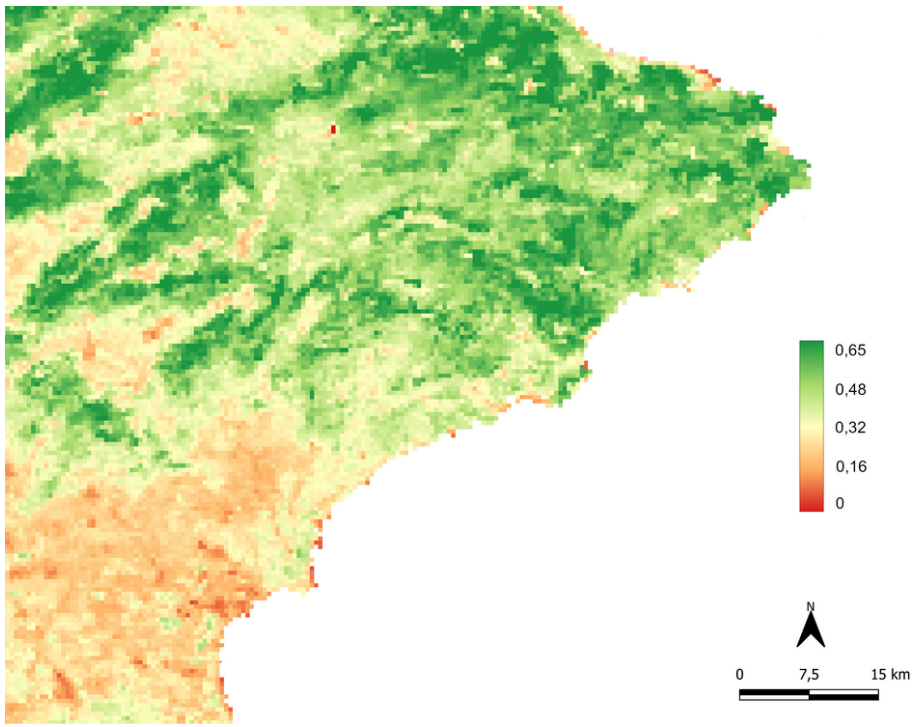

Figura 11. *Imagen compuesta del NDVI correspondiente al producto MODIS (MOD13A1) del 31-10-2013. Fuente: Servicio Geológico de Estados Unidos (USGS).*

En el caso de la publicación ***"Assessing water availability in Mediterranean regions affected by water conflicts through MODIS data time series analysis"*** incluida en esta tesis, se utilizaron las imágenes obtenidas del sensor MODIS para el periodo de 2001 a 2014 del índice de Vegetación de Diferencia Normalizada (NDVI), y de Temperatura de la Superficie Terrestre (LST).

Para extraer los valores de los píxeles que se encuentran dentro del área de estudio de forma individual, y obtener las imágenes de la media y desviación estándar anuales de NDVI y LST, se creó una máscara utilizando los límites de las cuencas hidrográficas de los ríos Amadorio y Guadalest, obtenidos de la Confederación Hidrográfica del Júcar. Al igual que en trabajos anteriores, el uso de máscaras sobre las imágenes de tipo ráster permite delimitar la zona objeto de estudio, evitando sobredimensionar el espacio.

Por otro lado, los datos diarios de precipitación se obtuvieron de 11 estaciones meteorológicas repartidas tanto dentro como fuera del área de estudio, con el objetivo de obtener unos valores representativos de las condiciones climáticas de la zona.

Posteriormente, se calculó con modelos de regresión múltiple la precipitación media anual teniendo en cuenta la localización de las estaciones y el Modelo Digital de Elevaciones y con ello se representaron mapas anuales de precipitación.

Los datos anuales de volumen almacenado de los embalses localizados en cada río se obtuvieron de los anuarios de aforo de la página de Redes de Seguimiento del Estado e Información Hidrológica.

En la representación de los escenarios futuros asociados al cambio climático, se utilizaron proyecciones de modelos climáticos globales de precipitación para el 2050 para cuatro trayectorias de concentración representativas de gases de efecto invernadero (RCP): RCP2.6, RCP4.5, RCP6 y RCP8.5 W/m², obtenidos de la página WorldClim (76) subvencionado por el Consorcio de Sistemas Geoespaciales y Agrícolas del Laboratorio de Innovación para la Intensificación Sostenible dentro de la iniciativa Feed the Future de Estados Unidos *(Geospatial and Farming Systems Consortium of the Sustainable Intensification Innovation Lab)*.

Para analizar la relación entre el volumen de agua almacenado en los embalses y las variables seleccionadas (NDVI, LST y precipitación) se calculó en primer lugar las anomalías de las series de datos utilizando el z-score que permite visualizar los patrones de cambio espacio-temporales. Posteriormente, se calculó el coeficiente de correlación de Spearman para los z-score de las variables y comprobar así, las relaciones entre ellas y la significancia. Posteriormente, se utilizaron correlogramas construidos con los valores de z-score del volumen de agua embalsado con cada una de las otras variables para representar espacialmente las correlaciones obtenidas.

La capacidad de predicción del NDVI y LST sobre el almacenamiento de agua teniendo en cuenta los escenarios de cambio climático con las 4 trayectorias de concentración, se evaluó mediante una regresión espacial de mínimos cuadrados.

4.4. Análisis e interpretación de imágenes satelitales para la evaluación de los recursos hídricos

Uno de los objetivos principales en teledetección es la clasificación de las imágenes obtenidas en función de las variables analizadas, en las que se definen las diferentes clases a las que pertenecen los píxeles y que forman parte del área de estudio.

Esta clasificación se puede realizar de dos formas: mediante una clasificación supervisada o una clasificación no supervisada.

Con la supervisada, se clasifican los píxeles de la imagen en función de las variables de estudio según valores asignados de acuerdo con las firmas espectrales de las superficies. Para ello, se realizan áreas de entrenamiento, en las que los valores de reflectividad de las diferentes superficies u objetos están definidos de forma clara dentro de una única clase (34).

En la clasificación no supervisada, no se determina ninguna clase, sino que se utilizan algoritmos automáticos de clasificación que buscan clases espectrales (o clústeres) en una imagen de forma que la variabilidad entre los píxeles incluidos en esa categoría sea la mínima posible.

En el artículo ***"Using Landsat images to determine water storing capacity in Mediterranean environments"*** que forma parte de esta tesis, se utilizó la clasificación supervisada de imágenes para obtener los datos de superficie de lámina de agua que se incorporan a los modelos de predicción propuestos.

Para obtener la superficie de agua de los embalses seleccionados se utilizaron un total de 336 imágenes de Landsat; el 75% de Landsat 7 ETM+ (Nivel 2) para el entrenamiento correspondientes a fechas entre octubre de 1999 y mayo de 2003 y, el 25% de imágenes de Landsat 8 (OLI) (Nivel 2) adquiridas entre abril de 2013 y diciembre de 2015 para la validación independiente entre las estimaciones de agua superficial y los datos oficiales del volumen de agua.

En primer lugar, se delimitaron las imágenes mediante un área de influencia o *buffer* creado a partir de los archivos de datos geográficos de la superficie máxima de los embalses, disponibles como recursos cartográficos para descarga en el apartado de Infraestructura de Datos Espaciales de las diferentes Confederaciones Hidrográficas (Guadiana, Segura, Júcar y Guadalquivir).

Para calcular la superficie de agua de cada embalse (Figura 12), se definieron conjuntos de píxeles pertenecientes a las clases "agua" o "suelo". El algoritmo *Spectral Angle Mapper* (SAM) calcula las similitudes entre las firmas espectrales de la imagen de entrenamiento y las firmas espectrales de los píxeles de la imagen como vectores en una dimensión igual al número de bandas (77).

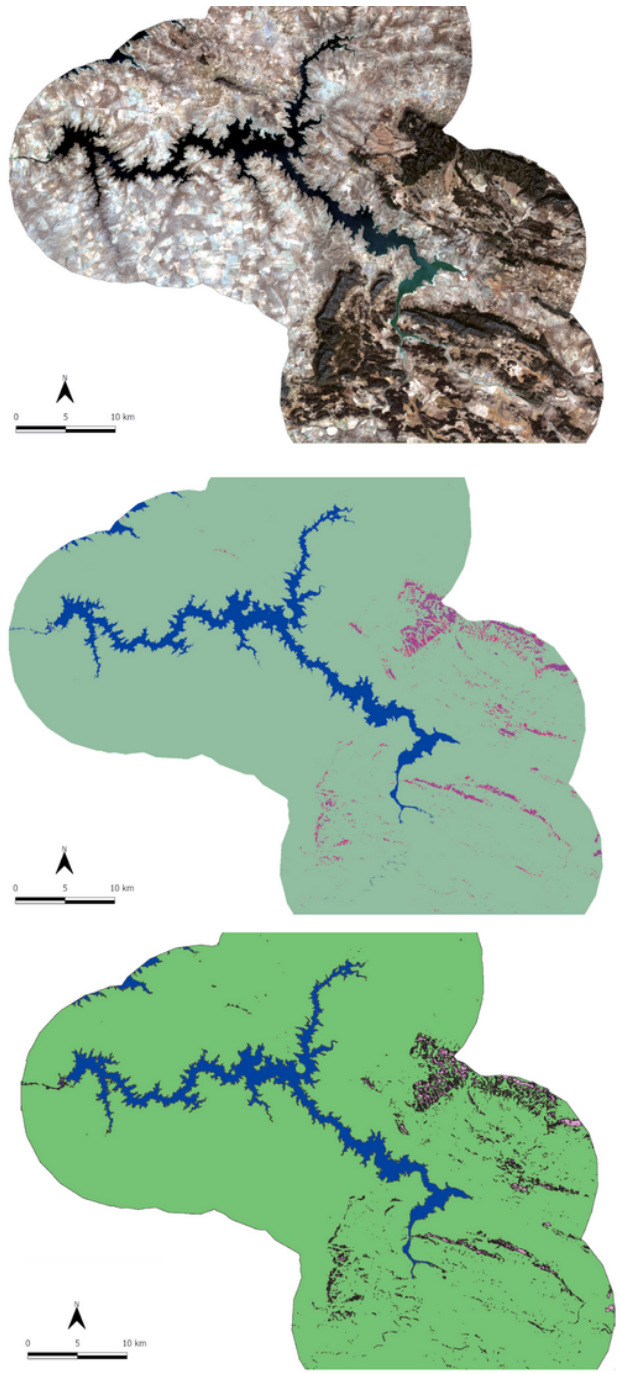

Figura 12. *Clasificación de las imágenes ráster durante el preprocesamiento de las imágenes Landsat 7 para la obtención de la superficie de la lámina de agua de los embalses. 1) Imagen Landsat 7 del embalse de La Serena obtenida en fecha 14-09-2000. 2) Clasificación "agua"-"suelo" de la imagen con SAM. 3) Vectorización de la imagen clasificada y cálculo de superficie. Fuente: elaboración propia.*

Los datos del volumen de agua almacenada, para las fechas en las que se obtuvieron las imágenes, proceden del visor de Redes de Seguimiento del Estado e Información Hidrológica del Ministerio de Agricultura y Pesca, Alimentación y Medio Ambiente (MAPAMA), actualmente del Ministerio para la Transición Ecológica y el Reto Demográfico (MITECO).

Se calcularon modelos de regresión para predecir el volumen de agua a partir de los mapas de agua superficial obtenidos, para posteriormente, evaluar el ajuste del modelo utilizando el Error Cuadrático Medio (RMSE). El RMSE mide el error del conjunto de datos de los valores estimados y los valores observados. Cuanto más pequeño es el valor de RMSE, más próximos son los datos estimados y los observados. Para comprobar la validez de las predicciones del modelo, se calculó la Desviación Predictiva Residual (RPD) que se define como el cociente entre la desviación estándar (σ) de los valores observados y la Raíz del Error Cuadrático Medio (RMSEP). En este caso, cuanto mayor sea el valor obtenido, mejor será la capacidad de predicción del modelo.

4.5. Estrategias para una economía circular: depuración y reutilización de aguas de riego

Uno de los sectores que más se ha beneficiado de la teledetección es la agricultura, tanto a nivel local para el seguimiento de las estadísticas agrarias, viabilidad o rendimientos, como a nivel más global para evaluar el impacto sobre el suelo, la biodiversidad, recursos hídricos, o estudiar los efectos del cambio climático. Para un sector sensible a esta elevada variabilidad, los efectos del cambio climático generan severas consecuencias debido a la disminución de los recursos disponibles o de las condiciones climáticas favorables (reducción de los recursos hídricos disponibles, el aumento de la temperatura, de eventos meteorológicos extremos, plagas vegetales o pérdida de suelo) enmarcado en un contexto de búsqueda de productividad para satisfacer la demanda alimentaria actual (78).

Como estrategia común para dar respuesta a las nuevas demandas a la vez que se garantiza la calidad del agua para nuestro desarrollo y los ecosistemas naturales, se ha propuesto como parte de los programas de medidas y acciones encaminadas a una gestión sostenible, la incorporación de recursos hídricos no convencionales (como la desalinización) en el que se puede reaprovechar del agua utilizada en el regadío de los propios cultivos (79).

Por ello, en el artículo ***"Agricultural drainage water characterization to determine the desalination possibilities for irrigation in a semi-arid environment"***, se realiza un análisis previo de caracterización y validación de la calidad de las aguas utilizadas en el riego con la finalidad de abastecer una planta desalinizadora por ósmosis inversa.

Para el análisis se seleccionaron 13 azarbes que recogen el agua de una densa red de canales de riego en la zona de la Depresión de Elche en la Cuenca del Bajo Segura. Estos azarbes son canales cementados en su mayor parte del recorrido, de bordes verticales y al aire libre. Se dividieron en dos grupos en función del río en el que desembocan el agua, el río Vinalopó y el río Segura (Figura 13), y se realizaron 12 muestreos repartidos entre septiembre de 2016 y julio de 2018, teniendo en cuenta la variabilidad estacional y, con 4 muestras por canal. Estas se tomaron al final del azarbe, pero lo suficientemente lejos de la costa para evitar la influencia del agua de mar.

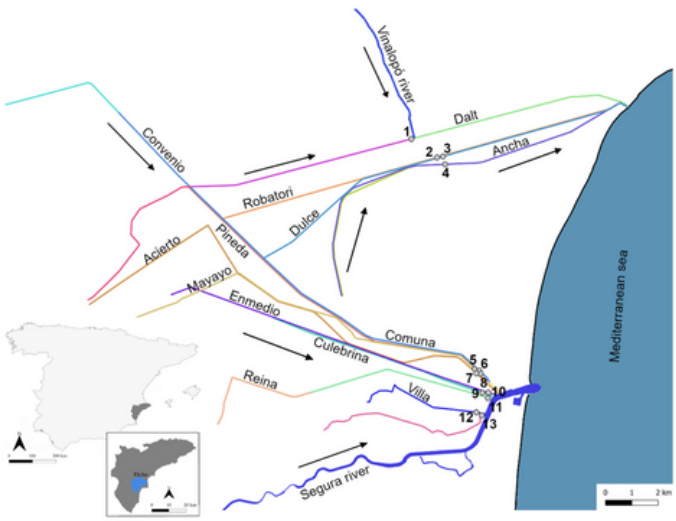

Figura 13. *Localización de los azarbes y puntos de muestreo de la zona de estudio.*

Por un lado, en las muestras de agua se analizó el pH, la salinidad determinando la conductividad eléctrica a 25ºC, cloruro y sodio siguiendo los métodos estándar para análisis de agua y aguas residuales, y los Sólidos en Suspensión por filtración en filtros de microfibra de vidrio de 1,2 µm. Por otro lado, para determinar si alguno de ellos podría proporcionar agua suficiente para mantener un cauce de una planta de sistema de ósmosis inversa de tamaño pequeño o mediano, se estimó el caudal de los azarbes siguiendo la metodología basada en el método de flotación (80,81).

5. Resultados generales y discusión

Con esta serie de publicaciones, se pretende destacar el potencial del uso de la teledetección y los SIG, para su incorporación como herramientas para mejorar la gobernanza del agua frente a escenarios de menor disponibilidad de recursos hídricos, no solo gestionando de forma adecuada y sostenible los existentes, sino también evaluar y fomentar la incorporación de recursos no convencionales, como el agua desalinizada, para aumentar y garantizar el acceso al agua en zonas áridas y semiáridas, de acuerdo con las estrategias, planes y programas desarrollados por el gobierno para el cumplimiento de los objetivos de la planificación hidrológica.

5.1. Cambios de usos del suelo, transformación agrícola y gestión del agua

Los cambios de uso del suelo es uno de los principales factores que más afecta negativamente al funcionamiento de los sistemas naturales y, por tanto, monitorizar los cambios e identificar las condiciones que determinan la vulnerabilidad de los ecosistemas frente a esos cambios juega un papel decisivo en la toma de decisiones y la aplicación de medidas en la planificación hidrológica. Los usos que mayor transformación ha sufrido a lo largo de los últimos años, es para el sector agrícola. De hecho, el estudio de la evolución de la demanda hídrica agraria a lo largo del tiempo es uno de los aspectos más significativos dentro del cómputo global de presiones sobre el agua y uno de los más costosos de hacer el seguimiento, ya que plantear una toma de datos en campo a gran escala resulta en muchas ocasiones, inviable. Es por ello que, a través de una metodología basada en datos obtenidos de sensores remotos, permite recolectar la información necesaria para analizar la evolución de las superficies y evaluar y cuantificar los cambios que se han producido.

Con el objetivo de analizar los cambios producidos en el uso del suelo y su relación con las actividades agrícolas y el riego a partir de datos obtenidos de sensores remotos, se utilizó un área de estudio localizada en una región semiárida de la península en la que la transformación agrícola en los últimos años ha supuesto que en la actualidad sea una de las principales actividades económicas.

En primer lugar, en la publicación ***"Water management in irrigation systems by using satellite information"*** se realizó el análisis de la localización de las balsas de riego en el Campo de Cartagena. Este análisis persigue demostrar la validez del uso de la fotografía aérea, que es la técnica pionera en teledetección, para determinar el cambio de usos del suelo y, sobre todo, en este caso determinar el cambio en la agricultura entre dos periodos de tiempo y el incremento en sistemas de regadío debido,

entre otros factores, a la llegada de aguas procedentes del Trasvase Tajo-Segura a la zona analizada.

A partir de la comparación de la información de las fotografías aéreas del vuelo interministerial de 1973-1986 y de las ortofotografías del PNOA de 2016, se determinó el número de balsas reguladoras de riego presentes en la cuenca del Mar Menor en cada uno de los periodos. El resultado más significativo fue el incremento de la densidad de la nube de puntos hacia el noreste de la cuenca, cerca de la costa en la que, además, coincide con una mayor presencia de cultivos en invernaderos. Desde el periodo de 1973-1986 a 2016 se ha estimado un incremento en el número de balsas 4 veces superior.

Con la información obtenida, y según los resultados derivados de la digitalización de los embalses, se muestra que la superficie de la lámina de agua expuesta a la atmósfera se ha incrementado casi 14 veces en 2016, al igual que la evaporación, con una diferencia de 15.62 hm^3/año entre ambos periodos.

Teniendo en cuenta el volumen de recursos y presiones que ejerce el sector agrario, se desarrollan de manera continua actuaciones encaminadas fundamentalmente a reducir las presiones por extracción, la modernización de regadíos e infraestructuras como depósitos o embalses, o el control y reducción de las fuentes de contaminación a masas de agua superficiales y subterráneas.

5.2. Índices de vegetación derivados de la teledetección para el estudio de zonas húmedas

Otro de los pilares en la gestión del agua es la protección de los ecosistemas acuáticos asociados, que juegan un papel imprescindible no solo para el mantenimiento de la biodiversidad, sino también como función integradora y reguladora en la protección de los recursos hídricos. Por ello, la caracterización, el estudio de los valores ecológicos, análisis hidrogeológico o la estimación de las necesidades hídricas son fundamentales para realizar un seguimiento y control del estado actual.

El uso de índices derivados de la teledetección puede ayudar en el estudio y estimación de los recursos hídricos disponibles, incluso, ayudar a predicción de futuros escenarios de variaciones climáticas que puedan afectar de manera negativa (82). Los índices de vegetación han sido ampliamente utilizados por su relación entre la respuesta espectral de la vegetación según diferentes propiedades biofísicas, con la disponibilidad de agua (83).

En el caso de este artículo, ***"A review of Landsat TM/ETM based vegetation indices as applied to wetland ecosystems"*** se realizó una revisión general de los principales índices utilizados para el estudio de la vegetación y zonas húmedas.

Para todos ellos, aplicado a un ejemplo concreto ecosistema acuático de una zona semiárida, se obtuvo el valor de la pendiente y el coeficiente de correlación para cada par de índices evaluados dentro de cada grupo.

Para los índices de estimación de la biomasa, se encontró una relación directa (con valores de pendiente positivos) y una gran correlación entre ellos con valores de r^2 por encima de 0.9. Sin embargo, en el caso de los índices del contenido de humedad, se encontró relaciones directas e inversas dependiendo del par de índices comparado, y además no muestran en general una buena correlación entre ellos.

Gracias a la resolución espacial y temporal de las imágenes de satélite y a los productos derivados, como los índices de vegetación y el NDVI, se pueden realizar análisis detallados para incorporar los resultados obtenidos a la planificación hidrológica. Un ejemplo de ello son los proyectos de la Confederación Hidrográfica del Júcar en colaboración con la Universidad de Castilla La Mancha, en los que se realiza la identificación de cultivos mediante el cálculo del NDVI utilizando imágenes de satélite, se estudia la evolución de las superficies de regadío (84) o el desarrollo de una plataforma de información para facilitar la planificación de los recursos hídricos para el riego en el ámbito del acuífero de la Mancha Oriental.

5.3. Teledetección en la evaluación de la disponibilidad de recursos hídricos bajo la perspectiva del cambio climático

Las imágenes obtenidas por teledetección han demostrado ser de gran utilidad en la detección y monitorización de las prácticas agrícolas y los sistemas de riego. Las nuevas reformas legislativas y propuestas específicas para la planificación hidrológica inciden sobre la construcción de un nuevo modelo de gobernanza del agua en un nuevo contexto de cambio climático, en el que se requiere un planteamiento de políticas de agua integradas, flexibles y adaptadas capaces de hacer frente a los posibles impactos sobre nuestras actividades socioeconómicas y el mantenimiento de los ecosistemas naturales.

Como parte del conjunto de principios básicos que plantea el Libro Verde de la Gobernanza del Agua en España para la gestión del agua, se identifican como elementos esenciales la obtención de datos e información, monitoreo y evaluación de los recursos hídricos para mejorar la capacidad de respuesta y optimización de los procesos.

Por ello, como parte de los objetivos de esta tesis, se plantea, a través de la combinación y correlación espacial de variables de teledetección y medidas directas, desarrollar modelos empíricos de aplicación en la planificación hidrológica.

Para analizar el comportamiento, patrones y distribución de las variables de teledetección seleccionadas y de los datos hidrológicos, se utilizaron en la ***"Assessing water availability in Mediterranean regions affected by water conflicts through MODIS data time series analysis"***, las imágenes de la media y desviación estándar de las series temporales de: NDVI (Índice de Vegetación de Diferencia Normalizado), LST (Temperatura de la Superficie Terrestre), precipitación y almacenamiento de agua en los dos embalses de la zona de estudio. En los resultados se observa que, a pesar de ser una superficie relativamente pequeña (unos 440 km^2), existe una gran variabilidad espacial de la precipitación muy influenciada por la altitud, al igual que en las imágenes de LST. En las áreas más bajas y cercanas a la costa, la precipitación es menor y los valores de LST mayores. Los valores más altos de precipitación se dan en las zonas divisorias más elevadas de ambas cuencas. Sin embargo, los mayores valores de NDVI no aparecen asociados a la precipitación sino a la presencia de zonas de cultivo permanente y de vegetación natural mediterránea. Del análisis de la correlación entre las series temporales de las diferentes variables se observan comportamientos similares en ambas cuencas. Se encontró una correlación significativa positiva entre el NDVI y los valores de reserva de agua de ambos embalses. Sin embargo, aunque se observó una relación negativa entre LST-NDVI y LST-almacenamiento de agua, no se encontró una correlación significativa entre esas combinaciones.

Para evaluar la capacidad de predicción de escenarios de precipitación futuros utilizando variables de teledetección, se relacionó los valores medios de NDVI y LST con la diferencia en la precipitación actual y las cuatro trayectorias de concentración y parámetros topográficos. Las variables significativas para los modelos de predicción obtenidos fueron principalmente LST con una relación inversa y la altitud, con un r^2 superior a 0.7 en todos los casos.

5.4. Incorporación de la teledetección a los modelos de gestión y planificación del agua

Con el objetivo de modelizar y estimar de forma sencilla la capacidad de almacenamiento de agua en embalses para su incorporación en sistemas de control y gestión basado en las imágenes de satélite obtenidas periódicamente, en el artículo ***"Using Landsat images to determine water storing capacity in Mediterranean environments",*** se desarrollaron modelos de regresión a partir de la clasificación supervisada de imágenes Landsat y datos oficiales de reserva de agua de los anuarios de aforo en 5 embalses (La Serena, Cubillas, La Pedrera, Beniarrés y Negratín).

En la fase de entrenamiento para el desarrollo de los modelos de regresión, se utilizaron los datos oficiales de volumen de agua y los valores de superficie de agua calculados con las series temporales de las imágenes de Landsat 7. Posteriormente, en la validación de los modelos, se utilizaron las imágenes de Landsat 8 y se compararon con los datos oficiales para las mismas fechas.

Para aumentar el conocimiento sobre el desempeño de los modelos de regresión, se calcularon el coeficiente de correlación de Pearson junto con el RMSE y RMSE normalizado (nRMSE) para determinar el ajuste de forma comparable entre los diferentes embalses (Tabla 1). Los valores de R^2 fueron en los cinco casos superiores a 0,9. Además, se obtuvieron valores adecuados para el ajuste de los modelos (valores bajos de nRMSE), ya que los resultados se encuentran entre el 24-25%, incluso del 13,4% en el caso del embalse de La Pedrera. En la validación de los modelos se obtuvieron el mismo rango de valores de RMSE que en la fase de entrenamiento. En el caso de los valores de RPD, todos estaban por encima de 2, lo que indica una buena capacidad de predicción de reserva de agua de los modelos desarrollados.

Algunas de las limitaciones que pueden surgir para la determinación de la superficie de agua son, por ejemplo, la presencia de una densa vegetación en los márgenes de los embalses, una marcada sinuosidad, o una elevada nubosidad que reduzca la disponibilidad de imágenes válidas. Además, se deben tener en cuenta en la estimación del volumen de agua de los embalses, los procesos de sedimentación y colmatación que pueden reducir considerablemente la capacidad de almacenamiento.

Sin embargo, y a pesar de la gran variabilidad estacional en el agua embalsada y de las consideraciones anteriores, los resultados de los modelos presentados en este estudio revelan la gran utilidad de las series temporales de imágenes multiespectrales en el seguimiento de los recursos hídricos.

Tabla 1. *Resultados de la validación cruzada entre la estimación del volumen de agua obtenido por teledetección y los datos oficiales de anuario de aforos de las Confederaciones Hidrográficas.*

	Training			Validation			
Reservoir	**R^2**	**RMSE**	**nRMSE**	**R^2**	**RMSE**	**nRMSE**	**RPD**
La Serena	0.967	72.352	25.0%	0.939	37.408	33.2%	3.01
La Pedrera	0.991	3.288	13.4%	0.991	3.926	12.7%	7.90
Beniarrés	0.970	0.713	24.0%	0.973	1.018	22.3%	4.49
Cubillas	0.975	0.742	21.7%	0.990	0.378	13.7%	7.32
Negratín	0.969	14.721	24.2%	0.930	11.644	35.8%	2.79

5.5. Recursos hídricos no convencionales

España es uno de los países europeos que más ha impulsado el aprovechamiento de las aguas depuradas como fuente alternativa para el abastecimiento y la agricultura, generando alrededor de 400 km^3/año, y que juega un papel fundamental para garantizar la seguridad hídrica y hacer frente a la reducción en la disponibilidad de los recursos hídricos naturales como efecto del cambio climático.

Más de la mitad del volumen de agua regenerada, tanto de agua desalada como depurada, se destina principalmente al riego agrícola, siendo uno de los sectores que más presión genera sobre el agua, sobre todo en la mitad sur de la península (85).

Con el objetivo de mejorar la gobernanza del agua, se han elaborado una serie de programas de actuaciones y estrategias entre las que se encuentra el Plan Nacional de Depuración, Saneamiento, Eficiencia, Ahorro y Reutilización (Plan DSEAR). De esta manera, el fomento de la reutilización del agua como recursos hídricos adicionales, y su incorporación en la planificación hidrológica, constituye el eje de actuación para lograr reducir el impacto sobre las masas de agua y alcanzar un desarrollo más sostenible.

Bajo esta perspectiva, en el artículo ***"Agricultural drainage water characterization to determine the desalination possibilities for irrigation in a semi-arid environment",*** se analizan la calidad de las aguas de drenaje agrícola de una zona de escasez hídrica

con el objetivo de estudiar la posibilidad de la implantación de un sistema de desalinización que contribuya a la mejora de la eficiencia y la sostenibilidad ambiental del agua.

Para el diseño de una planta de ósmosis inversa, se necesita seleccionar de forma adecuada las características operativas del sistema teniendo en cuenta los principales parámetros que afectan a una planta desalinizadora. Aquellos más relevantes y que influyen de manera significativa en el coste de tratamiento son la conductividad eléctrica y los sólidos disueltos totales. También es fundamental conocer las características del cultivo y el suelo sobre el que se desarrolla para el diseño de una planta desalinizadora.

El pH medio obtenido se encontraba entre 7,8 - 8,1. La conductividad eléctrica (CE) media oscilaba entre 3,1 y 12,8 mS/cm, y valores de sólidos disueltos totales (TDS) de 2.300 a 12.700 mg/l, cuando la concentración aceptable para el riego es de 750 mg/l. Esto supone un grado alto de salinidad del agua, que es un factor crítico para el coste energético en una planta de ósmosis inversa.

Los valores medios de sólidos en suspensión totales (TSS) estaban comprendidos entre 24-62 mg/l, excepto en el azarbe de Pineda, con una media de 104 mg/l. El valor máximo fue de 399 mg/l. Para evitar la rápida saturación de las membranas de ósmosis inversa, incrustaciones o el crecimiento de microorganismos es necesario incluir un pretratamiento que acondicione las características fisicoquímicas del agua de alimentación.

Para alimentar una planta de ósmosis inversa de menor tamaño, se debe proporcionar al menos un caudal constante de entre 0,5 y 1 m^3/s. En este caso, los valores de caudal presentaban una gran variación para cada azarbe con una media por debajo de 1 m^3/s, pero con valores comprendidos entre 0,001 y 4,18 m^3/s. Los cambios en el caudal debidos a la estacionalidad pueden variar la cantidad de sales disueltas y afectar al proceso de desalinización.

Los SIG pueden desempeñar un papel eficaz en el tratamiento de la información obtenida a través tanto de datos espaciales, como medidos en campo para la resolución de problemas en la gestión del agua. De esta forma, se crea una base de datos completa e integrada en la que se tienen en cuenta multitud de criterios que permite crear y dar soporte a un sistema de toma de decisiones basadas en información actualizada. Asimismo, ayudan a simular posibles escenarios y en la evaluación de la implementación de los diferentes planes, incluso sistemas de preferencia basados en la legislación o en juicios de valor (86) de acuerdo con los resultados que se van obteniendo en la incorporación y actualización de nueva información.

6. Conclusiones generales

La planificación es la principal herramienta para la gestión integrada y sostenible de los recursos hídricos y la mejor estrategia en la mitigación de los efectos del cambio climático. Con esta tesis se pretende aportar información sobre el potencial de la teledetección para mejorar y ampliar el conocimiento del estado de los recursos e integrar información de detección remota en los modelos de planificación y climáticos a través de los SIG.

En la última década, se han estado realizando proyectos de teledetección, analizando las imágenes obtenidas por los sensores remotos que han contribuido enormemente a tener una visión más completa y global del estado hidrológico de las cuencas. Estas imágenes tienen la ventaja de que aportan información de una forma continua en el tiempo, con una cobertura a escala mundial y disponibles gratuitamente. Con lo que es posible extraer multitud de información adicional a partir de las series temporales de imágenes y análisis estadísticos.

Aunque los problemas relacionados con la precisión y la incertidumbre en los datos de detección remota sigan siendo un reto, a medida que ha crecido la demanda de datos continuos se ha demostrado con numerosos estudios que la correlación entre las variables calculadas mediante teledetección y los datos obtenidos en campo es significativa, por lo que la integración de esta información es un avance importante en la monitorización a largo plazo de los recursos. Uno de los pilares más importantes para garantizar una asignación de recursos eficiente, es conocer el estado de las masas de agua y la determinación del consumo en los diferentes sectores, principalmente para la planificación y el suministro en escenarios futuros en los que se espera una disminución en las precipitaciones. Debido a que la agricultura es uno de los sectores que más puede verse perjudicada, en los últimos años, se ha venido desarrollando metodologías basadas en teledetección cada vez más precisas para la detección de zonas de regadío, del agua consumida o para la estimación de la evapotranspiración. De hecho, los índices de vegetación obtenidos a partir de series temporales de imágenes espectrales son ya una herramienta básica en los estudios para la gestión del agua en agricultura y ecosistemas naturales.

La tendencia actual en los estudios de investigación se está centrando en la determinación de las necesidades hídricas específicas para cada cultivo, de forma que pueda ajustarse la cantidad de agua de forma precisa a los requerimientos reales en cada momento.

La obtención de información de manera continua, la reducción de costes y la operabilidad de las técnicas utilizadas son algunos de los factores que deben tenerse en cuenta en la gestión del agua. Además, conocer el estado de los embalses y analizarla evolución del nivel de agua es un aspecto determinante en la gobernanza del agua, teniendo en cuenta que el déficit de precipitaciones año tras año contribuye a la disminución de la reserva total, principalmente en situaciones de sequía. Asimismo, la colmatación o aterramiento de los embalses también juega un papel importante no solo en la capacidad de almacenamiento, sino también en la calidad del agua y en la seguridad de la presa. Esta situación, si bien no sucede en todos los embalses, y en las construcciones más modernas ya se tiene en cuenta y existen mecanismos para el desagüe de sedimentos, se puede agravar en aquellos con más de 50 años, aunque depende de multitud de factores. Por lo tanto, las perspectivas de futuro van encaminadas en mejorar la capacidad de almacenamiento de aquellas construcciones menos recientes, conocer la tasa de erosión del vaso del embalse y el volumen de sedimentos que se depositan en el fondo.

Una de las medidas que se han adoptado para incrementar la cantidad de recursos hídricos disponibles, es la incorporación de recursos no convencionales como desalinización y reutilización, mayoritariamente para el riego agrícola. Estas medidas predominan en las cuencas hidrográficas como potencial solución a la garantía de suministro en periodos de mayor escasez para reducir la presión de recursos convencionales.

Por todo ello, se enumeran a continuación las conclusiones más relevantes según los resultados obtenidos en esta tesis:

1. En la publicación ***"Assessing water availability in mediterranean regions affected by water conflicts through MODIS data time series analysis"***, se ha observado una elevada correspondencia temporal entre la cantidad de agua de los embalses y las series temporales de las imágenes multiespectrales de NDVI y LST. De hecho, la mejor correlación con el almacenamiento de los dos embalses coincide con las zonas donde se esperan las disminuciones más significativas en la precipitación según los modelos de cambio climático. Estos resultados evidencian la capacidad de los datos obtenidos por teledetección para evaluar diferentes prácticas de gestión del agua.

2. En el caso de la publicación ***"Water management in irrigation systems by using satellite information",*** se observaron pérdidas significativas por evaporación de agua de las balsas de riego, unos 16,82 hm^3/año para las imágenes de PNOA 2016-2017, un dato especialmente relevante en zonas con una elevada insolación y problemas de escasez hídrica.

3. Los resultados obtenidos en el artículo ***"A review of Landsat TM/ETM based vegetation índices as applied to wetland ecosystems",*** muestran que otros índices, como el SAVI, pueden ser una alternativa al tradicional NDVI, ya que corrige la influencia y distorsiones que ejerce el suelo sobre los valores obtenidos del análisis de manera que, resulta mucho más conveniente en aquellas zonas en las que existe una baja densidad vegetal y mayor exposición de suelo, como pueden ser las áreas cultivadas.

4. El artículo ***"Using Landsat images to determine water storing capacity in mediterranean environments"***, muestra la posibilidad de incorporar el uso de sensores remotos a los sistemas de gestión como herramienta auxiliar para el control de embalses de una manera menos costosa. Este tipo de metodología sistemática se puede automatizar fácilmente e integrarla en los modelos de planificación hidrológica con la finalidad de establecer estrategias más precisas para el abastecimiento de agua.

5. Con la publicación ***"Agricultural drainage water characterization to determine the desalination possibilities for irrigation in a semi-arid environment"***, se muestra que la caracterización de los parámetros fisicoquímicos de las aguas de los drenajes agrícolas es un factor imprescindible para optimizar el proceso y diseñar una planta de desalinización, teniendo en cuenta que se debe conocer tanto la demanda real como los gastos que conllevaría el tratamiento para la regeneración del agua y cualesquier otra inversión necesaria.

Algunos de los objetivos básicos en la planificación hidrológica para asegurar la calidad y cantidad del agua es monitorizar, controlar y reducir el consumo de los recursos hídricos. Integrando toda la fuente de datos e información que ofrece la teledetección en un SIG se consigue un mayor conocimiento del estado de las masas de agua y de los ecosistemas asociados, más allá de las delimitaciones geográficas, posicionamiento de fuentes de contaminación o cálculo de superficie regada. La utilización de métodos indirectos, como la teledetección, consigue que, a partir de imágenes multiespectrales, datos meteorológicos y pequeños muestreos *in situ*, sea una alternativa viable para mantener en el tiempo de forma rápida y económica.

Por lo tanto, una tarea pendiente es potenciar y poner en marcha todo el conocimiento adquirido en los últimos años para incorporarlo de manera real a las estrategias y gobernanza del agua.

7. Referencias

1. Ministerio para la Transición y el Reto Demográfico. Libro Verde de la gobernanza del agua en España. 2020, 172.

2. Hassing, J.; Ipsen, N.; Clausen, T.J. Integrated Water Resources Management (IWRM) in Action. *United Nations World Water Assess. Program.* 2009, 1–18.

3. ONU Medio Ambiente. Progreso sobre gestión integrada de recursos hídricos. Referencia global para el indicador ODS 6 6.5.1: Grado de aplicación de la ordenación integrada de los recursos hídricos. *Sustain. Sanit. water Manag.* 2010.

4. Ministerio de Agricultura Alimentación y Medio ambiente. Sistema Español de Gobernanza del Agua. 2005.

5. United Nations. Managing Drought and Water Scarcity for Nature-Positive Food Production Impacts of Drought. United Nations Convention to Combat Desertification (UNCCD); 2021.

6. Olmos, P., García-Galiano, S., Martínez-Pérez, J. A. Mejora en la calibración de un modelo hidrológico distribuido en base a teledetección. In *Nuevas plataformas y sensores aplicados a la gestión del agua, la agricultura y el medio ambiente.*; Ángel Ruíz, L., Estornell, J., Erena, M.; Ed.; XVII Congreso de la Asociación Española de Teledetección. Universidad Politécnica de València, 2017; pp. 109–112. ISBN 9788490486504.

7. Ministerio para la Transición y el Reto Demográfico. Plan Nacional de Adaptación Al Cambio Climático 2021-2030; Madrid, Spain, 2020; ISBN 9788418508325.

8. Confederación Hidrográfica del Segura. Plan Hidrológico de la Demarcación del Segura 2015/21. Anejo 3 Usos y Demandas de Agua; 2015.

9. Confederación Hidrográfica del Júcar. Plan Hidrológico de La Demarcación Hidrográfica Del Júcar. Anejo 3 Usos y Demandas de Agua. Ciclo de Planificación Hidrológica 2015-2021. 2015.

10. Instituto Nacional de Estadística (INE). Encuesta sobre el suministro y Saneamiento del agua en España. Disponible en: http://www.ine.es/jaxi/menu.do?type=pcaxis&path=/t26/p067/p01&file=inebase.

11. Instituto Nacional de Estadística (INE). Encuesta sobre el uso del agua en el sector agrario (EUASA) Año 2018; 2020. Disponible en: https://www.ine.es/prensa/euasa_2018.pdf

12. Ministerio para la Transición y el Reto Demográfico Plan Nacional de Depuración, Saneamiento, Eficiencia, Ahorro y Reutilización. Plan DSEAR; 2021.

13. Ministerio para la Transición Ecológica y el Reto Demográfico. El MITECO Destaca El Papel de La Reutilización y La Desalación Del Agua Para Hacer Frente a Los Desafíos Del Cambio Climático En Materia de Seguridad Hídrica; 2021. Disponible en: https://www.miteco.gob.es/es/prensa/ultimas-noticias/el-miteco-destaca-el-papel-de-la-reutilización-y-la-desalación-del-agua-para-hacer-frente-a-los-desafíos-del-cambio-climático-en-materia-de-segu/tcm:30-533895

14. Asociación Española de desalación y reutilización. Cifras de desalación en España. 2019. Disponible en: https://aedyr.com/cifras-desalacion-espana/

15. ESYRCE. Encuesta sobre superficies y rendimientos de cultivos. 2020. Disponible en: https://www.mapa.gob.es/es/estadistica/temas/estadisticas-agrarias/boletin2020_tcm30-564330.pdf

16. SEPREM. Inventario de presas. Disponible en: http://www.seprem.es/presases.php

17. Pérez, E.P. V. Disposiciones decimononicas sobre aguas. Ley de 1879. Disponible en: https://www.mapa.gob.es/ministerio/pags/Biblioteca/fondo/pdf/9999_7.pdf

18. Ley 29/1985, de 2 de agosto, de Aguas.

19. Ley 46/1999, de 13 de diciembre, de modificación de la Ley 29/1985, de 2 de agosto, de Aguas.

20. Real Decreto Legislativo 1/2001, de 20 de julio, por el que se aprueba el texto refundido de la Ley de Aguas.

21. Real Decreto 907/2007, de 6 de julio, por el que se aprueba el Reglamento de la Planificación Hidrológica.

22. Real Decreto 1159/2021, de 28 de diciembre, por el que se modifica el Real Decreto 907/2007, de 6 de julio, por el que se aprueba el Reglamento de la Planificación Hidrológica.

23. Real Decreto 1664/1998, de 24 de julio, por el que se aprueban los Planes Hidrológicos de cuenca.

24. Ministerio de Agricultura, Alimentación y Medio ambiente. Libro Blanco del Agua en España; 1998, 40.

25. Directiva 2000/60/CE del Parlamento Europeo y del Consejo, de 23 de octubre de 2000, por la que se establece un marco comunitario de actuación en el ámbito de la política de aguas.

26. Ley 10/2001, de 5 de julio, del Plan Hidrológico Nacional.

27. Ministerio para la Transición Ecológica y el Reto Demográfico. Informe de Seguimiento de Planes Hidrológicos y Recursos Hídricos En España. Año 2020. Disponible en: https://www.miteco.gob.es/es/agua/temas/planificacion-hidrologica/memoria_infoseg_2020_tcm30-531935.pdf

28. Calvario Sanchez, G.; Dalmau, O.; Alarcon, T.E.; Sierra, B.; Hernandez, C. Selection and Fusion of Spectral Indices to Improve Water Body Discrimination. *IEEE Access* 2018, 6, 72952–72961, doi:10.1109/ACCESS.2018.2881430.

29. Ley 27/2006, de 18 de julio, por la que se regulan los derechos de acceso a la información, de participación pública y de acceso a la justicia en materia de medio ambiente (incorpora las Directivas 2003/4/CE y 2003/35/CE).

30. Ley 7/2021, de 20 de mayo, de cambio climático y transición energética.

31. Jensen, J.R. Remote Sensing of the Environment. An Earth Resource Perspective; Howard, J.&, Kaveney, D., Eds.; Second Edi.; Pearson Education, Inc., 2007; ISBN 0-13-188950-8.

32. Chuvieco, E. Fundamentals of Satellite Remote Sensing. An Environmental Approach; Edition, T., Ed.; CRC Press, 2020; ISBN 9780429506482. https://doi.org/10.1201/9780429506482

33. Reddy, M.A. Textbook of Remote Sensing and Geographical Information Systems.; Third Edit.; BS Publications, 2008; ISBN 978-81-7800-135-7.

34. Jensen, J.R. Introductory Digital Image Processing a Remote Sensing Perspective; Hall, U.S.R.& N.J.P., Ed.; Third Edit.; 2005; ISBN 0131453610.

35. European Commission. Updated Guidance on Implementing the Geographical Information System (GIS) Elements of the EU Water Policy., 2009.

36. CSIC. Plataforma temática interdisciplinar. TELEDETECT. Disponible en: https://pti-teledetect.csic.es/teledetect-pti/

37. Universidad de Salamanca. Investigación en recursos hídricos. Disponible en: https://www.usal.es/investigacion-en-recursos-hidricos-hidrus

38. United Nations Economic Commission for Europe (UNECE). Working Group on integrated water resources management. Disponible en: https://unece.org/environment-policy/water/about-the-convention/convention-bodies/working-group-integrated-water-resources-management

39. Water Europe. Water Europe Working Groups. Disponible en: https://watereurope.eu/working-groups/

40. European Environment Agency. WISE Freshwater. Freshwater Information System for Europe. Disponible en: https://water.europa.eu/freshwater

41. Ma, L.; Liu, Y.; Zhang, X.; Ye, Y.; Yin G.; Johnson, BA. Deep learning in remote sensing applications: A meta-analysis and review. *ISPRS J Photogramm Remote Sens*. 2019, *152*, 166–77. Disponible en: https://linkinghub.elsevier.com/retrieve/pii/S0924271619301108

42. Li, J.; Huang, X.; Gong, J. Deep Neural Network for Remote-Sensing Image Interpretation: Status and Perspectives. *Natl. Sci. Rev.* 2019, 6, 1082–1086, doi:10.1093/nsr/nwz058.

43. Francés, F., Ruiz-Pérez, G. ¿Es posible calibrar un modelo eco-hidrológico en una cuenca no aforada utilizando exclusivamente el NDVI de satélite? In *Nuevas plataformas y sensores aplicados a la gestión del agua, la agricultura y el medio ambiente.*; Ángel Ruíz, L., Estornell, J., Erena, M.; Ed.; XVII Congreso de la Asociación Española de Teledetección. Universidad Politécnica de València, 2017; pp. 55–58 ISBN 9788490486504.

44. Chen, L.; Wang, L. Recent Advance in Earth Observation Big Data for Hydrology. Big Earth Data 2018, 2, 86–107, doi:10.1080/20964471.2018.1435072.

45. Shao, Z.; Fu, H.; Li, D.; Altan, O.; Cheng, T. Remote Sensing Monitoring of Multi-Scale Watersheds Impermeability for Urban Hydrological Evaluation. Remote Sens. Environ. 2019, 232, 111338, doi:10.1016/j.rse.2019.111338.

46. Seth, I. GIS: A Useful Tool in Urban Water Management. In Geospatial Tools for Urban Water Resources; Springer Netherlands: Dordrecht, 2013; pp. 1–9.

47. Sánchez, B., González-Dugo, M. P., Mateos, L., Cifuentes, V. J., Escudero, R. Estimación de la superficie de los cultivos y la evapotranspiración de los regadíos de la cuenca del Guadalquivir por teledetección. In *Nuevas plataformas y sensores aplicados a la gestión del agua, la agricultura y el medio ambiente.*; Ángel Ruíz, L., Estornell, J., Erena, M.; Ed.; XVII Congreso de la Asociación Española de Teledetección. Universidad Politécnica de València, 2017; pp. 97–100 ISBN 9788490486504.

48. Martin-Vega, D., Pulido, J., Upegui, E. S. Análisis multitemporal de la pérdida de la capacidad hídrica a causa de los cambios generados en los suelos usando imágenes Landsat: Estudio de caso Córdoba-Colombia entre los sños 1985 y 2016. In *Nuevas plataformas y sensores aplicados a la gestión del agua, la agricultura y el medio ambiente.*; Ángel Ruíz, L., Estornell, J., Erena, M.; Ed.; XVII Congreso de la Asociación Española de Teledetección. Universidad Politécnica de València, 2017; pp. 105–108 ISBN 9788490486504.

49. Pavri, F.; Springsteen, A.; Dailey, A.; MacRae, J.D. Land Use and Socioeconomic Influences on a Vulnerable Freshwater Resource in Northern New England, United States. *Environ. Dev. Sustain.* 2013, 15, 625–643, doi:10.1007/s10668-012-9397-x.

50. Confederación Hidrográfica del Segura. Índice de estudios. Disponible en: https://www.chsegura.es/es/cuenca/planificacion/indice-estudios/

51. Confederación Hidrográfica del Júcar. Perfil de contratante. Cuadro-resumen anual. 2021. Disponible en: https://www.chj.es/es-es/ciudadano/perfildelcontratante/Paginas/Cuadroresumenanual.aspx

52. Directiva 2007/2/CE del Parlamento Europeo y del Consejo, de 14 de marzo de 2007, por la que se establece una infraestructura de información espacial en la Comunidad Europea (Inspire).

53. Ley 14/2010, de 5 de julio, sobre las infraestructuras y los servicios de información geográfica en España.

54. CHSIC. Visor cartográfico de la Confederación Hidrográfica del Segura. Disponible en: https://www.chsegura.es/portalchsic/apps/webappviewer/index.html?id=db44c41d2c7448409e9c4bab590e3828&codif=&nombre=Publico

55. SIA Júcar. Sistema de información del agua de la Confederación Hidrográfica del Júcar. Disponible en: https://aps.chj.es/siajucar/

56. IDE/Geoportal. Geoportal de la Confederación Hidrográfica del Guadalquivir. Disponible en: https://idechg.chguadalquivir.es/nodo/Visualiza/map.html

57. GeoGuadiana. Visor geográfico de la Confederación Hidrográfica del Guadiana. Disponible en: https://www.chguadiana.es/visorCHG/

58. Confederación Hidrográfica del Segura. Proyecto de Plan Hidrológico de la Demarcación Hidrográfica del Segura. Anejo X Programa de Medidas. 2022. Disponible en: https://www.chsegura.es/export/sites/chs/descargas/planificacionydma/planificacion21-27/docsdescarga/docplan2227Consolidado/A10_programa_medidas/Anejo_10_Programa_medidas.pdf

59. Confederación Hidrográfica del Júcar. Plan Hidrológico de la Demarcación Hidrográfica del Júcar. Anejo X Programa de Medidas. 2022. Disponible en: https://www.chj.es/es-es/medioambiente/planificacionhidrologica/Documents/Plan-Hidrologico-cuenca-2021-2027/PHC/Documentos/PHJ2227_Anejo10_PdM_20220329.pdf

60. Ministerio para la Transición y el Reto Demográfico. Plan PIMA Adapta AGUA. Disponible en: https://www.miteco.gob.es/es/agua/planes-y-estrategias/plan-pima-adapta-agua.aspx

61. Gutiérrez-Cánovas, C.; Arias-Real, R.; Bruno, D.; Cabrerizo, M.J.; González-Olalla, J.M.; Picazo, F.; Romero, F.; Sánchez-Fernández, D.; Pallarés, S. Multiple-Stressors Effects on Iberian Freshwaters: A Review of Current Knowledge and Future Research Priorities. *Limnetica* 2022, *41*, 1, doi:10.23818/limn.41.15.

62. Cau, P.; Manca, S.; Soru, C.; Muroni, D.; Gorgan, D.; Bacu, V.; Lehman, A.; Ray, N. An Interoperable, GIS-Oriented, Information and Support System for Water Resources Management. *Int. J. Adv. Comput. Sci. Appl.* 2013, *3*, doi:10.14569/SpecialIssue.2013.030309.

63. Ley 7/2021, de 20 de mayo, de cambio climático y transición energética.

64. Reglamento (UE) no 1089/2010 de la Comisión, de 23 de noviembre de 2010, por el que se aplica la Directiva 2007/2/CE del Parlamento Europeo y del Consejo en lo que se refiere a la interoperabilidad de los conjuntos y los servicios de datos espaciales.

65. The European Space Agency. About SPOT Series. Disponible en: https://earth.esa.int/eogateway/missions/spot

66. The European Space Agency. Sentinel Missions. Disponible en: https://sentinels.copernicus.eu/web/sentinel/missions

67. NASA. Missions: Earth Observing System (EOS). Disponible en: https://eospso.nasa.gov/mission-category/3

68. Jaiswal, R.K.; Bhatawdekar, S. Indian Earth Observation Program. In *Comprehensive Remote Sensing*. Elsevier; 2018. p. 280–98. Disponible en: https://linkinghub.elsevier.com/retrieve/pii/B9780124095489103215

69. Marco Dos Santos, G., Navarro-Pedreño, J., Meléndez-Pastor, I., Gómez Lucas, I. Research Trends in Water Management by Using Environmental Parameters Derived from Remote Sensing. J. Biosens. Renew. sources 2019, 1.

70. Alonso Sarría, F., Gomariz Castillo, F., Cánovas García, F. *Revista C. & G.* 2010, pp. 73–88.

71. Melendez-Pastor, I.; Navarro-Pedreño, J.; Koch, M.; Gómez, I.; Hernández, E.I. Land-Cover Phenologies and Their Relation to Climatic Variables in an Anthropogenically Impacted Mediterranean Coastal Area. *Remote Sens.* 2010, doi:10.3390/rs2030697.

72. West, H.; Quinn, N.; Horswell, M. Remote Sensing for Drought Monitoring & Impact Assessment: Progress, Past Challenges and Future Opportunities. *Remote Sens. Environ.* 2019, 232, 111291, doi:10.1016/j.rse.2019.111291.

73. Xue, J.; Su, B. Significant Remote Sensing Vegetation Indices: A Review of Developments and Applications. *J. Sensors* 2017, 2017, 1–17, doi:10.1155/2017/1353691.

74. Anselin, L.; Syabri, I.; Kho, Y. GeoDa: An Introduction to Spatial Data Analysis. Geogr Anal. 2006, 38 (*1*), 5–22.
Disponible en: https://onlinelibrary.wiley.com/doi/10.1111/j.0016-7363.2005.00671.x

75. Salinero, E.C. Teledetección Ambiental. La Observación de La Tierra Desde El Espacio.; Ariel Ciencia, 2002; ISBN 84-344-8047-6.

76. World Climate Research Programme. WorldClim. Future climate data. Disponible en: https://www.worldclim.org/data/cmip6/cmip6climate.html

77. Meneses. OA de CJ. PR. Spectral Correlation Mapper (SCM): An improvement on the Spectral Angle Mapper (SAM). 2000. Disponible en: https://popo.jpl.nasa.gov/pub/docs/workshops/00_docs/Osmar_1_carvalho__web.pdf

78. World Food Programme. Zero Hunger Strategic Reviews. Disponible en: https://www.wfp.org/zero-hunger-strategic-reviews

79. Zarzo, D.; Campos, E.; Terrero, P. Spanish Experience in Desalination for Agriculture. *Desalin. Water Treat.* 2013, *51*, 53–66, doi:10.1080/19443994.2012.708155.

80. Grundmann. AEHSJ. Flow velocity and discharge measurement in rivers using terrestrial and UAV imagery. *Hydrol Earth Syst Sci.* 2020, 24*(3)*, 1429–45.

81. Abed BS. Flow Measurements in Open Channels Using Integrating-Floats. J Eng [Internet]. 2021 Jan 1;27(1):130–41. Available from: https://joe.uobaghdad.edu.iq/index.php/main/article/view/j.eng.2021.01.09

82. Wang, Y. The Influence of Realistic Vegetation Phenology on Regional Climatemodeling. In Remote sensing of protected lands; CRC Press. Taylor & Francis Group, 2012. ISBN 9781439841884.

83. Ruíz-Verdú, A.; Delegido, J.; Verrelst, J.; Tenjo, C.; Pasqualotto, N.; Moreno, J. Objetivos y primeros resultados del proyecto SENSAGRI (Sentinels Synergy for Agriculture). In *Nuevas plataformas y sensores aplicados a la gestión del agua, la agricultura y el medio ambiente.* Ángel Ruíz, L., Estornell, J., Erena, M.; Ed.; XVII Congreso de la Asociación Española de Teledetección. Universidad Politécnica de València, 2017, 59–62. ISBN 9788490486504.

84. Calera A., Sánchez Pérez, D., Belmonte Mancebo, M., Arellano Alcázar, I. Teledetección para identificación de las superficies en Regadío TSUR. Convenio Confederación Hidrográfica del Júcar y Universidad de Castilla-La Mancha. 2020.

85. Morote Seguido, Á.F. La Desalinización. De Recurso Cuestionado a Recurso Necesario y Estratégico Durante Situaciones de Sequía Para Los Abastecimientos En la Demarcación Hidrográfica del Segura. *Investig. Geográficas* 2018, 47, doi:10.14198/INGEO2018.70.03.

86. Malczewski, J. GIS-based Multicriteria Decision Analysis: A Survey of the Literature. *Int. J. Geogr. Inf. Sci.* 2006, 20, 703–726, doi:10.1080/13658810600661508.

Ortofoto PNOA sobre invernaderos en San Pedro del Pinatar, Murcia.
Fuente. OrtoPNOA 2016 CC-BY 4.0

Marco Dos Santos, G. Meléndez-Pastor, I., Navarro-Pedreño, J., Gómez Lucas, I. (2018).

Water management in irrigation systems by using satellite information.

Satellite Information Classification and Interpretation.
IntechOpen. Chapter 6, 89-101.

https://doi.org/10.5772/intechopen.82368

Abstract

Changes in agriculture are associated to the availability of resources and the economic and social demands (market products). One of the most important transformation is to change rainfed crops into irrigated crops in order to increase yield. In most of the cases, water resource and irrigation reservoirs are needed to maintain the yield. However, evaporation from ponds can be an important economic loss for farmers and an unsustainable strategy for water management, especially in arid and semi-arid areas with water scarcity. Therefore, efficient methods of water storage should be established because of the availability of water is essential. In this study, a selected area located close to the city of Cartagena (Murcia) and the south of Alicante (Spain), has been studied. It is a traditional agricultural area where the transformation from rainfed to irrigated crops has been analyzed. This analysis was based on the study of the number of irrigation reservoirs and their size by using remote sensing data and GIS tools. Because of the high temperatures and insolation in the area, the increment of the number of reservoirs detected may be inefficient for water management. Therefore, the characterization of these reservoirs, to quantify the potential loss of water due to evaporation has been done by using remote sensing images. This analysis could be very interesting to find more efficient storage solutions (i.e. better spatial distribution of reservoirs, an increment of deep and reduction of surface exposure) improving the water storage and management.

Keywords

Arid environments; Evaporation; Irrigated agriculture; Spatial distribution; Water storage

1. Introduction

Water management is one of the most important problems for future decades. Although there are areas of the planet where the water availability is naturally scarce due to the rain and temperature patterns, human pressure on this resource is accentuating the problem of scarcity. As reflected in the World Water Assessment Program published by UNESCO (1), there are 3 types of pressures or “drivers” on water systems: demographic, economic and social. Population growth increases not only water consumption, also pollution, which is another way to decrease water availability. Furthermore, land occupation and urbanization affect the dynamics of the ecosystem due to soil sealing and consequently, the hydrological cycle is altered (infiltration processes, aquifer recharge, etc.). Protecting ecosystems is highly important to maintain the goods and services they offer us and it is so necessary for life. Economic growth has allowed the development of modern extraction and production techniques that aggravate water scarcity. Natural dynamics of water is affected, i.e. river flows are altered or the water table is reduced. The building of infrastructures that benefits the commerce of both products and services associated to water management have been increased. The change in the lifestyle of many countries is reflected in the amount of water consumed, principally in those in which access to drinking water is easy and immediate. In contrast, in developing countries where there is scarcity and water pollution, it is a great challenge. Therefore, there is a social inequality that must be resolved.

For example, in the case of arid and semi-arid areas (2) which the amount of available water is limited due to the shortage and irregularity of rainfall, the development of irrigated agriculture has caused an increase in pressure on water resources. This affects highly negatively the agriculture which is one of the biggest users of water with respect to the total demand of water (almost 80%) (3). In these areas where water is a limited resource, population growth exerts a great negative pressure on it. Agriculture must be able to supply the population even though the availability of water is the limiting factor for food production (4). To guarantee the continuous supply of water for irrigation, small ponds are built to store the water and manage it according to their needs (5).

These ponds are usually shallow constructions located near the crops that will supply. However, it seems that the management of these small reservoirs is based on the experience of the farmer and not on contrasted technical criteria (6). Water is a limited and essential resource for life that has to be managed efficiently, equitably and allow future generations to have access to it. Therefore, the current management model should be changed to make sustainable use of available water resources and develop strategies that promote savings and minimize losses in irrigation (7).

Evaporation is defined as a process by which liquid water turns to vapor state by heating it (energy breaks the bonds of the molecules) (8). The main factors that influence evaporation are: local climatic conditions such as air and water temperature, solar radiation, relative humidity, wind speed (9) and the geometry of the ponds, for example, evaporation is greater if the relationship between area and volume is large (10). In areas with high insolation, the evaporation from the sheet of water represents a significant loss from the environmental and also economic point of view (11). Different methods are being developed to avoid evaporation: there are chemical methods such as stearyl alcohol (12), floating modular systems that have different shapes and materials (13), floating photovoltaic panels (14), canvas or suspended coverages (15). Each method may be appropriate depending on the characteristics of the place where it will be installed (amount of water stored, area, costs, etc.) (16). Therefore, it is necessary to study tools and develop management strategies that improve the efficiency of water consumption and obtain the potential evaporation from the ponds and reservoirs.

The use of Geographic Information Systems (GIS) in the study of water resources allows us to know the dynamics of them, and therefore, models with different scenarios of water availability or demands can be developed (17). With these models, different projections can be made in order to develop management scenarios more suited to the state of resources. This technology, GIS, is very suitable due to the amount of information that can be incorporated into the models, and the possibility of viewing the information in the form of maps (18).

In developing countries, this tool can help the management of its resources with a relative low cost and the large number of free images obtained over many years from remote sensing. Moreover, in those countries in which it is not possible to collect data *in situ* because of the cost, time, or access due to legal causes or because of war conflicts. GIS combining remote sensing help to solve many problems related to resources management.

Remote sensing is being a very useful method to delimit and study water bodies, especially due to the difficulty of obtaining continuous information. Due to the contrast between the reflectance of the sheet of water and that of the earth surface (10), it is possible, through satellite images, to study and monitor the water storage (19), to observe the changes in the surface of water bodies over time, study the evolution of the irrigation reservoirs of an area (20), estimate its evaporation (important in arid and semi-arid zones) and volume.

The water absorbs the energy in wavelengths of the near and medium infrared, therefore, the reflected energy of these is low and the water bodies appear in dark color in both the multispectral images and the grayscale images (21). Moreover, satellite images facilitate the composition of RGB or False color images where water sheets can be detected and analyzed.

Facing of future scenarios of climate change (22), in which the availability and quality of water can be seriously affected (23), it is necessary to improve the use of water resources through the incorporation of new techniques and the modernization of infrastructures. This includes the application of regulations (24) that support integrated management techniques that guarantee a better resource quality and also promote citizen participation (25).

In this work, the combined use of remote sensing data and GIS tools, demonstrated with the example, the possibilities of managing and controlling water infrastructures and the evaporation of water in agriculture, one of the major consumers of water.

2. A study case: Campo de Cartagena, southeast of the Iberian Peninsula

2.1 Study area

The study area is located beside the Mar Menor in Murcia and south of Alicante (Figure 1), Spain. This basin is a sedimentary plain formed by conglomerates, marls, sandstones and clays (26) with approximately 152,000 hectares. The Mar Menor is the biggest coastal lagoon of Spain that is included in the RAMSAR convention. It is in serious danger of pollution as a result of nitrogen and phosphate contributions from agriculture that cause the loss of its water's quality, the decrease of the diversity and elimination of autochthonous species and induce the proliferation of algae blooms. The two factors that most affect this wetland are tourism (population growth) and agriculture; both generate polluting inputs that reach the Mar Menor through the different watercourses and infiltration processes. The climate is Bsh according to the Köppen classification, with low rainfalls (around 300 mm per year) of torrential type especially during the autumn. The average annual temperature is about 18ºC, with hot summer (about 32-35 ° C in august) and mild winters (the temperature usually does not drop below 5 ° C) (27).
Precisely the weather is one of the main reason why so many tourists (both Spanish and foreign) come every year to visit the Region of Murcia (more than 1 million people in 2015-2016) (28), especially near the coast.

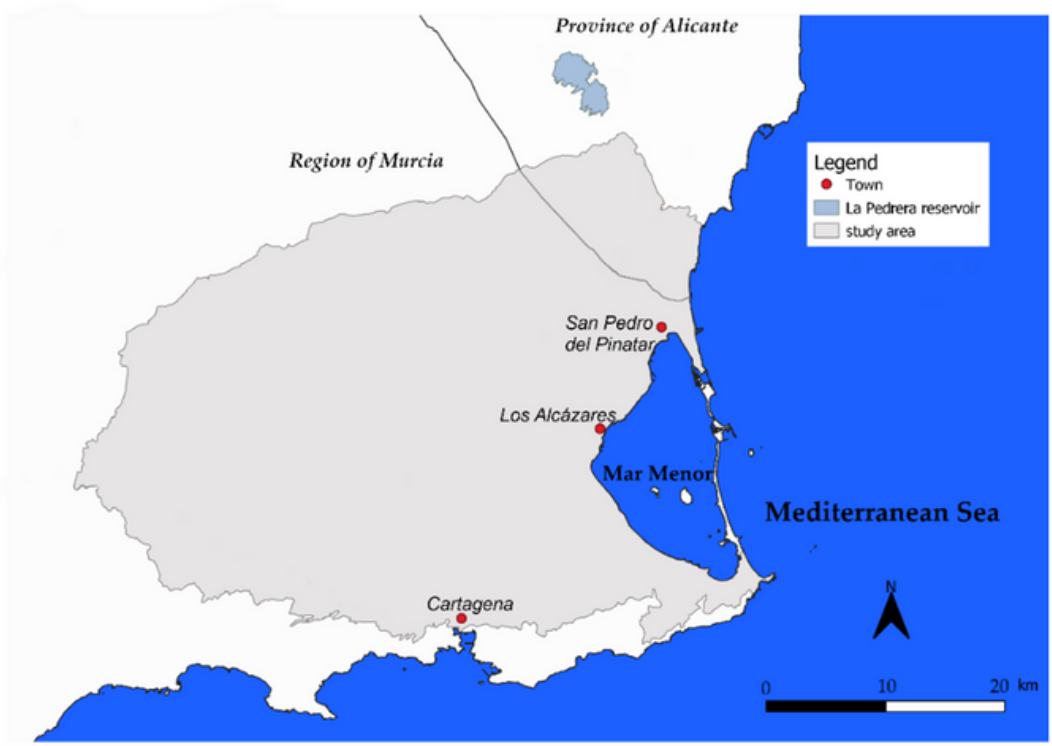

Figure 1. *Location of study area (Campo de Cartagena, Mar Menor watershed) in the region of Murcia and the south of the province of Alicante.*

Different improvements, mainly since the second half of the twentieth century in the region of Murcia and Alicante province, have favored the growth of population, principally located in coastal areas. This increase may be due to the improvement of communication channels (roads) and greater availability of water resources, which has allowed the development of agriculture. Agriculture is very important in the Region of Murcia, because of the good climate and a fertile soil in many river basins that allows suitable growth of crops, but the lack of water has limited the production. Therefore, the change of rainfed crops to irrigated crops was benefited by the capital investment (the Tajo-Segura water transfer in 1979, the exploitation of the aquifers and the obtaining of desalinated water) which increases the availability of water; the productivity of the crops has improved in spite of the severe shortage suffered by the area. La Pedrera reservoir (built in 1985), located in the province of Alicante, is responsible for regulating the water which comes from the Tajo-Segura transfer canal (agricultural and urban supply). This reservoir maintain adequate water availability despite the severe scarcity suffered in the area (29).

In fact, Murcia exports between 20 and 30% of fruits and vegetables in Spain, especially to the European Union (30). Even with the external contributions of water, it is not enough to supply the water needs of the area that often suffers serious droughts that cause cuts back not only for agriculture but also for urban supply. In addition, during the summer the demand for water for agriculture is higher because of the large water deficit and high temperatures. This situation also coincides with the period of greatest urban demand in the area due to tourism (31), especially in some areas closer to the coast. For example, it is estimated that on the Costa Cálida there were almost 4 million visitors in 2016 (28).

2.1 Methodology

The data were obtained from the National Geographic Institute (IGN). We used the geodesic reference system ETRS89 and UTM projection zone 30 (32).

The Mar Menor watershed was delimited with the Digital Terrain Model (MDT25 CC-BY 4.0 scne.es) and the GRASS software using the flow lines that run along the maximum slope. The basin covers 151,641 hectares and is located mainly in the Region of Murcia and a part in the province of Alicante. All the reservoirs found within the basin were digitized one by one by using high quality orthophotos of the Plan Nacional de Ortofotografía Aérea (PNOA) (FotoPNOA 2004-2016 CC-BY 4.0 scne.es) with pixel size of 25 cm. And the same process was done with old photographs taken from a photogrammetric flight along the period from 1973 to 1986 (Fotol 1973-1986 CC-BY 4.0 scne.es), scale 1: 18,000 and pixel size between 27 and 45 cm depending on the area. The digitization process was done with QGIS v.3.2. The ponds and reservoirs were marked with points to locate them and then they were digitalized to determine their surface taking into account the limits of the structure, when they were at maximum capacity. A field trip was also done to compare the results obtained from the images with the disposition in fact, checking close to a hundred elements (old mills, ponds and small reservoirs).

Figure 2. *Old mills and the new irrigation systems in the Campo de Cartagena.*

A heat map was developed from the density of points that identify the location of each irrigation ponds/reservoirs to understand better their distribution. Points interpolation aids to visualize in a map the concentration of these in a continuous surface. Three parameters are used to create a heat map: the cell size, the bandwidth and the type of calculation used in the interpolation. The cell size will determine the degree of detail on the surface. The larger the cell size, the less continuous the color gradient that represents the concentration of points will be. The bandwidth (or search radius) is the area around each point that the GIS will take into account for density calculation. The type of calculation used in the most common interpolation is inverse distance weighting (IDW), which assigns more importance to the functions that are closer than to those that are furthest away (33). In this case, we used a search radius of 5 km and 15 pixels of cell size.

To estimate annual evaporation losses in the study area, we have used as reference the evaporation values published in the article "Regional assessment of evaporation from agricultural irrigation reservoirs in a semiarid climate" by Martínez Alvárez *et al.* (2008) (34). They use measures done in the 2003 for the entire Segura River Basin (located in the southeast of Spain, including the study area). In this article, authors estimate the evaporation losses using daily, monthly and annual data on temperature, precipitation, relative humidity, wind speed, wind direction and solar radiation of 74 agro-meteorological stations for the period 2000-2006. In addition, some of them have class-A pan evaporometer in which evaporation was calculated by a sensor that determinate the difference in water level. The Class-A pan evaporometer standardized by the US National Weather Service is a 120.7 cm diameter and 15 cm deep cylinder made of galvanized iron.

It is elevated about 15 cm from the ground by a wooden platform. It must be located where the air circulates freely so that it does not affect the measurements (35). They use 14,145 irrigation reservoirs for the entire Segura basin, which occupied 4901 ha. They obtain as a result the annual evaporation loss in the Segura basin taking into account the maximum surface area, which was 68.8 hm^3. Based upon this value and considering the surface, the evaporation value of water used as a reference is 0.014 hm^3·year/ha. This help us to estimate the evaporation loss estimation in our study area.

3. Results and discussion

Figure 3 presents the digitized points that indicate the location of the irrigation ponds for both periods. There is a clear increase in the number of points currently with respect to the previous period.

In the image a (figure 3), the points do not appear distributed following any regular pattern; they are dispersed throughout the basin but especially near the coast and the urban cores, some of them forming small groups. In the top of the basin (NW), in the foothills of the Sierra de Carrascoy and El Valle, there are no irrigation ponds because at that time, mechanization and cultivation techniques did not allow working the land in areas with steep slopes. In the image b, there is a greater increase of irrigation ponds and small resorvoirs. Grouping of points can be observed mainly in the center of the basin which is quite flat, and in the top near La Pedrera reservoir. There is also a tendency for a high density of points near the coast as in the first image. In this case, due to the modern techniques, the irrigated crops occupy the foothills of the mountains.

In order to understand and visualize better the irrigation ponds distribution patterns in the area and compare them between two periods, a heat map (Figure 4) was created from the density of points. These maps confirm in a very clear way the changes produced in the area.

In the first image (Figure 4a), high density of points (in green) is observed in the lower part of the basin and following the coastline. This location may be associated with the extraction of water from the subsurface aquifers, following the patter of the traditional systems such as windmills (a pond was situated near the mill so that the water could fall into it). Moreover, extraction that is more efficient with pumps made possible to obtain water from the aquifers at a larger depth coming to cause an overexploitation of aquifers.

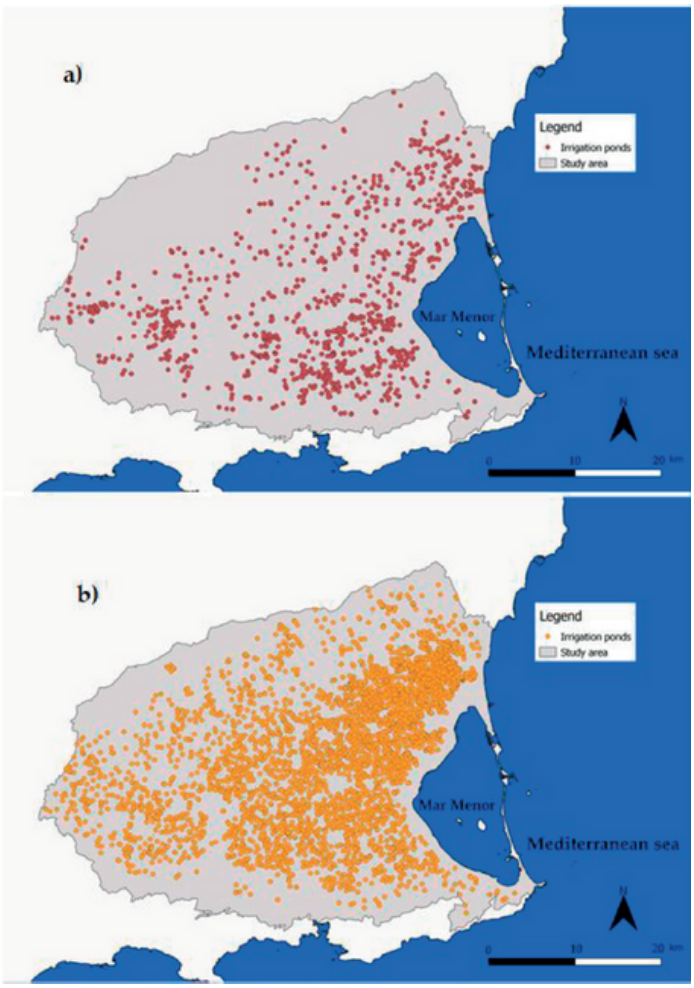

Figure 3. *Points marking the location of irrigation ponds in the Mar Menor basin in the 1973-1986 period (image a) and nowadays (2016-2017) (image b).*

The arrival of water from the Tajo-Segura transfer in 1979, increased the availability of water and relieved the pressure on groundwater (36). This situation benefited production and the expansion of intensive agriculture (with the corresponding construction of small reservoirs to store and supply water).

In the second image (Figure 4b), there is a generalized increament near the coast and a great increase in the upper part of the basin (NE). This difference could be explained by the construction in 1985 of the La Pedrera reservoir. It has 1272 hectares and can store 246 hm^3. This reservoir receives water from the Tajo-Segura transfer and distributed to the Campo de Cartagena by a great canal and others supplied conductions.

La Pedrera reservoir is also used for urban water supply through the Taibilla canal. Therefore, it is easier to supply the crop fields closest to the reservoir. Consequently, it has favoured a greater development of greenhouses (Figure 5). They are grouped near the towns of San Pedro del Pinatar (Murcia) and Pilar de la Horadada in the south of Alicante.

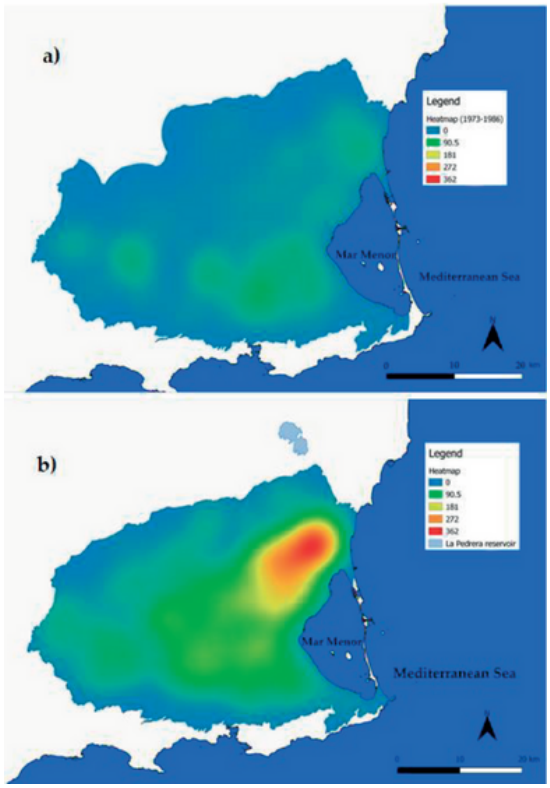

Figure 4. *Heat maps from dot density of the identified ponds with old photograph (figure a) and with those current (figure b).*

Figure 5. *Group of greenhoses near San Pedro del Pinatar in the study area. (Source: derived from FotoPNOA 2004-2016 CC-BY 4.0 scne.es).*

After the analysis of the data and the digitalization of the irrigation ponds from the images in both periods, table 1 shows a summary of them. 971 reservoirs were digitized from the data of the period 1973-1986. The sheet of water, according to the sum of the surface of all them, accounted to 88.63 hectares. The average surface area of the reservoir/pond was 318 m².

In the second period (2016-2017), 3,846 irrigation ponds were digitized from PNOA images. The total water surface were 1,201.32 hectares. The average surface area of the reservoirs increased to 1,631 m².

These values indicate that the number of reservoirs in this area has almost incremented 4 times. For the average surface of ponds, the size at present is 5 times higher than before, however not necessarily deeper than the oldest. Therefore, the total area occupied by the reservoirs has increased 14 times during the last decades when size only 5 times.

	Number of ponds	**Total area occupied (m²)**	**Mean area per pond (m²)**	**Estimated evaporation (hm³/year)**
1973-1986 period	971	886,34	318	1,24
2016-2017 period	3,846	12,013.189	1,631	16,82

Table 1. *Values obtained from the irrigation ponds digitalization and estimated values of evaporation in the study area for both periods.*

To estimate the possible evaporation losses from the sheet of water of the small reservoirs/ponds, we took as reference the value given for the area of 0.014 hm^3·year/ha (34). Considering all the reservoirs to their maximum capacity, the values estimated for each period were:

- For the 971 ponds in the first period (determined from the images obtained between 1973-1986), the annual losses would be close to 1.24 hm^3/year;
- and for the second one (mages of PNOA 2016-2017), it would be close to 16.82 hm^3/year.

This means that there is a difference of approximately 15.62 hm^3/year, parallel to the increment of the surface exposure of reservoirs and ponds. This amount of water that can be lost, is equal to that need for the supply of a city of 300,000 inhabitants for a year considering the average water consumption in Spain for inhabitant (37). Water scarcity in this area has always been a main concern for agricultural production. However, with the transfer from other river basins (i.e. Tajo river), water availability has been increased and along with the population growth and agricultural yield.
This was reflected in the construction of reservoirs/ponds in the last years, which has been increased. With this increment, the potential evaporation of water from reservoirs and ponds have been dramatically increased by the way.

According to a report managed by the Ministry of Agriculture and Water of the Region of Murcia with data from the Space Agency of Meteorology (AEMET), and with the collaboration of different universities and institutions, the evolution of rainfall does not follow a clear trend, a normal situation in that area with such irregularity. For temperatures, a slight tendency to increase is observed. In fact, according to this report from 1971 to 2009 the average annual temperature of the entire Region of Murcia increased from 15.5 to 17°C (38). Therefore, the evaporation loss could be aggravated considering the scenarios based on the climate change and the increase in temperature. In this sense, evaporation can be over the values estimated in this work.

In this line, it is important to study and development measures to avoid water evaporation and improve the efficiency of the irrigation system. For this reason, it is convenient to study a better spatial distribution of reservoirs and reduce the number of them. Moreover, an increment of deep in their construction can facilitate to storage the same amount of water with less surface exposure to evaporation. Finally, the use of some techniques to cover the ponds can reduce water surface exposure.

4. Conclusions

Remote sensing data is very useful to study and analyze the amount of water stored and the management of irrigation systems. The use of these technologies, both GIS and remote sensing, can help in the management decision-making about water resources.

The example given, shows that the amount of water that could evaporate represents a significant loss. In this case, the amount of water that could evaporate is almost 14 times higher now. This matches with the increase in the total surface occupied by the irrigation ponds. With only a 4 times increment in the number of reservoirs, the amount of water that could evaporate increases by 350%. Although it is an estimation, it is clear that water losses due to evaporation represent a high cost, especially in areas where this resource is scarce.

Despite the water limitations of the area, in the Mar Menor basin there are many agricultural fields that generate tons of fruits and vegetables that provide a great social and economic benefit to region. Even with the different sources of water, there is still a water deficit that generates (especially during droughts periods) economic, social and environmental instability.

In addition, with the possible effects of climate change that indicates less precipitation and higher temperatures, it is expected that the amount of water resources available can be seriously affected especially in arid and semi-arid areas such as Murcia and Alicante, which already suffer the effects of scarcity. Efforts should be done applying techniques to reduce the evaporation. Therefore, saving the resource to avoid losses as much as possible and be able to supply a growing population is a priority.

References

1. Nations U. Water in a Changing World [Internet]. Vol. 11, World Water. 2009. 349 p. Available from:http://www.esajournals.org/doi/abs/10.1890/1051-0761(2001)011[1027:WIACW]2.0.CO;2
2. Martínez Fernández J, Selma MAE. The dynamics of water scarcity on irrigated landscapes: Mazarrón and Aguilas in south-eastern Spain. Syst Dyn Rev. 2004;20(2):117–37.
3. European Environment Agency. El agua en la agricultura. Copenhagen; 2012.
4. El-Beltagy AMM. Impact of climate change on arid lands agriculture. Agric Food Secur. 2012;1(3).
5. Juan M, Casas J, Bonachela S, Fuentes-Rodríguez F, Gallego I, Elorrieta MA. Construction characteristics and management practices of in-farm irrigation ponds in intensive agricultural systems - agronomic and environmental implications. Irrig Drain. 2012;61(5):657–65.
6. Cazorla MJ. Gestión ecosistémica de las balsas de riego del litoral mediterráneo andaluz [Thesis]. Almería University; 2012.
7. Hamdy A, Abu-Zeid M, Lacirignola C. Water crisis in the mediterranean: Agricultural water demand management. Water Int. 1995;20(4):176–87.
8. USGS. The Water Cycle: Evaporation [Internet]. 2016 [cited 2018 Oct 16]. Available from: https://water.usgs.gov/edu/watercycleevaporation.html
9. Benzaghta MA, Mohamad TA. Evaporation from reservoir and reduction methods: An overview and assessment study. Int Eng Conv Domascus, Syria Medinah, Kingdom Saudi Arab. 2009; (May 11-18):9p.
10. Ibarra D, Salvador M, Conesa C. Estimación de evaporación en balsas de riego mediante el empleo de técnicas de teledetección . Estudio aplicado a la vertiente litoral sur de la Región de Murcia. 2014;8.
11. Lopez Moreno JI. Estimación de pérdidas de agua por evaporación en embalses del Pirineo. Cuad Investig Geográfica. 2008;34:61–81.
12. Gugliotti M, Baptista MS, Politi MJ. Reduction of evaporation of natural water samples by monomolecular films. J Braz Chem Soc. 2005;16(6 A):1186–90.
13. Segal L, Burstein L. Retardation of water evaporation by a protective float. Water Resour Manag. 2010;24(1):129–37.
14. KYOCERA TCL Solar begins operation of Japan’s largest 13.7MW Floating Solar Power Plant [Internet]. 2018 [cited 2018 Oct 16]. Available from: http://www.kyocerasolar.eu/index/news/news_details.L3NvbGFyX2VsZWN0cmljX3N5c3RlbXMvbmV3cy8yMDE4L0tZT0NFUkFfVENMX1NvbGFyX2JlZ2luc19vcGVyYXRpb25fb2ZfSmFwYW5fc19sYXJnZXN0XzEzXzdNV19GbG9hdGluZ19Tb2xhcl9Qb3dlcl9QbGFudA~~.html
15. Yao X, Zhang H, Lemckert C, Brook A. Evaporation Reduction by Suspended and Floating Covers : Overview , Modelling and Efficiency Urban Water Security Research Alliance Technical Report No . 28. Urban Water Secur Res Alliance Tech Rep No 28. 2010;(28).
16. Craig I, Green A, Scobie M, Schmidt E. Controlling Evaporation Loss from Water Storages. Natl Cent Eng Agric. 2005;(1000580/1):207.

17. Kawsar R. Water resource managment and Remote Sensing, a prospective issue that requires considerable attention [Internet]. 2015. Available from: http://geoawesomeness.com/water-resource-managment-and-remote-sensing-a-prospective-issue-that-requires-considerable-attention/
18. Tsihrintzis VA, Hamid R, Fuentes HR. Use of Geographic Information Systems (GIS) in water resources: A review. Water Resour Manag. 1996;10(4):251–77.
19. Pipitone C, Maltese A, Dardanelli G, Brutto M Lo, Loggia G La. Monitoring water surface and level of a reservoir using different remote sensing approaches and comparison with dam displacements evaluated via GNSS. Remote Sens. 2018;10(1):1–24.
20. Lin YCW, Hsiao L, Cheng K. A Multi-Decadal Change Analysis for Irrigation Ponds in Taoyuan , Taiwan Using Multi-source Data. 2018;(June):1–16.
21. Kite, Geoff; Pietroniro A. Remote Sensing of Surface Water. In: Schultz G.A. EET, editor. Remote Sensing in Hydrology and Water Management. Berlin, Heidelberg Springer; 2000. p. 217–38.
22. Porter, J.R., L. Xie, A.J. Challinor, K. Cochrane, S.M. Howden, M.M. Iqbal, D.B. Lobell MIT. Food security and food production systems. In: Field, C.B., V.R. Barros, D.J. Dokken, K.J. Mach, M.D. Mastrandrea, T.E. Bilir, M. Chatterjee, K.L. Ebi, Y.O. Estrada, R.C. Genova, B. Girma, E.S. Kissel, A.N. Levy, S. MacCracken, P.R. Mastrandrea and LLW, editor. Climate Change 2014: Impacts, Adaptation, and Vulnerability Part A: Global and Sectoral Aspects Contribution of Working Group II to the Fifth Assessment Report of the Intergovernmental Panel on Climate Change. Cambridge, United Kingdom and New York: Cambridge University Press; 2014. p. 485–533.
23. Hudson NW. 5. WATER CONSERVATION. In: FAO Land and Water Development Division, editor. Soil and Water Conservation in Semi-Arid Areas. Bedford, United Kingdom; 1987. p. 172.
24. Vargas-Amelin EPP. The challenge of climate change in Spain: Water resources, agriculture and land. J Hydrol. 2014;
25. FAO. Towards a water Critical Perspectives for Policy-makers. 2015;62.
26. Pérez Ruzafa, A. Marcos, C. Pérez Ruzafa IM. 30 años de estudios en la laguna costera del Mar Menor: de la descripción del ecosistema a la comprensión de los procesos y la solución de los problemas ambientales. In: Instituto Euromediterráneo del agua, editor. El Mar Menor: Estado del conocimiento actual. 1st ed. 2009. p. 18–40.
27. Blázquez, M.P. ; Pelegrín, G.B. ; Díaz MF. Ficha informativa de los humedales RAMSAR: Mar Menor. 2006.
28. Mompeán, Pedro Arroyo; Vegas Juez AM. Turismo en la región de murcia 2016. Instituto de Turismo de la Región de Murcia: ITREM; 2016.
29. Confederación Hidrográfica del Segura. Embalse de La Pedrera [Internet]. [cited 2018 Oct 8]. Available from: https://www.chsegura.es/chs/cuenca/infraestructuras/embalses/embalsedelaPedrera/index.html

30. FEDEX. Exportación/Importación españolas de frutas y hortalizas [Internet]. [cited 2018 Oct 17]. Available from: http://www.fepex.es/datos-del-sector/produccion-frutas-hortalizas
31. Candela L., Domingo F., Berbel J. AJJ. An overview of the main water conflicts in Spain: Proposals for problem-solving. In: El Moujabber M., Ouessar M., Laureano P. RR, editor. Water culture and water conflict in the Mediterranean area. Options Méditerranéennes: Série A. Séminaires Méditerranéens; n. 83; 2008. p. 197–203.
32. Real Decreto 1071/2007, de 27 de julio, por el que se regula el sistema geodésico de referencia oficial en España.
33. Dempsey C. Heat Maps in GIS [Internet]. GIS LOUNGE. 2012 [cited 2018 Oct 17]. Available from: https://www.gislounge.com/heat-maps-in-gis/
34. Martínez Alvarez V, González-Real MM, Baille A, Maestre Valero JF, Gallego Elvira B. Regional assessment of evaporation from agricultural irrigation reservoirs in a semiarid climate. Agric Water Manag. 2008;95(9):1056–66.
35. Toribio MIS. Métodos para el estudio de la evaporación y evapotranspiración. 1st ed. Sociedad Española de Geomorfología, editor. Logroño: Geomorga Ediciones; 1992.
36. Gil Meseguer E. Los paisajes agrarios de la región de Murcia. Papeles de Geografía. 2006;43:19–30.
37. Instituto Nacional de Estadística. España en cifras 2017. Madrid; 2018.
38. Victoria Jumilla F (coord.). Cambio Climático en la Región de Murcia. Murcia: Consejería de Agricultura y Agua; 2010.

Imagen Sentinel 2 sobre el Parque Natural de El Hondo y las Salinas de Santa Pola.
Fuente: MosaicoSentinel2Historico 2019-2021 CC-BY 4.0

Marco Dos Santos, G., Meléndez-Pastor, I., Navarro-Pedreño, J., Gómez Lucas, I. (2019).

A review of Landsat TM/ETM based vegetation indices as applied to wetland ecosystems.

Journal of Geographical Research, 2(1), 499.

https://doi.org/10.30564/jgr.v2i1.499

Abstract

A review of vegetation indices as applied to Landsat-TM and ETM+ multispectral data is presented. The review focuses on indices that have been developed to produce biophysical information about vegetation biomass/greenness, moisture and pigments.

In addition, a set of biomass/greenness and moisture content indices are tested in a Mediterranean semiarid wetland environment to determine their appropriateness and potential for carrying redundant information.

The results indicate that most vegetation indices used for biomass/greenness mapping produce similar information and are statistically well correlated.

Keywords

Arid wetlands; Leaf pigments; Spectral reflectance; Vegetation greenness; Vegetation biomass; Vegetation moisture; Vegetation canopy

1. Introduction

In the last decades a broad range of vegetation indices has been developed, showing an increased interest by the scientific community in measuring vegetation properties through remote sensing techniques. A great number of indices are developed with the aim to reduce their sensitivity to extraneous factors such as soil background or atmosphere [1], and several reviews of vegetation indices have been published (e.g. [2,3,4,5,6,7]).

Remote sensing tools are used for a large number of studies of natural areas [8,9], to assess the state of vegetation or crop yield [10], or for vegetation classification [11]. In addition, several authors [12,13] have highlighted the role of vegetation indices as valuable biophysical data for models and simulations. This work focuses on three biophysical properties, which are vegetation biomass/greenness, vegetation moisture, and plant pigments. Remote sensing of vegetation biomass is of great value in modelling vegetation stress and crop yield [14]. Numerous researches have shown the direct relationship that exists between spectral response in the near-infrared region and various biomass measurements [15,16,17,18,19]. Spatial and temporal change of vegetation moisture can be used for plant water stress estimations. Water stress detection by remote sensing as based on plant physiology can be successfully conduced for different vegetation types with little adjustment [20,21,22]. A great number of research work has been conducted for estimating vegetation moisture content (e.g. [6,21,22,23]) with a common goal: vegetation moisture content can be estimated more accurately using medium-infrared reflectance data. Chrolophylls, carotenoids and anthocyanins are optically detectable and have either photosynthetic or photoprotective functions [24]. Moreover, they also provide an accessible ‘handle’ for evaluating relative photosynthetic activity, which can vary with leaf type [25]. Reflectance assessment of leaf pigments can potentially provide indicators of integrated leaf physiology under a wide range of conditions [24]. For quantitative pigment content estimations, accurate data calibration methods must be carefully applied. As Gamon and Surfus (1999) [24] observed, comparisons of reflectance indices with extracted pigment levels suggest specie-specific relationships influenced by leaf structure properties [26]. This indicates a need for empirical calibration when using reflectance indices.

A great number of studies deal with vegetation index estimations for specific locations. These kinds of studies are of great value for these local studies, because vegetation indices can be estimated with great accuracy. In addition, due to the high availability of images, it is possible monitor the state of the vegetation over time [27]. However, applying these locally tested methods to other study areas is sometimes not possible because of the different vegetation species and communities, as well as the different

soils and lithology encountered in other areas. The objective of this paper is the review of several vegetation indices that can be computed with Landsat TM and ETM+ data in order to select the most representative of the Mediterranean wetland areas by first determining potentially redundant information among the tested indices.

2. Vegetation indices

Jensen (2000) [4] defines vegetation indices as “dimensionless, radiometric measures that function as indicators of relative abundance and activity of green vegetation, often including leaf-area-index (LAI), percentage green cover, chlorophyll content, green biomass, and absorbed photosynthetically active radiation (APAR)”. Huete and Justice (1999) [28] summarize as follows the main characteristics that a vegetation index must satisfy:

1. Maximize sensitivity to plant biophysical parameters, with mathematical relations as simple as possible.
2. Normalize or model external effects, such as Sun angle, scene geometry, and space-temporal atmospheric characteristics.
3. Normalize internal effects, such as canopy and soil background variations, illumination geometry, and phenological state.
4. Respond to specific measurable biophysical parameters, such as biomass, LAI, APAR, etc., that can be field validated and qualitatively controlled.

Vegetation spectral indices try to enhance the spectral contrast among different wavelengths as a response to characteristic absorption and/or reflectance features.

A crucial aspect is that the absorptions from different plant materials are similar and overlap, so that a single absorption band cannot be isolated and directly related to, for example, chemical abundances of one plant constituent [29]. Vegetation indices have been classified into four categories as a function of the following computation concepts (based partially on: Jackson and Huete (1991) [30] and Eastman (2003) [31]):

- **Slope-based indices:** any particular value of the index can be produced by a set of two bands (for example red/infrared reflectance values) that form a line emanating from the origin of coordinates of a bi-spectral plot (scattergram). Different levels of the index can be envisioned as producing a spectrum of such lines that differ in their slope [32].

- **Distance-based indices:** measure the degree of vegetation present by gauging the difference of any pixel's reflectance from the reflectance of bare soil [32]. A key concept here is that a plot of the positions of bare soil pixels of varying moisture levels (and soil organic matter contents [33] in a bi-spectral plot will tend to form a line (known as the soil line). As vegetation canopy cover increases, this soil background will become progressively obscured, with vegetated pixels showing a tendency towards increasing along a perpendicular distance from this soil line. All of the members of this group require that the slope and intercept of the soil line be defined for the particular image being analysed.

- **Orthogonal transformations:** undertake a transformation of the available spectral bands to form a new set of uncorrelated bands within which a green vegetation index band can be defined.

- **Continuum Removal and Band Depth:** the continuum is an estimate of the other absorptions present in the spectrum, not including the one of interest [33]. The continuum-removal process isolates spectral features, removes the continuum, and scales the band-depth (or band area) to be equal, to allow identification of subtle band shifts and shapes [34].

Table 1 provides a classification of the indices as a function of the calculation concept. All presented indices have been adapted so that they can be utilized with reflectance imagery provided by the Landsat Thematic Mapper sensor. Technical information about the Thematic Mapper sensor can be found at the U.S. Geological Survey Landsat Project web site (http://landsat.usgs.gov).

Table 1. *A classification of the indices as a function of the calculation concept.*

Index computation concept	Index
Slope-based	SR NDVI TVI OSAVI ARVI NDII LWCI MSI Red/Green ratio WDVI
Distance-based	PVI SAVI MSAVI TSAVI1 TSAVI2 GESAVI SARVI MSARVI EVI
Orthogonal transformation	Tasseled Cap-Greenness Tasseled Cap-Wetness Integral
Continuum Removal and Band Depth	Band-Depth TM5 (B-DTM5)

2.1 Slope-based indices

Generally, slope-based indices are easier to calculate than other indices. Some indices are normalized ratios where possible results are comprised between the range of –1 to 1. This approach facilitates the interpretation of the index. Selected slope-based indices are:

2.1.1. Normalized Difference Vegetation Index (NDVI)

NDVI original formulation is attributed to Rouse *et al.* (1974) [35]. This index has been widely used and tries to enhance reflectance differences between red and NIR spectral regions of plant spectral signatures. The NDVI index evolved from the Simple Ratio (SR) proposed by Birth and McVey (1968) [36].

$$SR = \frac{\rho_{TM4}}{\rho_{TM3}} \tag{1}$$

The NDVI is formulated as:

$$NDVI = \frac{\rho_{TM4} - \rho_{TM3}}{\rho_{TM4} + \rho_{TM3}} \tag{2}$$

Deering *et al.* (1975) [37] proposed the Transformed Vegetation Index (TVI) by adding a constant value of 0.5 to the NDVI to avoid negative values. They also included the square root transformation of the NDVI with the additional constant, to stabilize the variance. TVI is computed as:

$$TVI = \sqrt{\left(\frac{\rho_{TM4} - \rho_{TM3}}{\rho_{TM4} + \rho_{TM3}}\right) + 0.5} \tag{3}$$

NDVI has been related with a great number of parameters, such as changes in the amount of green biomass and chlorophyll content [4]. Several types of relationships with numerous parameters have been reported. A synthetic summary of some of them is presented below ([38] and references therein):

- Leaf chlorophyll content
- Leaf water content
- CO_2 net flux

- Absorbed Photosynthetically Active Radiation (APAR)
- Vegetation net productivity
- Leaf Area Index (LAI)
- Rainfall amount received by a vegetation canopy
- Phenological dynamics
- Potential plant transpiration

2.1.2. Optimized Soil-Adjusted Vegetation Index (OSAVI)

Additional modifications of NDVI have been developed to minimize the effect of soil background and atmospheric attenuation for the maximization of vegetation spectral response. Rondeaux *et al*. (1996) [39] proposed the OSAVI (Optimized Soil-Adjusted Vegetation Index) with the inclusion of an adjusting factor X to the NDVI denominator. They estimated, using the SAIL model [40] enhanced by the hot-spot effect [41], that the optimum X value was 0.16 units. OSAVI values range between the NDVI and SAVI estimations.

$$OSAVI = \frac{\rho_{TM4} - \rho_{TM3}}{\rho_{TM4} + \rho_{TM3} + 0.16} \quad (4)$$

Rondeaux *et al.* (1996) [39] also provided a test of the sensitivity to soil background for many vegetation indices. They evaluated the sensitivity of OSAVI to soil background effects and its relationship with NDVI and SAVI [42,43]. They concluded that: a) with low or relative low vegetation cover (< 50%, LAI ≤ 1) this index performs slightly worse than SAVI but better than NDVI; b) with high or relative high vegetation cover, (<50%, LAI ≥ 1) the index performs slightly worse than NDVI but better than SAVI. Steven (1998) [44] evaluated the OSAVI with a canopy model to observational parameters and concluded that the index can be used successfully for agricultural monitoring.

2.1.3. Atmospherically Resistant Vegetation Index (ARVI)

ARVI was proposed by Kaufman and Tanre (1992) [45]. The index tries to minimize atmospheric effects (molecular scattering and ozone absorption) due to the normalization of the blue, red, and near-infrared reflectance bands. Kaufman and Tanre (1992) [45] indicated that atmospheric aerosol influences vegetation indices in two ways [28]:

- Influence as path radiance: By an additive, effect due to land surface brightness.
- Influence through transmittance: By a multiplicative, effect due to surface brightness.

The ARVI uses blue band to reduce atmospheric effects in the red band, by using an experimental aerosol model (γ). Kaufman and Tanre (1992) [45] provided guidelines for aerosol model values selection. g is normally equal to 1 to minimize atmospheric effects.

$$ARVI = \frac{\rho^*_{TM4} - \rho^*_{rb}}{\rho^*_{TM4} + \rho^*_{rb}} \quad (5)$$

$$\rho^*_{rb} = \rho^*_{TM3} - \gamma \cdot (\rho^*_{TM1} - \rho^*_{TM3}) \quad (6)$$

where:
ρ^*_k = apparent reflectance of band k
γ = aerosol model

ARVI is similar to NDVI with respect to potentially related biophysical parameters.

2.1.4. Normalized Difference Infrared Index (NDII)

The original Infrared Index (II) was proposed by Hardisky *et al.* (1983) [46] and was cited by Hunt and Rock (1989) [22] as Normalized Difference Infrared Index (NDII). NDII differs from NDVI in that TM band 3 (red spectral region) is replaced by band 5 (mid-infrared spectral region).

TM band 5 can be related with a leaf water absorption band [4]. Carter (1991) [47] showed that mid-infrared reflectance increases are related with decreases in plant moisture.

$$NDII = \frac{\rho_{TM4} - \rho_{TM5}}{\rho_{TM4} + \rho_{TM5}} \quad (7)$$

NDII is highly correlated with canopy water content [46]. Jensen (2000) [4] highlighted that NDII is more sensitive to changes in plant biomass and water stress than NDVI in wetland studies.

Several studies have shown that these kinds of indices that combines near-infrared with mid-infrared bands is more appropriate than NDVI for estimating vegetation water contents (e.g. [6,23,48]).

A similar index to NDII is the Leaf Water Content Index (LWCI) proposed by Hunt *et al.* (1987) [21] for leaf Relative Water Content (RWC) estimations. It is based on the principle that, according to Beer's law, absorbance of infrared radiation by leaf water (A) is equal to the product of the equivalent water thickness (l), the extinction coefficient (ε_w), and the concentration of water (c_w , [21] computed it as 55.6 mol/L). The ratio of leaf absorbance to leaf absorbance at full turgor (A/AFT) is equal to the ratio of equivalent thickness (l/lFT) because ε_w and c_w cancel out. Consequently, A/AFT is equal to the ratio of water volumes averaged over the leaf area (V/VFT), which is RWC.

$$LWCI = \frac{-\log[1-(\rho_{TM4}-\rho_{TM5})]}{-\log[1-(\rho_{TM4\,FT}-\rho_{TM5\,FT})]} \tag{8}$$

where:

$\rho_{TM_k\,FT}$ = reflectance of TM band k when leaves area at full turgor

Hunt and Rock (1989) [22] reported that LWCI can measure leaf RWC directly and is useful to determine when certain plants are water stressed. However, the required reflectance measurements and two different but known RWC make it impractical for field applications.

2.1.5. Red/Green ratio

This index was proposed by Gamon and Surfus (1999) [24] to assess anthocyanin content. The role of this kind of plant pigment is unclear [24]: being both photoprotective [50] and defensive [51,52]. Gamon and Surfus (1999) [24] suggested the possible role of anthocianyns: "the complementary patterns of xanthophyll and anthocyanin pigmentation during early leaf development suggest that anthocianyns provide a critical, photoprotective role before xanthophylls pigments reach final levels" (not fully developed photosynthetic competence). The index is formulated as:

$$R/G = \frac{\rho_{TM3}}{\rho_{TM2}} \tag{9}$$

Gamon and Surfus (1999) [24] observed that the Red/Green ratio was strongly related to anthocyanin pigment content estimated by destructive sampling and spectrophotometric quantification.

2.2. Distance-based indices

A key concept for distance-based vegetation indices is the soil line. Richardson and Wiegand (1977) [53] discovered the concept of the soil line. It results from a linear relationship between the red and near-infrared reflectance values of bare soils:

$$y = ax + b$$

(10)

where:

x = reflectance of red band
y = reflectance of near-infrared band
a = slope of the soil line
b = intercept of the soil line

The soil line is dependent on individual soil types. Fox *et al.*, (2004) [54] affirmed that a global soil line representing all soil types is not possible due to the fact that the line would be linear in some portions of the entire range as a result of soil condition variations (soil type, moisture, organic matter content, etc.).

The original index for this group is the Perpendicular Vegetation Index (PVI) proposed by Richardson and Wiegand (1977) [53]. The derivation of the index requires several steps (based on Eastman, 2003 [31]):

A. Determination of the soil line equation by bare soil reflectance values for red (independent variable) vs. infrared (dependent variable) bands.

$$\rho_{g4} = a \cdot \rho_{g3} + b \qquad (11)$$

where:

ρ_{g4} = an x position on the soil line
ρ_{g3} = the corresponding y coordinate
a = the slope of the soil line
b = the y-intercept of the soil line

B. Determine the equation of the line that is perpendicular to the soil line, with the form:

$$\rho_{p4} = c \cdot \rho_{p3} + d \quad (12)$$

where:
ρ_{p4} = red reflectance
ρ_{p3} = infrared reflectance
c = -1/*a*
d = ρ_{p4} - $c \cdot \rho_{p3}$

C. Find the intersection of the two lines (i.e., the coordinate ...., ...).

$$\rho_{gg4} = \frac{c \cdot b - d \cdot a}{c - a} \quad (13)$$

$$\rho_{gg3} = \frac{b - d}{c - a} \quad (14)$$

D. Find the distance between the intersection and the pixel coordinate using Pythagoras' Theorem.

$$PVI = (\sqrt{(\rho_{gg4} - \rho_{gg4})^2 + (\rho_{gg3} - \rho_{gg3})^2} \quad (15)$$

Selected distance-based indices are:

2.2.1. Soil Adjusted Vegetation Index (SAVI)

SAVI results from a modification of NDVI by the addition of a soil adjustment factor (L) [42,43]. L value varies as a function of soil characteristics. The index is formulated as:

$$SAVI = \frac{(\rho_{TM4} - \rho_{TM3})}{(\rho_{TM4} + \rho_{TM3} + L)} \cdot (1 + L) \quad (16)$$

where:
L = soil adjustment factor

Originally, a graphical method was used for *L* value extraction. If *L* = 0, SAVI = NDVI, and if *L* = 100, SAVI ≅ PVI. Huete (1988) [42] suggested an *L* value of 1 for areas with low vegetation, *L* value of 0.5 for intermediate areas, and *L* value of 0.25 for densely vegetated areas. SAVI is similar to NDVI with respect to potentially related biophysical parameters.

Qi *et al.* (1994) [52] developed the MSAVI (Modified Soil Adjusted Vegetation Index) with the inclusion of a new *L* adjustment factor that considers the soil line, the NDVI and the WDVI (Weighted Difference Vegetation Index) [55, 56]. The new *L* factor is formulated as:

$$L = 1 - 2 \cdot a \cdot NDVI \cdot WDVI \quad (17)$$

where:

$$WDVI = \rho_{TM4} - a \cdot \rho_{TM3} \quad (18)$$

and:

a = slope of the soil line (for *L* and WDVI)

They proposed two formulations to the MSAVI, the first is identical to the original SAVI but with the new *L* soil adjustement factor, and the last one is as follows:

$$MSAVI = \frac{2 \cdot \rho_{TM4} + 1 - \sqrt{(2 \cdot \rho_{TM4} + 1)^2 - 8 \cdot (\rho_{TM4} - \rho_{TM3})}}{2} \quad (19)$$

2.2.2. Transformed Soil Adjusted Vegetation Index (TSAVI)

Baret *et al.* (1989) [57] argued that SAVI was only valuable if the soil line constants are a=1 and b=0. They developed the first modification of SAVI, the TSAVI1, which is formulated as:

$$TSAVI_1 = \frac{a \cdot ((\rho_{TM4} - a) \cdot (\rho_{TM3} - b))}{\rho_{TM3} + a \cdot \rho_{TM4} - a \cdot b} \quad (20)$$

where:

a = slope of the soil line

b = intercept of the soil line

TSAVI1 tries to combine the potentials of SAVI and PVI. The problem of TSAVI1 is that the index does not give good results in areas of heavy vegetation, because it is designed for semiarid areas. Baret et al. (1991) [57] proposed a modification of the first TSAVI. The TSAVI2 included a correction factor of 0.08 to minimize soil brightness background effects.

$$TSAVI_2 = \frac{a \cdot (\rho_{TM4} - a \cdot \rho_{TM3} - b))}{\rho_{TM3} + a \cdot \rho_{TM4} - a \cdot b + 0.08 \cdot (1 + a^2)} \quad (21)$$

where:
a = slope of the soil line
b = intercept of the soil line

2.2.3. Generalized Soil-Adjusted Vegetation Index (GESAVI)

Gilabert *et al.* (2002) [58] used the concept of vegetation isolines for the development of the Generalized Soil-Adjusted Vegetation Index (GESAVI), an index that belongs to the SAVI family. The index is based on the angular distance between the soil line and the vegetation isolines. They assume that vegetation isolines are linear but not parallel to the soil line, and the soil line is intercepted by the vegetation isolines at a cross point with a given red reflectance equal to:

$$R_{cross} = -\frac{b' - b}{a' - a} \quad (22)$$

where:
a = slope of the soil line
a' = slope of the vegetation isoline
b = intercept of the soil line
b' = intercept of the vegetation isoline

They also provided a geometrical interpretation of the index. The index is formulated as:

$$GESAVI = \frac{\rho_{TM4} - a \cdot \rho_{TM3} - b}{\rho_{TM3} + Z} \quad (23)$$

where:

$Z \equiv - R_{cross}$

2.2.4. Soil and Atmospherically Resistant Vegetation Index (SARVI)

SARVI results from the integration of the soil adjustment factor (*L*) of SAVI with the normalization of the blue, red, and near-infrared reflectance bands of ARVI [59]. The index is formulated as:

$$SARVI = \frac{\rho^*_{TM4} - \rho^*_{rb}}{\rho^*_{TM4} + \rho^*_{rb} + L} \quad (24)$$

$$\rho^*_{rb} = \rho^*_{TM3} - \gamma \cdot (\rho^*_{TM1} - \rho^*_{TM3}) \quad (25)$$

where:

ρ^*_k = apparent reflectance of band k

L = soil adjustment factor

γ = aerosol model

Huete and Liu (1994) [59] also proposed the MSARVI, a modification of SARVI.

$$MSARVI = \frac{2 \cdot \rho^*_{TM4} + 1 - \sqrt{\left[\left(2 \cdot \rho^*_{TM4} + 1\right)^2 - \gamma \cdot \left(\rho^*_{TM4} - \rho^*_{rb}\right)\right]}}{2} \quad (26)$$

$$\rho^*_{rb} = \rho^*_{TM3} - \gamma \cdot (\rho^*_{TM1} - \rho^*_{TM3}) \quad (27)$$

where:

ρ^*_k = apparent reflectance of band k

L = soil adjustment factor

γ = aerosol model

Huete and Liu (1994) [59] provided a sensitivity analysis of SAVI, ARVI, SARVI, and MSARVI with respect to NDVI. Jensen (2000) [4] reports several cases:

Case 1. Only soil noise (total atmospheric correction): SAVI and MSARVI are the best indices, and NDVI and ARVI are the worst.

Case 2. Partial atmospheric correction (Rayleigh and ozone components removed): SARVI and MSARVI are the best indices, and NDVI and ARVI are the worst.

Case 3. No atmospheric correction: SARVI are the best index, and NDVI and ARVI are the worst.

2.2.5. Enhanced Vegetation Index (EVI)

The EVI was developed by Huete and Justice (1999) [28] based on the MODIS sensor as an index with *"improved sensitivity into high biomass regions and improved vegetation monitoring through a de-coupling of the canopy background signal and a reduction in atmosphere influences"*. EVI is formulated as:

$$EVI = \frac{\rho^*_{TM4} - \rho^*_{TM3}}{\rho^*_{TM4} + C_1 \cdot \rho^*_{TM3} - C_2 \cdot \rho^*_{TM1} + L} \cdot (1 + L) \quad (28)$$

where:
ρ^*_k = apparent reflectance of band k
L = soil adjustment factor
C1, C2 = use of the blue band in correction of the red band for atmospheric aerosol scattering

EVI has been formulated for global vegetation studies and for the improvement in the extraction of canopy biophysical parameters. EVI application to global MODIS data is accessible as part of the NASA-Earth Observing System (EOS) program.

2.3. Orthogonal transformations

The derivation of orthogonal transformation indices is complicated. Principal Component Analysis can be considered as a reference point for orthogonal transformation indices. Selected indices are:

2.3.1. Tasseled Cap transformation

Kauth and Thomas (1976) [60] derived an orthogonal transformation with four components from original Landsat MSS data. They used an imagery repository of an agricultural area, and tried to make a synthesis of crops spectral variation axes. They obtained a 3-D figure, the 'Tasseled Cap'. The four components that Kauth and Thomas calculated, are soil brightness (B), vegetation greenness (G), yellow stuff (Y), and non-such (N):

$$B = 0.332 \cdot \rho_{mms1} + 0.603 \cdot \rho_{mms2} + 0.675 \cdot \rho_{mms3} + 0.262 \cdot \rho_{mms4} \quad (29)$$

$$G = -0.283 \cdot \rho_{mms1} - 0.66 \cdot \rho_{mms2} + 0.577 \cdot \rho_{mms3} + 0.388 \cdot \rho_{mms4} \quad (30)$$

$$Y = -0.899 \cdot \rho_{mms1} + 0.428 \cdot \rho_{mms2} + 0.076 \cdot \rho_{mms3} - 0.041 \cdot \rho_{mms4} \quad (31)$$

$$N = -0.016 \cdot \rho_{mms1} + 0.131 \cdot \rho_{mms2} - 0.452 \cdot \rho_{mms3} + 0.882 \cdot \rho_{mms4} \quad (32)$$

Crist (1985) [61] derived computed Tasseled Cap components for TM data. He derived three components, brightness (B), greenness (G), and wetness (W).

$$B = 0.0243 \cdot \rho_{TM1} + 0.4158 \cdot \rho_{TM2} + 0.5524 \cdot \rho_{TM3} + 0.5741 \cdot \rho_{TM4} + 0.3124 \cdot \rho_{TM5} - 0.2303 \cdot \rho_{TM7} \quad (33)$$

$$G = -0.1603 \cdot \rho_{TM1} - 0.2819 \cdot \rho_{TM2} - 0.4939 \cdot \rho_{TM3} + 0.794 \cdot \rho_{TM4} - 0.0002 \cdot \rho_{TM5} - 0.1446 \cdot \rho_{TM7} \quad (34)$$

$$W = 0.0315 \cdot \rho_{TM1} + 0.2021 \cdot \rho_{TM2} + 0.3102 \cdot \rho_{TM3} + 0.1594 \cdot \rho_{TM4} - 0.6806 \cdot \rho_{TM5} - 0.6109 \cdot \rho_{TM7} \quad (35)$$

TM brightness component is related with total reflectivity of the scene, the greenness component can be related with the concept of NDVI, and the wetness component is related with plant moisture [4,6]. A great amount of research work has been focused on the Tasseled Cap transformation concept [62-65]. For the computation of Tasseled Cap coefficients to local condition and for various sensors, Jackson (1983) [66] provides useful guidelines.

2.3.2. Integral

The basis of this index relies on the absorption effect of water on visible and SWIR bands. The index has been developed in the framework of forest fires research [6]. Integral is computed as:

$$Integal = 0.07 \cdot \rho_{TM1} + 0.08 \cdot \rho_{TM2} + 0.06 \cdot \rho_{TM3} + 0.2 \cdot \rho_{TM5} + 0.27 \cdot \rho_{TM7} \quad (36)$$

Integral is negatively related with Fuel Moisture Content (FMC). Chuvieco et al. (2002) [6] do not consider the near-infrared band to avoid indirect effects (LAI, grass curing) on FMC estimation.

2.4. Continuum Removal and Band Depth

Clark and Roush (1984) [67] established the bases of the Continuum Removal concept. This technique can be considered as the core of Imaging Spectroscopy.

- Continuum: is the 'background absorption' onto which other absorption features are superimposed.
- Individual features: attributed to individual components.

The depth of absorption can be related to the abundance of the absorber and the grain of the material [68]. By searching specific absorption features for individual components (e.g. H_2O, Fe_2S, lignin), and calibrating data with other analytical methods (e.g. X-ray chromatography, HPLC), an accurate quantitative estimation of components can be done.

Clark *et al.* (2003) [69] indicated that the apparent depth of an absorption feature (D) relative to the surrounding continuum in a reflectance or emittance spectrum [67] is:

$$D = 1 - \frac{R_b}{R_c} \tag{37}$$

where:
Rb = reflectance of the absorption-band centre (minimum of the continuum-removed feature)
Rc = reflectance value of the continuum at the wavelength of the band centre

Adapted from Kokaly and Clark (1999) [29], Van Niel (2003) [70] provided equations for continuum-removed band depth analysis of vegetation moisture. They used a very simplified version of band depth analysis with only tree bands, TM4 and TM7 as respectively left and right extremes of the continuum, and TM5 as the absorption-band centre. As previously mentioned, TM band 5 can be related with a leaf water absorption band [4]. TM adapted continuum-removed band depth analysis equations are as follow:

$$D_{TM5} = 1 - R' \tag{38}$$

$$R' = \frac{\rho_{TM5}}{(\rho_{TM4} \cdot (1-c)) + (\rho_{TM7} \cdot c)} \tag{39}$$

$$c = \frac{\lambda_{TM5} - \lambda_{TM4}}{\lambda_{TM7} - \lambda_{TM4}} \approx 0.59359 \tag{40}$$

3. Test site example: imagery and pre-processing

The selected test site is located in the southeast coast of Spain, in Alicante (figure 1). With a Mediterranean climate (hot summers and warm winters), and a semiarid rainfall regimen (mean annual rainfall lower than 300 mm), this test site is composed by a set of coastal wetlands surrounded by salt flats, agricultural and urban areas. These wetlands are included in the list of Ramsar sites and protected as Natural Parks (Salinas de Santa Pola and El Hondo in Crevillente-Elche). A key factor that characterizes these wetlands and their biodiversity is the electrical conductivity of the water bodies, ranging from 2.5 mS/cm, 10 mS/cm for salty waters to more than 220 mS/cm for hypersaline waters (in salt flats). Water inputs of these ecosystems are in the form of *in situ* rainfall, natural river basin runoff, agricultural channels, and seawater channels (for salt flats).

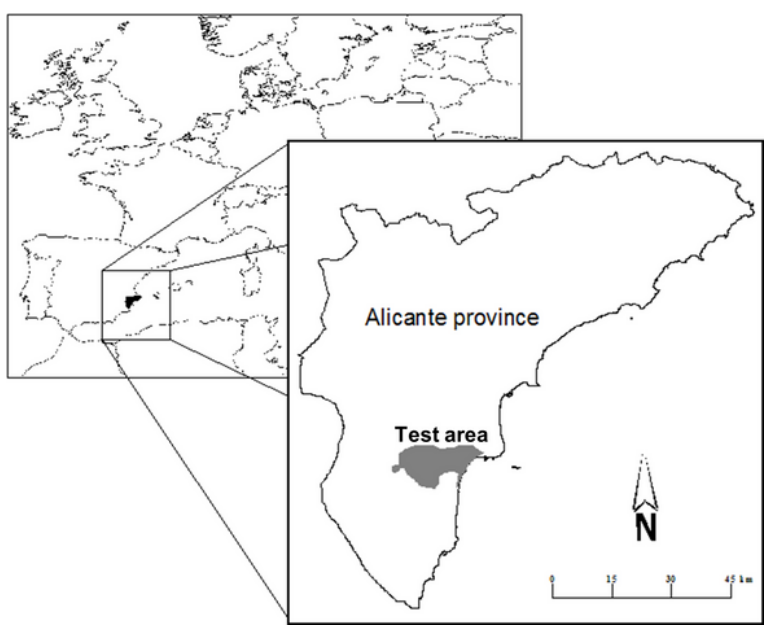

Figure 1. *Test area (Ramsar wetland site) located in south-eastern coast of Spain, in Alicante province.*

A LANDSAT 5 Thematic Mapper scene (path 199, row 33, WRS-2) acquired on 14/08/2005 (10:31:49 a.m.) by ESA (European Space Agency) ground receiving station in Matera (Italy) was used for the analysis. TM bands 2, 3, and 4 covering the study site are shown in figure 2.

An image to map geometric correction using the bilinear function and nearest neighbour resampling method was performed [6,71] using high precision vectorial cartography obtained by digitalisation of aerial orthophotographies at 1 m spatial resolution. The RMS error of the geometrically corrected TM scene was less than half a pixel (13.84 m).

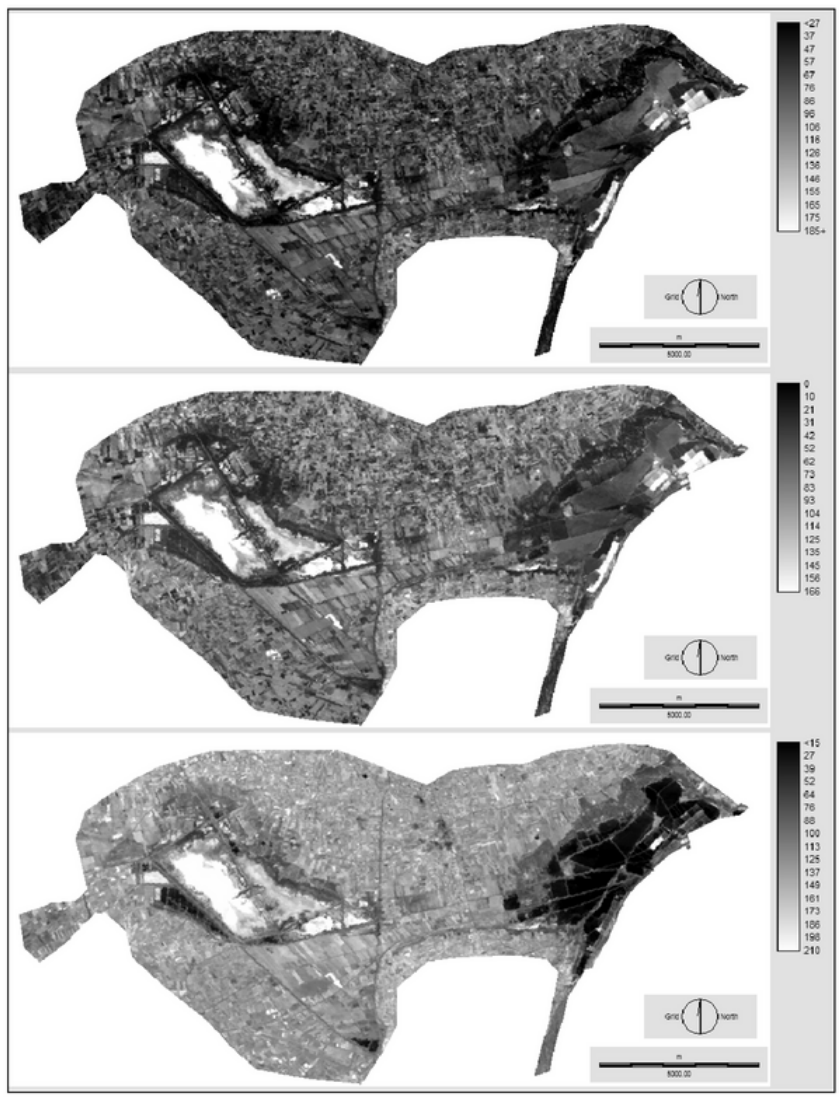

Figure 2. *LANDSAT-TM bands 2, 3, and 4 (from top to bottom) shown as greyscale images of the test area. The image was acquired on 08/14/2005 for path 199, row 33 (WRS-2) by Landsat-5.*

Radiometric calibration of optical bands was carried out according to the guidelines reported by Chander and Markham (2003) [72] for the calculation of exoatmospheric reflectance. They defined two necessary steps. The first one is the conversion of calibrated digital numbers (Qcal) to at-sensor spectral radiance (Lλ):

$$L_\lambda = \left(\frac{LMAX_\lambda - LMIN_\lambda}{Q_{cal\,\max}} \right) \cdot Q_{cal} + LMIN_\lambda \quad (41)$$

where:

Lλ = spectral radiance at the sensor's aperture (W/m²·sr·µm)

Qcal = quantized calibrated pixel value in DNs

Qcal max = maximum quantized calibrated pixel value (DN=255) corresponding to LMAXλ

LMINλ = spectral radiance as scaled to Qcal min in W/(m²·sr·µm)

LMAXλ = spectral radiance as scaled to Qcal max in W/(m²·sr·µm)

LMAXλ and LMINλ values are provided by Chander and Markham [72]. The second step is the conversion from at-sensor radiance (Lλ) to exoatmospheric reflectance (ρP):

$$\rho_P = \frac{\pi \cdot L_\lambda \cdot d^2}{ESUN_\lambda \cdot \cos\theta_S} \quad (42)$$

where:

ρP = planetary or apparent reflectance

Lλ = spectral radiance at the sensor's aperture (W/m²·sr·µm)

d = Earth-Sun distance (A.U.)

ESUNλ = mean solar exoatmospheric irradiances

θS = solar zenith angle (degrees)

Chander and Markham [72] also list the ESUNLλ and *d* values.

Because haze is the most important atmospheric attenuation element [73], a simple dark object subtraction by minimum value of histogram [71] was done in order to obtain an approximation of ground reflectance. Previous studies in Spain have used this atmospheric correction successfully (e.g. [6,74,75]).

In order to improve the visual interpretation of the results and the statistical analysis, a water body mask was built. A normalized ratio of TM bands 1 and 5 reflectance data was calculated based on the singularity of spectral characteristics of water bodies, which show higher reflectance values in the blue spectral region and lower reflectance values in the SWIR spectral region. This ratio was designed as the Normalized Water Bodies Surface Index (NWBSI) and the following formulation is proposed for TM bands based on the spectral characteristics of the water bodies:

$$NWBSI = \frac{\rho_{TM1} - \rho_{TM5}}{\rho_{TM1} + \rho_{TM5}} \tag{43}$$

The selection of TM band 5 as the band representing the SWIR spectral region is due to the occurrence of very intense water band absorption in soils and vegetation with very high moisture contents (typical in wetland ecosystems) in TM band 7 [76] which may generate some confusion. The thresholds selected for the discrimination of water bodies are: NDWSI > 0 for water bodies; NDWSI ≤ 0 for non-water bodies.

For distance-based indices, slope line calculation was done by extracting reflectance data at known bare soil areas. 1,013 pixels were used for the slope line regression analysis (figure 3). Slope coefficient (a = 1.0657) and interception coefficient (b = 0.1059) were calculated. A correlation coefficient (r2) of 0.915 was then obtained.

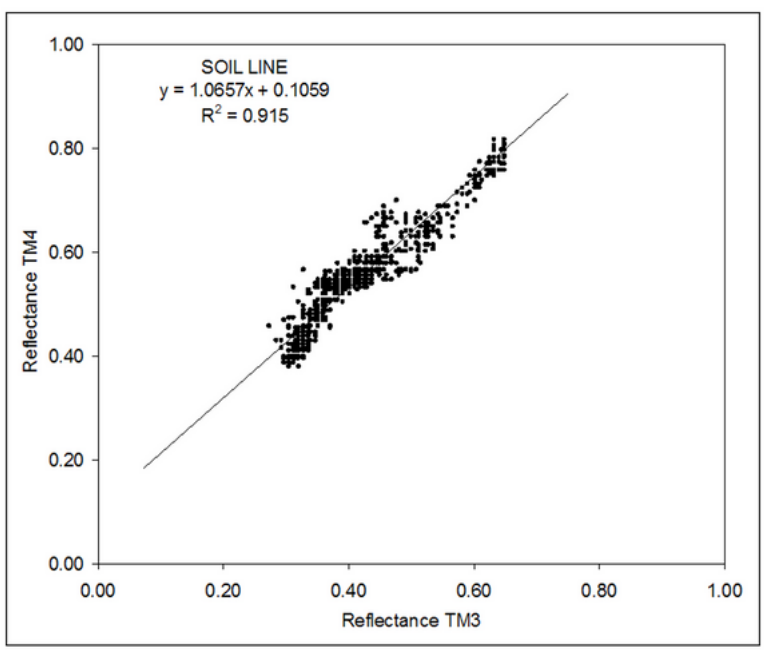

Figure 3. *Linear regression analysis for estimating the soil line using reflectance values of TM bands 3 and 4 (1,013 pixels were used for the regression analysis).*

The high variability within the soils (in relation to moisture, organic matter content, salinity, etc.) required the sampling of a great number of pixels to capture the different soil variations. A smaller number of pixel sampling may provide a higher correlation coefficient value but will not capture accurately the soil variations found in the study area.

4. Experiment: statistical procedure

The computed vegetation indices are presented in Table 1 as classified by the mathematical conceptualization. All the indices were analyzed and tested to determine their potentially redundant information content. Several descriptive values and statistics were computed for all reviewed indices (Table 2).

Table 2. *Descriptive values obtained by the application of the indices to the test area.*

Vegetation index	Mean	Min.	Max.	Std. dev.	Error
ARVI	0.095	-0.600	0.773	0.131	3.286E-04
B-DTM5	0.280	-0.154	0.734	0.058	1.0455E-04
EVI	0.207	-0.111	0.793	0.088	2.207E-04
Greenness	0.089	-0.163	0.556	0.080	2.007E-04
Integral	0.237	0.000	0.45	0.075	1.881E-04
MSARVI	0.009	-0.055	0.07	0.013	3.261E-04
MSI	0.656	0.000	2.000	0.122	3.060E-04
NDII	0.214	-0.333	0.773	0.093	2.333E-04
NDVI	0.282	-0.471	0.844	0.128	3.211E-04
R/G ratio	1.025	0.000	1.458	0.088	2.207E-04
SARVI	0.058	-0.252	0.502	0.080	2.007E-04
SAVI	0.251	-0.185	0.802	0.103	2.584E-04
TSAVI2	0.111	-0.964	0.675	0.114	2.860E-04
Wetness	-0.256	-0.705	0.071	0.094	2.358E-04

For the analysis, 158,938 pixels were used within the study area (and outside the water mask). Mean value, minimum and maximum values, standard deviation, and error (as standard deviation divided by the square root of the number of pixels) were determined for each vegetation index.

For testing the redundant information, a pixel by pixel linear regression analysis was performed on all indices (each index was compared individually against all other indices) in order to evaluate their respective degree of correlation. Slope (*a*) and correlation coefficient (r^2) parameters of the linear regression analysis were used for testing the redundant information. Slope coefficient indicates the type of relation between two indices. This relation can be direct if the slope coefficient is positive, or it can be indirect if the slope coefficient is negative.
Correlation coefficient (r^2) provides a method to assess the degree of similarity between a pair of variables. A high correlation coefficient value indicates a great degree of similarity between both independent and dependent variables. Correlation coefficients (r^2) vary between 0 and 1. As the correlation coefficient nears to 1, the larger is the similarity between the variables.
Slope (*a*) and correlation coefficient (r^2) parameters can provide a method of comparison among vegetation indices. Differences in atmospheric effects, vegetation patterns, and other local characteristics can be ignored, because we assume that they have the same effect on all indices. With this assumption, we can estimate if there are potentially redundant information in the selected indices. Linear regression analysis was done for those indices that provide the same kind of vegetation biophysical information. The two groups are: greenness/biomass indices (ARVI, EVI, Greenness, MSARVI, NDVI, SARVI, SAVI, TSAVI2), and vegetation moisture indices (B-DTM5, Integral, MSI, NDII, Wetness). Other third group can be differentiated based on specific vegetation pigment contents. Within this last group, only Red/Green ratio was included.

5. Results of the experiment

Table 2 provides descriptive values and statistics as obtained from the application of the indices in the test area. Greenness/biomass indices mean values are comprised within the range of 0.009 for MSARVI to 0.282 for NDVI. Vegetation moisture indices mean values are comprised within the range of -0.256 for Wetness to 0.656 for MSI. Error values are low and homogeneous between indices. The lower error value corresponds to MSARVI with an order of magnitude lower than the other indices.

Tables 3 and 4 provide slope (*a*) and correlation coefficient (r^2) values of greenness/biomass indices for the redundant information test. Slope coefficients are presented in table 3 where independent variables are ordered by columns and dependent variables are ordered by rows. In all cases, slope coefficient values are positive, showing that all greenness/biomass indices have a direct relationship.

Table 3. *Slope coefficients (a) of linear regression analysis for greenness/biomass indices.*

		Slope coefficients of regression lines (*a*)							
Dependent variables (*y*)	ARVI		1.44	1.50	10.04	1.01	1.63	1.22	1.09
	EVI	0.64		1.05	6.63	0.64	1.08	0.83	0.76
	Greenness	0.56	0.87		5.86	0.58	0.94	0.76	0.67
	MSARVI	0.10	0.14	0.15		0.10	0.16	0.12	0.11
	NDVI	0.96	1.37	1.50	9.65		1.57	1.20	1.07
	SARVI	0.60	0.89	0.94	6.17	0.61		0.75	0.67
	SAVI	0.76	1.16	1.26	7.81	0.78	1.26		0.90
	TSAVI2	0.81	1.25	1.33	8.23	0.83	1.34	1.07	
		ARVI	EVI	Greenness	MSARVI	NDVI	SARVI	SAVI	TSAVI2
		Independent variables (*x*)							

The correlation coefficients for greenness/biomass indices are shown in table 4. In general, a high degree of correlation between all selected greenness/biomass indices was found as the number of high correlation coefficients shows (for $r^2 \geq 0.9$). As an example, SAVI is highly correlated with all other selected greenness/biomass indices. EVI is also highly correlated with all other selected greenness/biomass indices except for NDVI. On the contrary, Greenness and TSAVI2 are only highly correlated with EVI and SAVI. ARVI, MSARVI, NDVI and SARVI are highly correlated with 4 or 5 indices. SAVI is the highest correlated index for selected greenness/biomass indices.

Table 4. *Correlation coefficients (r^2) of linear regression analysis for greenness/biomass indices.*

	Correlation coefficients (r^2)						
EVI	0.919						
Greenness	0.835	0.914					
MSARVI	0.971	0.949	0.891				
NDVI	0.969	0.877	0.871	0.941			
SARVI	0.987	0.957	0.883	0.992	0.952		
SAVI	0.925	0.967	0.957	0.947	0.941	0.951	
TSAVI2	0.879	0.944	0.895	0.884	0.883	0.893	0.967
	ARVI	EVI	Greenness	MSARVI	NDVI	SARVI	SAVI

Tables 5 and 6 provide slope (*a*) and correlation coefficient (r^2) values of vegetation moisture indices. Slope coefficients are presented in table 5 where independent variables are ordered by columns and dependent variables are ordered by rows.

Table 5. *Slope coefficients (a) of linear regression analysis for vegetation moisture indices.*

		Slope coefficients of regression lines (*a*)				
Dependent variables (*y*)	B-D_{TM5}		-0.15	-0.35	0.46	0.25
	Integral	-0.27		0.40	-0.53	-0.71
	MSI	-1.54	0.97		-1.29	-1.02
	NDII	1.21	-0.76	-0.77		0.79
	Wetness	0.66	-1.06	-0.63	0.82	
		B-D_{TM5}	Integral	MSI	NDII	Wetness
		Independent variables (*x*)				

Selected vegetation moisture indices show direct or inverse relations as a function of the cross-pair of indices. Therefore, their relation is not as clear as greenness/biomass indices.

As an example, MSI shows a direct relation with Integral, and an inverse relation with B-DTM5, NDII, and Wetness. In other case, B-DTM5 shows a direct relation with NDII and Wetness, and an inverse relation with Integral and MSI.

Table 6 shows that highly correlated indices (for $r^2 \geq 0.9$) are not frequent within selected vegetation moisture indices. Only MSI and NDII show a high correlation ($r^2 = 0.988$) between them.

Table 6. *Correlation coefficients (r^2) of linear regression analysis for vegetation moisture indices*

	Correlation coefficients (r^2)			
Integral	0.039			
MSI	0.544	0.384		
NDII	0.563	0.402	0.988	
Wetness	0.161	0.755	0.645	0.648
	$B\text{-}D_{TM5}$	Integral	MSI	NDII

6. Conclusions

The great pool of existing vegetation indices provides important tools for vegetation monitoring and analysis. These indices have the potential to be applied as a common tool for agricultural and natural resources management studies. The indices of greenness/biomass, vegetation moisture, and vegetation pigments content were reviewed and formulated so that they can be easily computed with reflective values of LANDSAT Thematic Mapper (TM) data.

Additionally, a simple method for redundant information testing has been used in order to discriminate similar information contained in these indices. Linear regression analysis has the potential for providing an ubiquitous test, since similar scene conditions are assumed for all computed indices. Detection of direct or inverse relations and the degree of correlation or similarity between indices can be successfully determined.

Although these indices can be grouped according to the purpose for which they were designed and the correlated between them, assuming that they lead to the same biophysical parameter information, several differences have been observed, especially in the magnitude of the values calculated from the reflectance of the bands used. For the area used in this experiment, SAVI appears to be the most appropriate index for greenness/biomass determination although no specific index appears to be the most appropriate in the case of vegetation moisture estimation.

References

1. Steven, M.D., Malthus, T.J., Baret, F., Xu, H., Chopping, M.J. (2003). Intercalibration of vegetation indices from different sensor systems [C]. Remote Sensing of Environment, 88: 412-422. (https://doi.org/10.1016/j.rse.2003.08.010)
2. Richardson, A.J., Everitt, J.H. (1992). Using Spectral Vegetation Indices to Estimate Rangeland Productivity [C]. Geocarto International, 1: 63-77. (DOI: 10.1080/10106049209354353)
3. Lyon, J.G., Yuan, D., Lunetta, R.S., Elvidge, C.D. (1998) A Change Detection Experiment Using Vegetation indices [C]. Photogrammetric Engineering & Remote Sensing, 64, 2: 143-150.
4. Jensen, J.R. (2000). Remote Sensing of the Environment: An Earth Resource Perspective [M]. Upper Saddle River (NJ), USA: Prentice Hall.
5. Jensen, J.R. (2004). Introductory Digital Image Processing. A Remote Sensing Perspective. Third edition. [M] Upper Saddle River (NJ), USA: Prentice Hall.
6. Chuvieco, E., Riaño, D., Aguado, I., Cocero, D. (2002). Estimation of fuel moisture content from multitemporal analysis of Landsat Thematic Mapper reflectance data: applications in fire danger assessment [C]. International Journal of Remote Sensing, 23, 11: 2145-2162. (https://doi.org/10.1080/01431160110069818)
7. Xue, J., Su, B. (2017). Significant Remote Sensing Vegetation Indices: A Review of Developments and Applications [C]. Journal of Sensors, 2017, Article ID 1353691. (https://doi.org/10.1155/2017/1353691)
8. Cetin, M., Sevik, H. (2016). Evaluating the recreation potential of Ilgaz Mountain National Park in Turkey [C]. Environmental Monitoring and Assessment, 188, 52. (https://doi.org/10.1007/s10661-015-5064-7)
9. Potapov, P., Yaroshenko, A., Turubanova, S., Dubinin, M., Laestadius, L., Thies, C., Aksenov, D., Egorov, A., Yesipova, Y., Glushkov, I., Karpachevskiy, M., Kostikova, A., Manisha, A., Tsybikova, E., Zhuravleva, I. (2008). Mapping the World's Intact Forest Landsacapes by Remote Sensing [C]. Ecology and Society, 13, 2: 51. (http://www.ecologyandsociety.org/vol13/iss2/art51/)

10. Curran, P. (1980). Multiespectral remote sensing of vegetation amount [C]. Progress in Physical Geography: Earth and Environment, 4, 3: 315-341. (https://doi.org/10.1177/030913338000400301)
11. Running, S.W., Loveland, T.R, Pierce, L.L., Nemani, R.R., Hunt, E.R. Jr. (1995). A Remote Sensing Based Vegetation Classification Logic for Global Land Cover Analysis [C]. Remote Sensing of Environment, 51: 39-48. (https://doi.org/10.1016/0034-4257(94)00063-S)
12. Estes, J.E., Jensen, J.R., Simonett, D.S. (1980). Impacts of remote sensing on the U.S. Geography [C]. Remote Sensing of Environment, 10: 43-80. (https://doi.org/10.1016/0034-4257(80)90098-X)
13. Houborga, R., Soegaard, H., Boeghb, E. (2007). Combining vegetation index and model inversion methods for the extraction of key vegetation biophysical parameters using Terra and Aqua MODIS reflectance data [C]. Remote Sensing of Environment, 106, 1: 39-58. (https://doi.org/10.1016/j.rse.2006.07.016)
14. Jensen, J.R. (1983). Biophysical Remote Sensing. Review Article [C]. Annals of the Association of American Geographers, 73, 1: 111-132. (https://doi.org/10.1111/j.1467-8306.1983.tb01399.x)
15. Jensen, J.R., Coombs, C., Porter, D., Jones, B., Schill, S., White, D. (1998). Extraction of Smoth Cordgrass (Sparthina alterniflora) Biomass and Leaf Area Index Parameters from High Resolution Imagery [C]. Geocarto International, 13, 4:25-46. (https://doi.org/10.1080/10106049809354661)
16. Hanna, M.M., Steyn-Ross, D.A., Steyn-Ross, M. (1999). Estimating Biomass for New Zealand Pasture Using Optical Remote Sensing Techniques [C]. Geocarto International, 14, 3: 89-94. (https://doi.org/10.1080/10106049908542121)
17. Haboudane, D., Miller, J.R., Pattey, E., Zarco-tejada,P., Strachan, I.B. (2004). Hiperespectral vegetation indices and novel algorithms for predicting green LAI of crop canopies: Modelling and validation in the context of precision agriculture [C]. Remote Sensing of Environment, 90: 337-352. (DOI:10.1016/j.rse.2003.12.013)
18. Muukkonen, P. & Heiskanen, J. (2005). Estimating biomass for boreal forests using ASTER satellite data combined with standwise forest inventory data [C]. Remote Sensing of Environment, 99, 4: 434-447. (DOI: 10.1016/j.rse.2005.09.011)
19. Gitelson, A.A. (2004) Wide Dynamic Range Vegetation Index for Remote Quantification of Biophysical Characteristics of Vegetation [C]. Journal of Plant Physiology. 161, 2: 165-173. (https://doi.org/10.1078/0176-1617-01176)
20. Jackson, R.D. (1982). Canopy temperature and crop water stress [C]. Advances in Irrigation Research, 1:45-85. (https://doi.org/10.1016/B978-0-12-024301-3.50009-5)
21. Hunt, E.R., Rock, B.N., Nobel, P.S. (1987). Measurement of Leaf Relative Water Content by Infrared Reflectance [C]. Remote Sensing of Environment, 22: 429-435. (https://doi.org/10.1016/0034-4257(87)90094-0)

22. Hunt, E.R., Rock, B.N. (1989). Detection of Changes in Leaf Water Content Using Near- and Middle-Infrared Reflectances [C]. Remote Sensing of Environment, 30: 43-54. (https://doi.org/10.1016/0034-4257(89)90046-1)
23. Gao, B.C. (1996). NDWI. A normalized difference water index for remote sensing of vegetation liquid water from space [C]. Remote Sensing of Environment, 58: 257-266. (https://doi.org/10.1016/S0034-4257(96)00067-3)
24. Gamon, J.A., Surfus, J.S. (1999). Assessing leaf pigment content and activity with a reflectometer [C]. New Phytologist, 143: 105-117. (https://doi.org/10.1046/j.1469-8137.1999.00424.x)
25. Gamon, J.A., Serrano, L., Surfus, J.S. (1997). The photochemical reflectance index: an optical indicator of photosynthetic radiation use efficiency across species, function types, and nutrient levels [C]. Acta Oecologica, 112: 492-501. (https://doi.org/10.1007/s004420050337)
26. Sims, D.A., Gamon, J. (2002). Relationships between leaf pigment content and spectral reflectance across a wide range os species, leaf structures and developmental stages [C]. Remote Sensing of Environment, 81, 2-3: 337-354. (DOI: 10.1016/S0034-4257(02)00010-X)
27. Schultz, M., Clevers, J.G.P.W., Carter, S., Verbesselt, J., Avitabile, V., Quang, H.V., Herold, M. (2016). Performance of vegetation indices from Landsat time series in deforestation monitoring [C]. International Journal of Applied Earth Observation and Geoinformation, 52: 318-327. (https://doi.org/10.1016/j.jag.2016.06.020)
28. Huete, A., Justice, C. (1999). MODIS Vegetation Index (MOD 13) Algorithm Theoretical Basis Document. Version 3 [S]. Greenbelt (MD), USA: NASA Goddard Space Flight Center.
29. Kokaly, R.F., Clark, R.N. (1999). Spectroscopic Determination of Leaf Biochemistry using Band-Depth Analysis of Absorption Features and Stepwise Multiple Linear Regression [C]. Remote Sensing of Environment, 67: 267-287. (https://doi.org/10.1016/S0034-4257(98)00084-4)
30. Jackson, R.D., Huete, A.R. (1991). Interpreting vegetation indices [C]. Preventive Veterinary Medicine, 11: 185-200. (https://doi.org/10.1016/S0167-5877(05)80004-2)
31. Eastman, J.R. (2003). IDRISI Kilimanjaro. Guide to GIS and Image Processing [S]. Worcester (MA), USA: Clark University.
32. Fox, G.A., Sabbagh, G.J. (2002). Estimation of Soil Organic Matter from Red and Near-Infrared Remotely Sensed Data Using a Soil Line Euclidean Distance Technique [C]. Soil Science Society of America Journal, 66, 6: 1922-1929. (DOI:10.2136/sssaj2002.1922)
33. Clark, R.N., Roush, T.L. (1984). Reflectance spectroscopy: quantitative analysis techniques for remote sensing applications [C]. Journal of Geophysical Research, 89: 6329-6340. (https://doi.org/10.1029/JB089iB07p06329)
34. Clark, R.N. (1999). Chapter 1: Spectroscopy of Rocks and Minerals, and Principles of Spectroscopy. In: Rencz, A.N. (ed.) [M]. Manual of Remote Sensing, Volume 3, Remote Sensing for the Earth Sciences. New York (USA): John Wiley & Sons, Ltd.: 3-58. (ISBN: 0471-29405-5)

35. Rouse, J.W., Haas, R.H., Schell, J.A., Deering, D.W. (1974). Monitoring Vegetation Systems in the Great Plains with ERTS [S]. Proceeding, Third Earth Resources Technology Satellite-1 Symposium, NASA SP-351. Goddard Space Flight Center, Greenbelt (MD), USA: 309-317.
36. [36] Birth, G.S., McVey, G. (1968). Measuring the Color of Growing Turf with a Reflectance Spectrophotometer [C]. Agronomy Journal, 60, 6: 640-643. (DOI:10.2134/agronj1968.00021962006000060016x)
37 [37] Deering, D.W., Rouse, J.W., Haas, R.H., Schell, J.A. (1975). Measuring Forage Production of Grazing Units from Landsat MSS data [S]. Proceedings of the 10th International Symposium on Remote Sensing of Environment, ERIM 2. Ann Arrbor, USA: 1169-1178.
38. [38] Chuvieco, E. (2002). Teledetección ambiental. La observación de la Tierra desde el espacio [M]. Barcelona (Spain): Ariel Ciencia. (ISBN: 8434480727)
39. [39] Rondeaux, G., Steven, M., Baret, F. (1996) Optimization of Soil-Adjusted Vegetation Indices [C]. Remote Sensing of Environment, 55: 95-107. (https://doi.org/10.1016/0034-4257(95)00186-7)
40. [40] Verhoef, W. (1984). Light scattering by leaf layers with application to canopy reflectance modelling: the SAIL model [C]. Remote Sensing of Environment, 16, 2: 125-141. (https://doi.org/10.1016/0034-4257(84)90057-9)
41. [41] Kuusk, A. (1991). The hot-spot effect in plant caopy reflectance [M]. In R.B. Myneni and J. Ross Eds.), Photon-Vegetation interactions, Application in Optical Remote Sensing and Plant Ecology. New York: Springer Verlag.: 139-159. (DOI: 10.1007/978-3-642-75389-3_5)
42. [42] Huete, A.R. (1988) A Soil Adjusted Vegetation Index (SAVI) [C]. Remote Sensing of Environment, 25, 3: 295-309. (https://doi.org/10.1016/0034-4257(88)90106-X)
43. [43] Huete, A.R., Hua, G., Qi, J., Chehbouni, A., Van Leeuwem, W.J. (1992). Normalization of Multidirectional Red and Near-Infrared Reflectances with the SAVI [C]. Remote Sensing of Environment, 41, 2-3: 143-154. (https://doi.org/10.1016/0034-4257(92)90074-T)
44. [44] Steven, M.D. (1998). The sensitivity of the OSAVI vegetation index to observational parameters [C]. Remote Sensing of Environment, 63, 1: 49-60. (https://doi.org/10.1016/S0034-4257(97)00114-4)
45. [45] Kaufman, Y.J., Tanre, D. (1992). Atmospherically Resistant Vegetation index (ARVI) for EOS-MODIS [C]. IEEE Transactions on Geosciences and Remote Sensing, 30, 2: 261-270. (DOI: 10.1109/36.134076)
46. [46] Hardisky, M.A., Klemas, V., Smart, M. (1983). The Influence of Soil Salinity, Growth From, and Leaf Moisture on the Spectral Radiance of Spartina alternifolia Canopies [C]. Photogrammetric Engineering and Remote Sensing, 49, 1: 77-83. (DOI: 0099-1112183/4901-77$02.25/0)
47. Carter, G. (1991). Primary and Secondary Effects of Water Content on the Spectral Reflectance of Leaves [C]. American Journal of Botany, 78, 7: 916-924. (https://doi.org/10.1002/j.1537-2197.1991.tb14495.x)

48. Ceccato, P., Flasse, S., Tarantola, S., Jacquemound, S., Grégoire, J.M. (2001). Detecting vegetation leaf water content using reflectance in the optical domain [C]. Remote Sensing of Environment, 77, 1: 22-33. (https://doi.org/10.1016/S0034-4257(01)00191-2)
49. Gould, K.S., Kuhn, D.N., Lee, D.W., Oberbauer, S.F. (1995). Why leaves are sometimes red [S]. Nature, 378, 6554: 241-242. (DOI: 10.1038/378241b0)
50. Coley, P.D., Aide, T.M., (1989). Red coloration of tropical young leaves: a possible anti-fungal defence? [C]. Journal of Tropical Ecology, 5, 03: 293-300. (DOI:10.1017/S0266467400003667)
51. Coley, P.D., Barone, J.A. (1996). Herbivory and plant defenses in tropical forest [C]. Annual Review of Ecology and Systematics, 27: 305-335. (https://doi.org/10.1146/annurev.ecolsys.27.1.305)
52. Qi, J., Chehbouni, Al, Huete, A.R., Kerr, Y.H., Sorooshian, S. (1994). A modified soil adjusted vegetation index (MSAVI) [C]. Remote Sensing of Environment, 48, 2: 119-126. (DOI: 10.1016/0034-4257(94)90134-1)
53. Richardson, A.J., Wiegand, C.L. (1977). Distinguishing vegetation from soil background information [C]. Photogrammetric Engineering & Remote Sensing, 43, 12: 1541-1552. (ISSN: 0099-1112)
54. Fox, G.A., Sabbagh, G.J., Searcy, S.W., Yang, C. (2004). An Automated Soil Line Identification Routine for Remotely Sensed Images [C]. Soil Science Society of America Journal, 68, 4: 1326-1331. (DOI:10.2136/sssaj2004.1326)
55. Clevers, J.G.P.W. (1988). The derivation of a simplified reflectance model for the estimation of leaf area index [C]. Remote Sensing of Environment, 25, 1:53-69. (https://doi.org/10.1016/0034-4257(88)90041-7)
56. Clevers, J.G.P.W., Verhoef, W. (1993). LAI estimation by means of the WDVI: A sensitivity analysis with a combined PROSPECT-SAIL model [C]. Remote Sensing Reviews, 7, 1: 43-64. (DOI:10.1080/02757259309532165)
57. Baret, F., Guyot, G.; Major, D. (1989). TSAVI: A Vegetation Index Which Minimizes Soil Brightness Effects on LAI and APAR Estimation [S]. 12th Canadian Symposium on Remote Sensing and IGARSS' 90. Volume 4. Vancouver, Canada.: 10-14. (DOI: 10.1109/IGARSS.1989.576128)
58. Gilabert, M.A., González-Piqueras, J., García-Haro, F.J., Meliá, J. (2002). A generalizad soil-adjusted vegetation index [C]. Remote Sensing of Environment, 82, 2-3: 303-310. (https://doi.org/10.1016/S0034-4257(02)00048-2)
59. Huete, A.R., Liu, H.Q. (1994). An Error and Sensitivity Analysis of the Atmospheric- and Soil-Correcting Variants of the Normalized Difference Vegetation Index for the MODIS-EOS [C]. IEEE Transactions on Geosciences and Remote Sensing, 32, 4: 897-905. (DOI: 10.1109/36.298018)

60. Kauth, R.J., Thomas, G.S. (1976). The Tasseled Cap: A Graphic Description of the Spectral Temporal Development of Agricultural Crops as Seen By Landsat [S]. In Proceedings, Machine Processing of Remotely Sensed Data. Laboratory for the Applications of Remote Sensing (LARS), Purdue University, West Lafayette (IN), USA: 41-51. (http://docs.lib.purdue.edu/lars_symp/159)
61. Crist, E.P. (1985). A Thematic Mapper Tasseled Cap Equivalent for Reflectance Factor Data [C]. Remote Sensing of Environment, 17, 3: 301-306. (https://doi.org/10.1016/0034-4257(85)90102-6)
62. Crist, E.P. (1983). The TM tasselled cap: A preliminary formulation [S]. In Proceedings of the Symposium on Machine Processing of Remotely Sensed Data. Laboratory for the Applications of Remote Sensing (LARS), Purdue University, West Lafayette (IN), USA: 357-364.
63. Crist, E.P., Cicone, R.C. (1984a). Comparison of the dimensionality and features of simulated Landsat-4 MSS and TM data [C]. Remote Sensing of Environment, 14, 1-3: 235-246. (https://doi.org/10.1016/0034-4257(84)90018-X)
64. Crist, E.P., Cicone, R.C. (1984b). A physically-based transformation of thematic mapper data – the TM Tasseled Cap [C]. IEEE Transactions on Geoscience and Remote Sensing, 22, 3: 256-263. (DOI: 10.1109/TGRS.1984.350619)
65. Crist, E.P., Kauth, (1986). The Tasselled Cap demystified [C]. Photogrammetric Engineering and Remote Sensing, 52, 1: 81-86. (DOI: 0099-1112186/5201-0081$02.25/0)
66. Jackson, R.D. (1983). Spectral Indices in n-Space [C]. Remote Sensing of Environment, 13, 5: 409-421. (https://doi.org/10.1016/0034-4257(83)90010-X)
67. Clark, R.N., Roush, T.L. (1984). Reflectance spectroscopy: quantitative analysis techniques for remote sensing applications [C]. Journal of Geophysical Research, 89, B7: 6329-6340. (DOI: 10.1029/JB089iB07p06329)
68. Clark, R.N. (1999). Chapter 1: Spectroscopy of Rocks and Minerals, and Principles of Spectroscopy [M]. In: Rencz, A.N. (ed.). Manual of Remote Sensing, Volume 3, Remote Sensing for the Earth Sciences. New York (USA): John Wiley & Sons, Ltd.: 3-58.
69. Clark, R. N., Swayze, G. A., Livo, K. E., Kokaly, R. F., Sutley, S. J., Dalton, J. B., McDougal, R. R., Gent, C. A. (2003). Imaging Spectroscopy: Earth and Planetary Remote Sensing with the USGS Tetracorder and Expert Systems [C]. Journal of Geophysical Research, 108, E12: 5131. (DOI:10.1029/2002JE001847.v)
70. Van Niel, T.G., McVicar, T.R., Fang, H., Liang, S. (2003). Calculating environmental moisture for perfield discrimination of rice crops [C]. International Journal of Remote Sensing, 24, 4: 885-890. (DOI:10.1080/0143116021000009921)
71. Mather, P.M. (2004). Computer Processing of Remotely Sensed Images. An Introduction [M]. Third edition. West Sussex (England), UK: John Wiley & Sons, Ltd. (ISBN: 9780470849187)
72. Chander, G., Markham, B. (2003). Revised Landsat-5 TM radiometric calibration procedures and postcalibration dynamic ranges [R]. IEEE Transactions of Geosciences and Remote Sensing, 41, 11: 2674-2677. (DOI: 10.1109/TGRS.2003.818464)

73. Chavez, P. (1988). An improved dark-object subtraction technique for atmospheric scattering correction of multispectral data [C]. Remote Sensing of Environment, 24, 3: 459-479. (https://doi.org/10.1016/0034-4257(88)90019-3)
74. Koch, M. (2000). Geological controls of land degradation as detected by remote sensing: a case study in Los Monegros, north-east Spain [C]. International Journal of Remote Sensing, 21, 3: 457-473. (DOI:10.1080/014311600210687)
75. Dewa, R.P., Danoedoro, P. (2017). The effect of image radiometric correction on the accuracy of vegetation canopy density estimate using several Landsat-8 OLI's vegetation indices: A case study of Wonosari area, Indonesia [S]. IOP Conference Series: Earth and Environmental Science, 54, 012046. (DOI:10.1088/1755-1315/54/1/012046)
76. Hoffer, R.M. (1978). Biological and physical considerations in applying computer-aided analysis techniques to remote sensor data. In Swain, P.H. and Davis, S.M. (eds.), Remote Sensing: The Quantitative Approach, McGraw- Hill Book Company, New York: 227-289.

Embalse de la Pedrera, Alicante.
Fotografía: Gema Marco Dos Santos

Marco Dos Santos, G., Meléndez-Pastor, I.. Navarro-Pedreño, J., , Koch, M. (2019).

Assessing water availability in Mediterranean regions affected by water conflicts through MODIS data time series analysis.

Remote sensing, 11(11), 1355.

https://doi.org/10.3390/rs11111355

Abstract

Water scarcity is a widespread problem in arid and semi-arid regions such as the western Mediterranean coastal areas. The irregularity of the precipitation generates frequent droughts that exacerbate the conflicts among agriculture, water supply and water demands for ecosystems maintenance. Besides, global climate models predict that climate change will cause Mediterranean arid and semi-arid regions to shift towards lower rainfall scenarios that may exacerbate water conflicts. The purpose of this study is to find a feasible methodology to assess current and monitor future water demands in order to better allocate limited water resources. The interdependency between a vegetation index (NDVI), land surface temperature (LST), precipitation (current and future), and surface water resources availability in two watersheds in southeastern Spain with serious di culties in meeting water demands was investigated. MODIS (Moderate Resolution Imaging Spectroradiometer) NDVI and LST products (as proxy of drought), precipitation maps (generated from climate station records) and reservoir storage gauging information were used to compute times series anomalies from 2001 to 2014 and generate regression images and spatial regression models. The temporal relationship between reservoir storage and time series of satellite images allowed the detection of di erent and contrasting water management practices in the two watersheds. In addition, a comparison of current precipitation rates and future precipitation conditions obtained from global climate models suggests high precipitation reductions, especially in areas that have the potential to contribute significantly to groundwater storage and surface runo , and are thus critical to reservoir storage. Finally, spatial regression models minimized spatial autocorrelation e ects, and their results suggested the great potential of our methodology combining NDVI and LST time series to predict future scenarios of water scarcity.

Keywords

Vegetation index; precipitation; LST; water supply; semiarid; Mediterranean; spatial regression

1. Introduction

Spain is among the countries at higher risk of climate change [1,2] due to its geographical location, the complex topography and the high population density, especially in coastal regions [3]. The risk of water resources overexploitation is evident and requires the development of integrated and sustainable strategies in order to maintain socioeconomic activities [4] and preserve natural resources and ecosystems [5].

In this sense, remote sensing has demonstrated its enormous capabilities to retrieve information and to assess, monitor and predict environmental processes and functions [6,7]. Geospatial research programs that combine multiple platforms and sensors have allowed for the collection of an exceptional body of knowledge of the evolution of the Earth in recent decades. Projects such as the Earth Observing System (EOS) from the United States National Aeronautics and Space Administration (NASA) or the Copernicus Earth Observation Program from the European Space Agency (ESA) are outstanding platforms of knowledge generation for sustainable natural resources planning and control.

The semiarid Mediterranean climate greatly influences seasonal water availability for human use. The growing demand for food due to the increase in the world's population has meant a great change in the agricultural sector with an increasing demand for water resources [8] to enable the intensification of agricultural activities to meet those needs. Irrigation systems promote the development of crops and thus increase water demands in areas where water is scarce by default [9] at the expense of losing natural ecosystems.

In addition, tourism contributes to the increase in water demands, which has a great impact on the Mediterranean coast of SE Spain. For example, in the present study area, during the summer (and water shortage period), a city like Benidorm can double or more the number of inhabitants [10]. In this sense, dams and reservoirs have an important role in securing water for domestic use and irrigation in periods of scarcity and high demand [3,11].

General Circulation Models (GCMs) are used to make future climate projections and simulate the response of the global system to di erent scenarios of increasing greenhouse gases concentrations. There are many GCMs that o er di erent results depending on the model used and the chosen emission scenario [12]. In southern Europe, the Intergovernmental Panel for Climate Change (IPCC) models for the end of the 21st century [8] predicts a temperature increase and an even more intense decrease

in precipitation rates. These scenarios of higher water scarcity will mean more intense summer droughts and longer periods of inter-annual droughts. They will promote a decrease of soil water content, as well as aquifers recharge. Future lower precipitations would result in increased pressure on water resources by di erent sectors, which would worsen the problem of water demands in areas already dealing with this issue [9]. Under these conditions of demographic changes and uncertain global climate change scenarios, in which the availability of water is threatened, the e cient management of water resources in semi-arid zones should focus on a sustainable economic, social and environmental use that guarantees the supply for all uses in an equitable manner [13,14].

The e fect of climate change on Mediterranean arid and semi-arid regions will most likely be a shift towards lower rainfall scenarios that accelerate the desertification process [15]. Under these conditions in which precipitation decreases and the temperature increases, semi-arid zones can face large water losses due to high evapotranspiration and aggravate scarcity [16]. Remote-sensing products such as NDVI and LST have proven to be valuable proxies for monitoring vegetation dynamics [17], land surface moisture conditions [18], yield estimates [19], soil evaporation rates [20], and drought vulnerability [21]. In the context of generating early alert systems, various spectral indexes have been developed for monitoring droughts, such as the Vegetation Temperature Condition Index-VTCI [22,23], the Vegetation SupplyWater Index-VSWI [24] or the Soil Moisture Agricultural Drought Index-SMADI [25] among others.

The relationship between LST and NDVI has been generally described as having a negative correlation (e.g., Refs. [21,26]) with steeper slopes for dryer conditions [25]. However, the relationship between LST and NDVI may exhibit notable spatial [27] and temporal [26] alterations, and new research is needed in order to assess the sensitivity and resilience of ecosystems to climate variability [28]. In order to examine and understand the response patterns of vegetation indices to current climate variability (from 2001 to 2014) and water demands in the study area, the following questions are explored in this work: (1) Does a significant correlation exist between NDVI, LST and precipitation time series anomalies? (2) Similarly, does a significant correlation exist between NDVI, LST and water reservoir storage anomalies? (3) Can remotely sensed time series data (NDVI, LST) be used together with water reservoir storage changes to spatially and temporally assess current water demands and predict future water needs?
The objective of our research is the development of a feasible methodology to assess current and monitor future water demands with remote sensing in order to better allocate limited water resources and alleviate water conflicts. In this sense, this work presents an approach to evaluate the spatial-temporal relationships among remotely-sensed vegetation spectral indices (specifically NDVI) and land surface temperature (LST)

vegetation time series, in relation to precipitation (current rates and future predictions) and available water resources (i.e., volume of water stored in reservoirs) over two medium-small-sized western Mediterranean watersheds. Both Mediterranean watersheds were selected because they constitute a conjunctive water resources management system and their climatic variability, limited availability of water resources, and vast demands for anthropic activities during dry periods generate socio-economic and environmental water use conflicts. The paper is organized in the following manner:

- Time series of MODIS data (i.e., NDVI and LST) were compiled and used to compute their time series anomalies for temporal change detection. Current precipitation and reservoir storage time series anomalies were also computed.
- The correlation among time series anomalies was statistically assessed. Additionally, correlation images between reservoir storage and the spatial variables (NDVI, LST and current precipitation) were computed. The use of a land cover map, along with bibliographic references and the knowledge of the study area allowed the identification of areas and land uses that may influence the availability of water resources.
- Finally, spatial regression analysis was used to evaluate the potential of NDVI and LST time series as predictors of future precipitation changes by taking into account the spatial autocorrelation of the variables.

2. Materials and Methods

The study area lies in the Comarca of Marina Baja in northern Alicante Province (SE Spain). It is located around 38 360 N and 0 100 W. This region is part of the Subbaetic Range [29]. It is characterized by its very steep orography, including beaches and coves surrounded by large cli s and rugged mountains (Figure 1).

The Marina Baja encloses densely populated coastal urban areas and tourist resorts (e.g., Benidorm). The main agricultural activities comprise irrigated fruit trees (loquat and citrus) in areas of low to moderate elevation and slope, and rainfed crops such as olive and almond trees [30]. Antique cultivation terraces are still being used. Natural Mediterranean vegetation includes pine forests (Pinus sp.) and xerophytic shrubs (e.g., Rosmarinum o cinalis, Thymus sp., etc.). The area is prone to natural or man-induced summer wildfires, which greatly impact the natural vegetation landscape, wildlife and human activities. Based on theWorld Reference Base for Soil Resources [31], the dominant soil types are Calcisols in the lowlands and Leptosols at the mountain slopes [32].

This study focuses on two main watersheds of the Comarca of Marina Baja, namely Algar-Guadalest and Amadorio (Figure 1). Both basins are similar in size and orography, each one contains a reservoir, and their slightly di erent topographic orientation induces climatic variations. They are separated by a line of summits of more than 1400 m of elevation (Aitana is the highest peak with 1557 m a.s.l.) that are at a distance of less than 10 km from the coastline. The Algar-Guadalest watershed covers an area of 215 km2 and its dominant orientation is NW-SE. The mean elevation is 555 m a.s.l. (meters above sea level), and the average slope is 19.6 . Two main rivers (Algar and Guadalest) drain the basin. The Guadalest river sub-basin includes a reservoir with a total volume of 0.013 km³. The Amadorio watershed covers an area of 225 km², and the dominant orientation is N-S. The mean elevation is 610 m a.s.l. and the average slope is 18.3 . The Amadorio river includes a reservoir with a total volume of 0.016 km³. The climate is typically Mediterranean with annual average values of mean air temperature higher than 17 C along the coastline. The orographic characteristics greatly influence spatio-temporal precipitation patterns. Dominant Köppen-Geiger climate classes are Bsk (cold steppe) in the lowlands and Csb (temperate with dry or temperate summer) in the mountains [33].

The Marina Baja is an interesting case of water resources management in semi-arid areas. It is a region with a high competition for land occupation, evidenced by the abandonment of traditional agricultural practices in favor of intensive irrigated agriculture and a massive urban development [34]. This process leads to a progressive increase in water demands, in a region where the availability of water resources is really scarce. It is evident that there is a conflict between the uses of water and the need for integrated water management in the area [35]. The great problem of water management in the Marina Baja has motivated the development of multidisciplinary studies to optimize the use of water resources, such as procedures for water exchange contracts instead of emerging water markets [35] among others.

The Comarca of Marina Baja has a complex system of conjunctive use of diverse water resources. The Consorcio de Aguas de la Marina Baja is the organism devoted to manage those water resources (http://www.consorciomarinabaja.org/). The main components of the system are Guadalest and Amadorio reservoirs that are mainly used for urban supply.

Both reservoirs were originally built for irrigation purposes, but the Consorcio de Aguas de la Marina Baja has promoted agreements with farmers by which these trade their water with Benidorm and other towns' treated wastewater of enough quality to be used for irrigation, and obtain several compensations in return [36]. The availability of natural water resources (i.e., precipitation, river flow and groundwater) in the watersheds has been highly irregular over time and still is. However, the system has been able to serve urban water demands since the 1970s. The continued use of groundwater as input to the Guadalest reservoir permits a higher regularity in water releases [37].

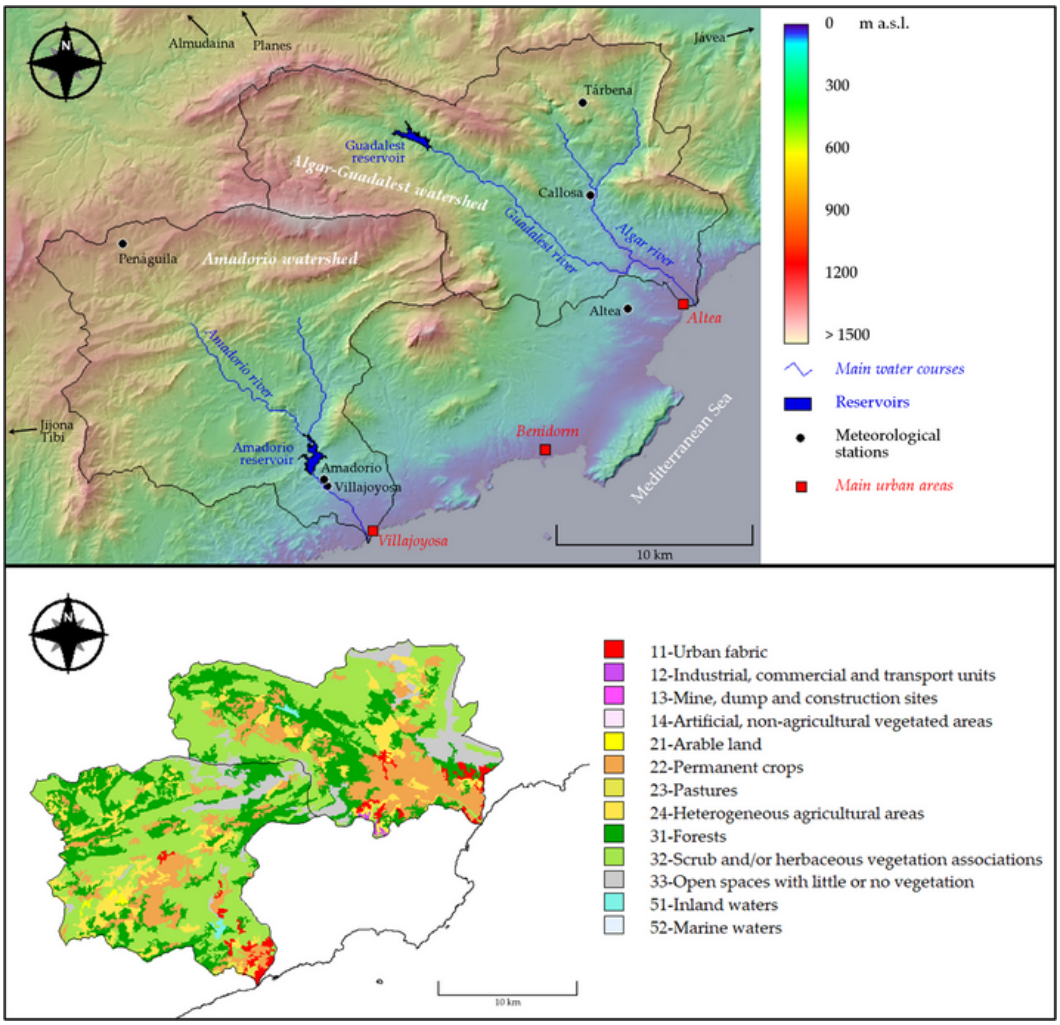

Figure 1. *Maps describing the study area. (Top) Delineation of the Amadorio and Algar-Guadalest watersheds. Main rivers and reservoirs are shown. Meteorological stations are indicated by black dots and stations outside the map boundary by arrows. The background image is the digital elevation model employed in the analyses. (Bottom) CORINE 2012 land cover map. Level 2 of the legend schematization is shown.*

2.1. Remote-Sensing images and ancillary geospatial information

Vegetation and LST dynamics were observed with a time series of TERRA-MODIS images (Moderate Resolution Imaging Spectroradiometer) from 2001 to 2014. Vegetation status was assessed with a spectral vegetation index, namely the Normalized Di erences Vegetation Index (NDVI). The NDVI [38] has been extensively employed as a way to monitor vegetation status by computing seasonal and temporal profiles of vegetation activity (e.g., seasonal and phenologic activity, length of the growing season, peak greenness, onset of greenness, and leaf turnover or 'dry-down' period), which enable inter-annual comparisons of vegetation status [39]. Furthermore, LST was retrieved from the thermal bands of the MODIS sensor. LST is an indicator for evapotranspiration, soil moisture and vegetation water stress [27].

Two types of high processing level MODIS products (Level 3-Land products) were employed for our analyses: (1) NDVI composite images acquired at 16-day time interval and 500 m spatial resolution (MOD13A1); and (2) LST composite images acquired at 8-day time interval with a spatial resolution of 1 km (MOD11A2). All the images were obtained from the U.S. Geological Survey-Earth Explorer geodatabase (URL: https://earthexplorer.usgs.gov/). The study area expands across two MODIS tiles. Therefore, the original images had to be mosaicked pairwise for each date. Subsequently, MODIS data were transformed from Sinusoidal projection to UTM-European Terrestrial Reference System 1989 (ETRS89) projection for extracting a subset of 38 28 km over the study area. The nominal spatial resolution selected for all the analyses was 1 km. Annual average and standard deviation images were computed. The number of spurious pixels was very low due to the sunny and clear sky condition of the study area throughout the year. However, spurious pixel values were replaced with the average value from the surrounding pixels (3x3 filter).

For the geospatial analyses, several cartographic data sources were employed. A digital elevation model (DEM) from the National Institute of Geography of Spain (IGN) was used for watershed analysis. Topographic characteristics of the watershed were computed utilizing the original resolution of the DEM (25 m). Land cover information was obtained from the European Union CORINE Land Cover project (URL: https://land.copernicus.eu). A land cover map from 2012 (Figure 2b) was used to assist in the interpretation of remote-sensing data results. Furthermore, o cial watershed boundaries and main river courses were obtained from the Hydrographic Confederation of the Júcar River, a national public organism in charge of the planning and control of the watersheds nearby the Júcar River basin (situated in East Spain). A mask of the watersheds was developed and employed to extract individual pixel values for further analyses. ENVI 5 (Harris Geospatial Solutions, Broomfield, CO, USA) and TerrSet

(Clark Labs,Worcester, MA, USA) software were used for digital image processing and GIS (Geographical Information System) analyses.

2.2. Climate and reservoirs storage data

Climatic variables were obtained from the 11 meteorological stations from the Ministry of Agriculture and Fisheries, Food and Environment of Spain (MAPAMA), that area located within the study area and surroundings (Figure 1). Eight of them are maintained by the Spanish Meteorological Agency (AEMET) and the others by the Agroclimatic Information System for Irrigation (SIAR). The meteorological stations are located at di erent elevations, orientations and distances from the coast, in order to obtain information about the variability of climatic conditions in the area. Therefore, they can be assumed to be representative of the present climatic conditions of the study area. For each meteorological station, daily values of precipitation were compiled and used to develop annual time series of total precipitation. Precipitation maps were needed to develop spatial analyses along with the remote-sensing variables. For this reason, we computed annual precipitation maps for each year from 2001 to 2014. Multiple regression models were developed for each year in order to predict annual precipitation (dependent variable) based on geographical variables (elevation and spatial location of the meteorological stations). Previous studies have revealed the importance of distance to the coastline and local orography as a trigger mechanism of rain events [40]. Stepwise method for variable entry and removal was the selected statistical technique. Model performance was based on higher adjusted R^2, lower Akaike Information Criterion (AIC) [41], and minimum collinearity measured with the variance inflation factor (VIF) [42]. Regression models were built with the R statistical programming language [43]. Model parameters fitting was used to compute annual precipitation estimation maps based on geographical position and elevation from a DEM.

Future climate conditions were obtained from the WorldClim repository (URL: http://www.worldclim.org) [44]. Precipitation projections for 2050 were obtained from the global climate model developed by Schmidt *et al.* [45]. We used their climate projections for four representative concentration pathways (RCPs), namely: RCP2.6, RCP4.5, RCP6, and RCP8.5 (+2.6, +4.5, +6.0, and +8.5 W/m², respectively) [46]. Original geographic coordinates data (0.5 degrees of spatial resolution) were reprojected in order to match MODIS spatial resolution characteristics.

Water volume of the Amadorio and Guadalest reservoirs are continuously monitored by Spanish authorities.

This is a web tool (http://sig.mapama.es/redes-seguimiento/) owned by the Ministry of Agriculture and Fisheries, Food and Environment (MAPAMA) with information about river gauges and reservoirs water volume. Average monthly water volume records of Guadalest and Amadorio reservoirs were used to compute time series of annual reservoir storage for the period of 2001–2014. Current and future precipitation, along with the reservoir storage volume date, were employed to investigate the occurrence and magnitude of drought/wet periods that may hamper the availability of water resources for natural processes and human activities.

2.3. Statistical methods

Annual time series of selected variables (i.e., average NDVI and LST, mean reservoir storage and total precipitation) were statistically analyzed in order to better understand temporal change patterns and their inter-relationships. Understanding the past evolution of studied variables and their possible cause–e ect relationships is essential to model their future spatial-temporal patterns and determine the usefulness of our remote-sensing time series for the improvement of water management. In this sense, time series anomalies (2001–2014) were computed on an annual basis. The time series anomaly (z-score) was computed according to the following expression [47,48]:

$$Z = \frac{x_i - \mu}{\sigma}$$

where *xi* is the time series value for a given moment *i*, and μ and σ are respectively the mean value and the standard deviation value of the time series. When the z-score is negative, it indicates below normal conditions of the selected variable, and when it is positive, it indicates above normal conditions. Vegetation index time series anomalies are a useful method for assessing the degree of wetness or dryness for each time unit in relation to the average value of the time series [49]. A negative z-score value indicates below-average vegetation conditions, thereby pointing to prevailing drought; and when it is positive, it indicates above-average vegetation conditions [49]. The interpretation of positive and negative z-score values for LST, precipitation and reservoir storage time series anomalies follows the same guidelines. Its physical interpretation depends on the variable. When the z-score is negative, it indicates below-normal temperature, precipitation or reservoir storage values, and when it is positive, it indicates above-normal values, thereby pointing to warm/wet seasons or periods [48].

The spatial-temporal relationships among NDVI, LST, precipitation (current or future), and reservoir storage volume time series are the core of our investigation (with the aim of developing fast early detection systems of water supply limitations through remote-sensing images) and were evaluated with three di erent statistical methods. Firstly, the Spearman rank-order correlation test was used to compute the correlation among z-score time series of average NDVI, LST, current precipitation, and total reservoir storage for both watersheds from 2001 to 2014. Correlation coe cients and significance levels were computed. This test allowed the identification of similar temporal patterns of selected variables. Secondly, correlation images were obtained by computing the correlograms of the annual z-score reservoir storage time series for each reservoir, with respect to the computed annual z-score of NDVI, LST and current precipitation time series of the pixels located within the same watershed. Correlogram results were employed to build correlogram images that express the spatial relationship among reservoir storage anomalies (point data) with respect to the spatial variables. Finally, spatial regression models were used to assess the relationship between precipitation and remote-sensing variables, taking into account the autocorrelation e ects. OpenGeoDa software [50] was used for this analysis. This software is part of a suite of GeoDa software tools designed for spatial analysis of geographical information, including spatial autocorrelation and spatial regression algorithms [51]. Ordinary Least Squares spatial regression models were computed, employing future precipitation data as the dependent variable and remotely-sensed variables and topographic parameters as explanatory variables.

3. Results

3.1. Correlation between NDVI, LST and precipitation

Our first research question was related to the possible existence of significant correlations between NDVI, LST and precipitation time series anomalies. Before addressing that question, we explored the temporal-spatial patterns of remote-sensing variables (i.e., NDVI and LST) and current precipitation maps. The time series of NDVI images exhibits great spatial and temporal variability. Figure 2a,b shows the average and standard deviation values of the NDVI between the years 2001 and 2014. Large areas of the Algar-Guadalest basin report average NDVI values higher than 0.37 and low standard deviations. In fact, the average NDVI value from 2001 to 2014 for this watershed was 0.47 with a coe cient of variation lower than 5%. NDVI values higher than 0.53 are associated with irrigation crops (fruit trees) in mid and low elevations, and dense forest patches in the most remote areas.

Conversely, the average NDVI value from 2001 to 2014 for Amadorio watershed was 0.38 with a coe cient of variation higher than 8%. A cluster of high NDVI standard deviation pixels in the NW of the Amadorio basin was observed. A visual inspection of recent aerial orthophotos revealed that it is associated with a forest fire.

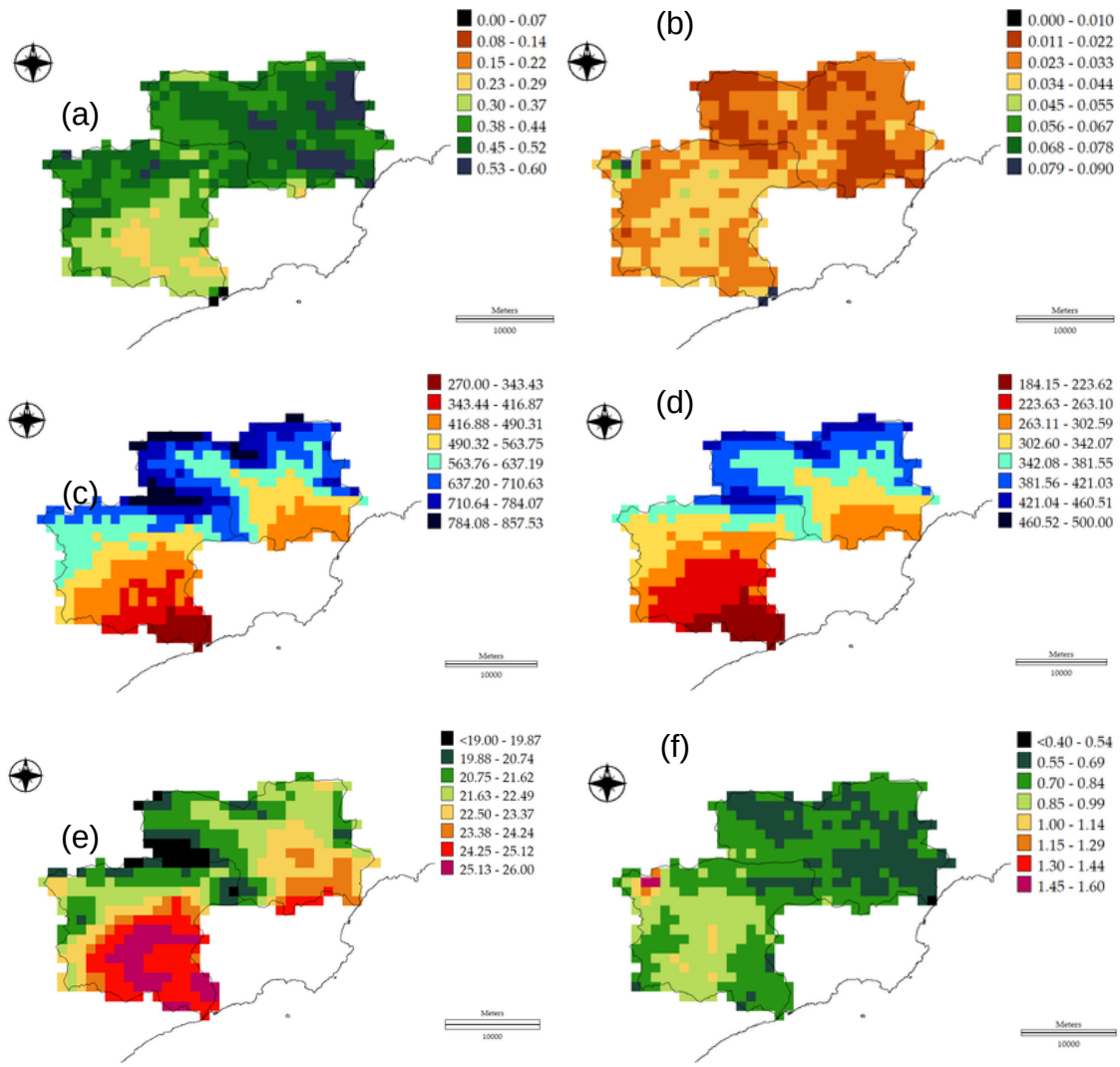

Figure 2. *Average (a) and standard deviation (b) NDVI images of the study area for the period 2001 to 2014. Average (c) and standard deviation (d) estimated precipitation images (in mm) of the study area for the period 2001 to 2014. Average (e) and standard deviation (f) LST images (in Celsius degrees) of the study area for the period 2001 to 2014. The delineation of the watersheds and the coastline are shown (black lines).*

Precipitation of the study area is largely affected by the elevation and position with respect to the coastline [40]. For this reason, multiple regression models combining precipitation data, elevation and spatial location of the meteorological stations were applied. All statistical models reported adjusted R^2 values higher than 0.7, and their parameters were employed to predict precipitation at unknown locations. Precipitation maps were produced for each year of the study period.

Figure 2c,d shows the average and standard deviation values of estimated precipitation between the years 2001 and 2014. The most remarkable observation of the maps is the high spatial variability over a relatively small area. Average precipitation of the Algar-Guadalest basin was 632 mm while average precipitation for the Amadorio basin was 523 mm. Low precipitation areas were found at low elevations near the coastline and southern half of the Amadorio river basin. Larger average precipitation and standard deviation values were found at the highest points of the drainage divide. These areas are very steep and often show bare rock outcrops (this explains their low NDVI values in Figure 2a).

Figure 2 e,f shows the average and standard deviation values of the LST between the years 2001 and 2014. LST images revealed relevant altitudinal variations of the temperature. The highest average LST was 25.7 °C and was obtained in the lower sector for the Amadorio watershed, just a few kilometers from the coastline. The lowest average temperature was 18.9°C and is associated with the location of the highest mountain found in the study area, namely the Aitana peak. LST spatial patterns are clearly affected by the altitudinal gradient (i.e., lower temperatures at higher elevations) and the influence of the sea (coastline temperatures were slightly lower than temperatures in some inland areas). Standard deviation was higher at the lower sector of the more continental Amadorio watershed with respect to the higher areas or the wettest Algar-Guadalest basin. A cluster of high standard deviation LST values spatially correlates with the previously mentioned forest fire area. The removal of the vegetation cover (as detected by the NDVI time series) greatly influenced LST variability.

3.2. Time series anomalies patterns

Time series of selected variables (i.e., average NDVI and LST, and total precipitation) were used to compute annual time series anomalies for each pixel in each of the two watersheds. In addition, reservoir storage time series anomalies were computed too.

Figure 3 shows the original time series of the three selected variables for Algar-Guadalest and Amadorio basins as well as their corresponding time-series anomalies (z-score values).
The general pattern of NDVI time series was the same for both watersheds. NDVI values of the Algar-Guadalest basin ranged between 0.6 and 1.0 and were higher than those of the Amadorio basin. The general pattern of both time series was very similar, with subtle but very informative temporal variations. The time series of NDVI anomalies reveals positive values between 2007 and 2011, in addition to the year 2013. Beyond these values, the local maximums of the years 2002 and 2004, which correspond to slightly humid years, are very revealing.

In this sense, the time series of precipitation is very irregular, with abnormally wet years closely followed by years of severe droughts (e.g., 2005). As a result of this great irregularity, the time series of precipitation anomalies exhibits great variations, reflecting instances of drought and wet years very well. The most distinctive feature is the concatenation of a period of above-average precipitation (2006 to 2009) followed by a very severe drought in 2010.
Average LST values were always higher for the southern Amadorio basin but the temporal temperature pattern was very similar for both watersheds.

A more detailed analysis revealed two different periods. The first one ranged from 2001 to 2007 and is characterized by a great homogeneity and subtle z-score changes. The second period (2008 to 2014) is dominated by much more extreme LST variations, with two very acute negative z-score values (for 2008 and 2010) followed by rising temperatures, reaching a maximum absolute temperature and z-score value in 2014.
After exploring the relationships between remote-sensing variables and current precipitation time series anomalies (research question #1), we dealt with the second research question: a possible significant correlation between NDVI, LST and water reservoir storage anomalies. The general pattern of the reservoir storage time series shows a gradual increase between 2001 and 2005. From that year on, the time series of anomalies reveals moderate interannual oscillations, with alternating maximum storage volumes between the two reservoirs. The final decline of the reservoir storage coincided with low NDVI and precipitation values, and the highest LST records. All these complex temporal patterns suggested the necessity for employing some statistical methods to shed some light and better understand the relationships among them.

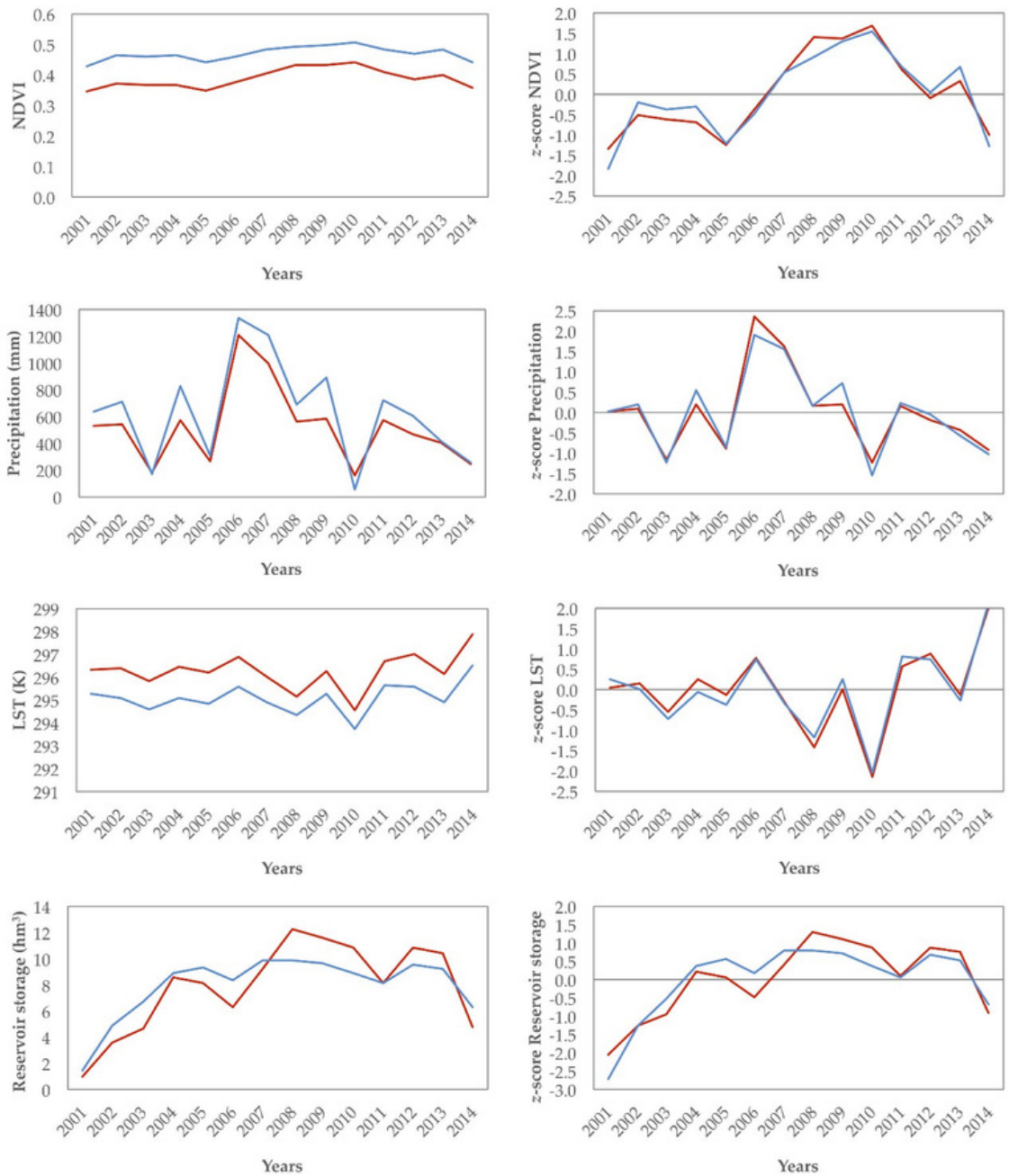

Figure 3. *Raw data and z-score time series of average NDVI, average precipitation, LST, and total reservoir storage for Algar-Guadalest (blue lines) and Amadorio (red lines) watersheds from 2001 to 2014.*

3.3. Spatial-temporal relationships between reservoir storage, vegetation greenness, LST and precipitation

Once the general patterns of the time series of anomalies were known, the next step was to analyze the relationships between the different variables. Our last research question was related to the possibility of employing remotely sensed time series data (NDVI, LST) together with water reservoir storage changes to spatially and temporally assess current water demands and predict future water needs. With this objective in mind, three different types of analyses were performed: (1) Spearman rank correlation test of z-score time series; (2) correlation images of spatial variables vs. reservoir storage volume; and (3) spatial regression of future precipitation with respect to remote-sensing variables.

Firstly, the correlations between z-score time series for both watersheds were calculated (Table 1). The results obtained for each watershed were quite similar. Highly significant correlations (p-value ≤ 0.01) among the same variables were obtained. It suggests a similar behavior of both basins for the studied variables. We also found significant correlations between different variables. Significant (p-value ≤ 0.05) and highly significant (p-value ≤ 0.01) correlations between NDVI and reservoir storage time series anomalies were found. No significant correlations were reported for other variable combinations. We can observe negative correlation values between LST with respect to NDVI and reservoir storage. Correlation analysis results reinforced our previous observation of similar temporal patterns of the time series anomalies for both watersheds but with some subtle differences (e.g., a magnitude offset between the time series).

Table 1. *Spearman rank correlation test results for z-score time series of NDVI, precipitation, LST, and reservoir storage for Algar-Guadalest (A-G) and Amadorio (Am.) watersheds.*

Variables		NDVI		Precipitation		LST		Reservoir Storage	
		A-G	Am.	A-G	Am.	A-G	Am.	A-G	Am.
NDVI	A-G	1	0.956 **	0.103	0.125	−0.376	−0.473	0.565 *	0.824 **
	Am.	0.956 **	1	0.165	0.196	−0.305	−0.433	0.565 *	0.802 **
Precipitation	A-G	0.103	0.165	1	0.996 **	0.349	0.288	0.262	0.090
	Am.	0.125	0.196	0.996 **	1	0.323	0.257	0.310	0.143
LST	A-G	−0.376	−0.305	0.349	0.323	1	0.930 **	−0.403	−0.363
	Am.	−0.473	−0.433	0.288	0.257	0.930 **	1	−0.370	−0.367
Reservoir storage	A-G	0.565 *	0.565 *	0.262	0.310	−0.403	−0.370	1	0.843 **
	Am.	0.824 **	0.802 **	0.090	0.143	−0.363	−0.367	0.843 **	1

Significance levels: [*] = p ≤ 0.05; [**] = p ≤ 0.01.

Secondly, we developed an image product, called correlation images (Figure 4), that expresses the spatial relationship among reservoir storage anomalies and the explanatory spatial variables. They were obtained by computing the pixel-by-pixel correlation between the z-score values of the NDVI, LST and current precipitation time

High positive correlation values reflected some kind of synchronization among the time series, while high negative correlation values suggested a differential behavior among the reservoir storage and explanatory variables. The NDVI correlation image was quite complex with high correlation values for a large portion of the Amadorio watershed, and some clusters of low correlation values at the lower portion of the Algar-Guadalest watershed and the highest elevations. The LST correlation image showed a large cluster of pixels with high correlation values in the middle and lower part of the Algar-Guadalest watershed. On the contrary, a cluster of pixels with negative correlation values was observed in the warmest sector of the Amadorio river basin. The correlation image for the current precipitation adopts a clear trend of negative correlations in the sectors with less precipitation (see Figure 2c), moving to positive correlation values as the precipitation increases.

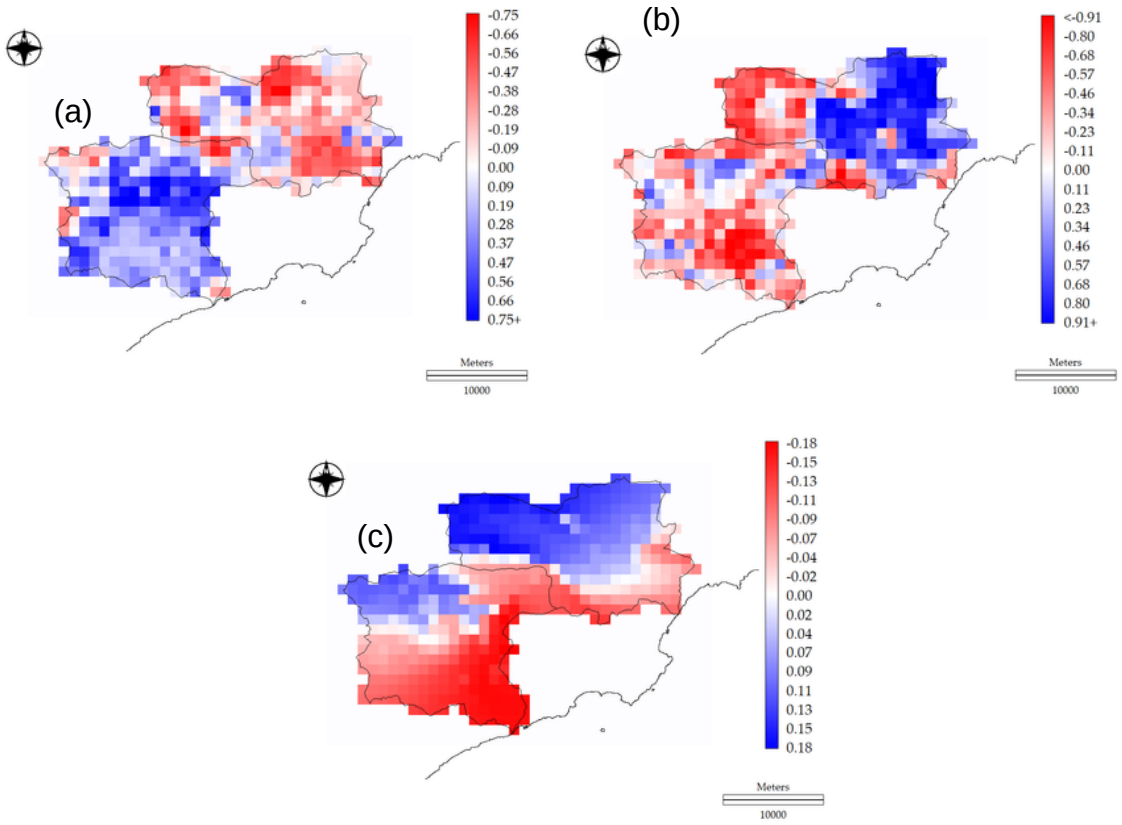

Figure 4. *z-score correlation image among reservoir storage vs. (a) NDVI, (b) LST, and (c) current precipitation time-series anomalies.*

Finally, we used spatial regression methods to evaluate the predictive capability of our remote-sensing time series (NDVI and LST) with respect to future precipitation scenarios (Table 2).

Two types of dependent variables were used: (a) original data from Schmidt *et al.* [45] for four representative concentration pathways that allow for the prediction of precipitations in 2050; and (b) the difference between our current precipitation maps (2001–2014) with respect to the Schmidt *et al.* [45] dataset. This second type of data allows for the identification of areas with expected lower/higher precipitation in the future. Predictive variables were the average values of NDVI and LST (see Figure 2) for each pixel of the study area and also their corresponding correlation images (see Figure 4). We also included topographic parameters obtained from the DEM (see Figure 1). Spatial correlograms of predictive variables were used to identify a suitable threshold distance of 4 km for the weights of the regression. Regression models were interactively pruned in order to exclude non-significant predictive variables.

Table 2. *Spatial regression model results. Model adjustment statistics and the explanatory variables information are shown.*

	Precipitation Predictions	Adj. R^2	*p*-Value	Variables	Coefficient	Std. Error	*p*-Value
Future precipitation predictions	RCP26	0.819	<0.001	Constant	1006.885	25.508	<0.001
				Elevation	0.043	0.005	<0.001
				LST (mean 2001–2014)	−22.478	1.016	<0.001
	RCP45	0.829	<0.001	Constant	927.370	23.672	<0.001
				Elevation	0.049	0.005	<0.001
				LST (mean 2001–2014)	−20.206	0.942	<0.001
	RCP60	0.835	<0.001	Constant	898.844	22.895	<0.001
				Elevation	0.051	0.005	<0.001
				LST (mean 2001–2014)	−19.607	0.911	<0.001
	RCP85	0.828	<0.001	Constant	937.138	23.380	<0.001
				Elevation	0.045	0.005	<0.001
				LST (mean 2001–2014)	−20.557	0.931	<0.001
Precipitation change (future prediction-present)	RCP26	0.722	<0.001	Constant	70.006	4.533	<0.001
				Elevation	−0.214	0.007	<0.001
				LST correlogram image	−42.773	4.093	<0.001
				NDVI correlogram image	57.910	5.863	<0.001
	RCP45	0.725	<0.001	Constant	47.297	4.610	<0.001
				Elevation	−0.217	0.007	<0.001
				LST correlogram image	−44.878	4.162	<0.001
				NDVI correlogram image	62.657	5.961	<0.001
	RCP60	0.727	<0.001	Constant	33.717	4.637	<0.001
				Elevation	−0.219	0.007	<0.001
				LST correlogram image	−45.595	4.187	<0.001
				NDVI correlogram image	64.455	5.997	<0.001
	RCP85	0.731	<0.001	Constant	48.234	4.587	<0.001
				Elevation	−0.220	0.007	<0.001
				LST correlogram image	−44.471	4.142	<0.001
				NDVI correlogram image	62.243	5.932	<0.001

We obtained adjusted R^2 values higher than 0.8 for the models predicting future precipitation scenarios. Predictive significant variables were elevation and LST, with an inverse relationship between future prediction and LST. With respect to the expected precipitation change dataset, we also obtained high adjusted R^2 values (>0.7) for all the spatial regression models. Predictive significant variables were elevation, LST correlation image and also NDVI correlation image. The relationship between future precipitation changes is positive for the NDVI and negative for LST.

4. Discussion

4.1. Impacts of predicted precipitation scenarios

The precipitation regime of the study area is highly variable both spatially and temporally. Orography greatly influences precipitation patterns [40] and the presence of dry areas, such that the conditions may vary within a short distance [15]. Precipitation also changes from year to year and interannually. Higher precipitation volumes are usually obtained in autumn in the form of torrential rains. In this sense, high-intensity precipitation events (>400 mm in 24 h) are feasible in this area, due to the advection of maritime winds across the Western Mediterranean, driving moist air towards the Alicante Province coast, and the presence of an upper level isolated low pressure system over Eastern Iberian Peninsula [40]. This phenomenon is characteristic of the study area and greatly impacts socio-economic activities and environmental processes. For example, severe flash foods are recurrent each autumn and could promote dramatic consequences like the destruction of infrastructures and even human lives. The high rainfall erosivity induces land degradation process (i.e., soil erosion) by extreme runoff. It greatly endangers soil resources due to the vulnerability of dominant soil types (especially Leptosols). Besides, the occurrence of extreme autumn precipitation events just after the devastation of summer wildfires may increase the risk of soil degradation.

Water resources are quantitatively and qualitatively affected by these kinds of land degradation processes [52,53]. This is particularly concerning for an area facing severe problems of managing highly fluctuating seasonal water demands.

Precipitation estimations by global climate prediction models (such as Schmidt *et al.* [46], and used in this work) are revealing future scenarios of even worse water scarcity for many arid and semiarid regions (Figure 5). This is an alarming situation because many of those areas are densely populated and potentially face a future with less water resources (intensification of drought periods) and higher water demands (e.g., urban water supply, agriculture irrigation).

Fortunately, drought assessment through remote sensing—although a complex research topic—has been achieving highly successful results obtained by combining the time series of NDVI and LST [54].

Both remote-sensing variables may be synergistically combined to develop easy-to-implement empirical indices based on the assumption of a negative correlation between both variables [55]. However, their correlation may be much more complex than previously thought and may change from negative to positive as the climatic conditions change [27].

Further, spatial autocorrelation may alter the conclusion of statistical analyses performed without the allowance for it [56,57]. This type of correlation has been investigated in the past but this work differs from previous work by showing/investigating the complexity of this relationship with respect to changing climatic conditions. For these reasons, this work is a multistage approach to evaluate the spatial-temporal relationships of NDVI and LST time series, with respect to precipitation (current and future predictions) and available water resources (i.e., volume of water stored in reservoirs) time series.

We combined three different data analysis procedures: (1) time series anomalies analysis to detect general temporal patterns of the variables; (2) image correlation to detect through remote-sensing areas whose environmental characteristics and land management could greatly affect available water resources; and (3) spatial regression analysis to assess the predictive capabilities of NDVI and LST time series to quantify current and future precipitation.

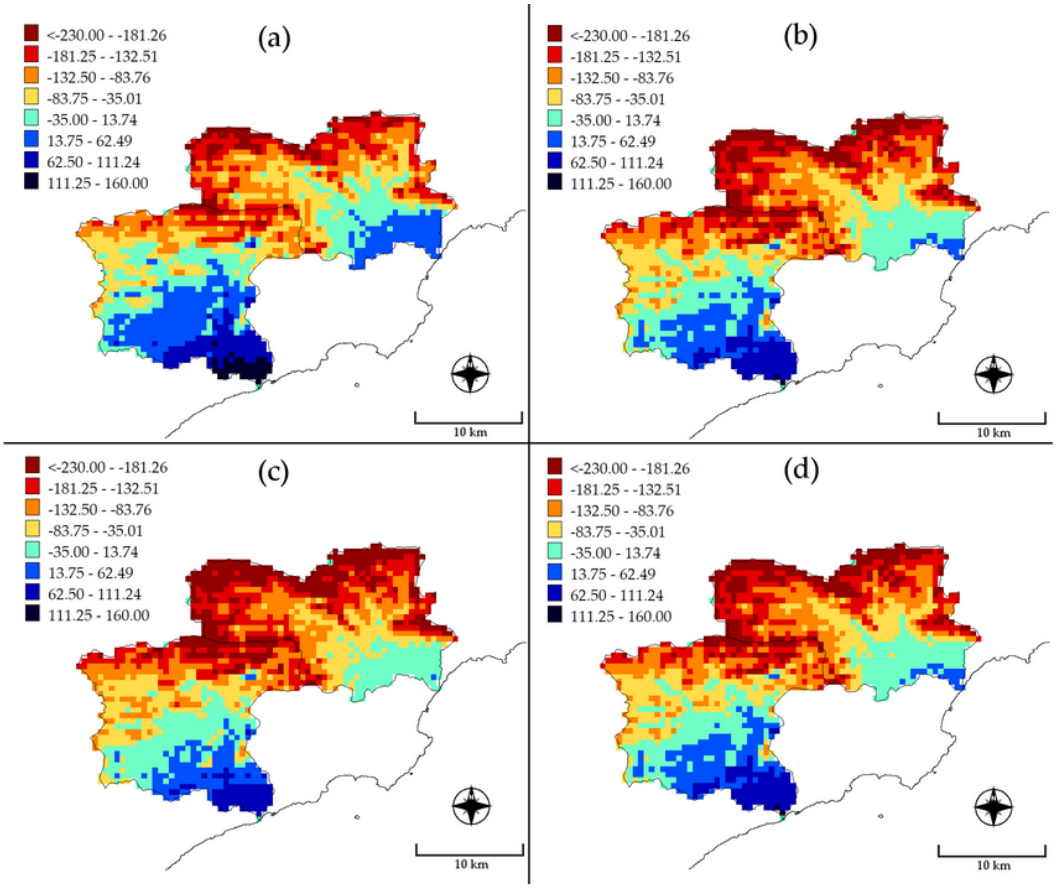

Figure 5. *Differences between current precipitation and 2050 predicted precipitation under RCP2.6, RCP4.5, RCP6, and RCP8.5 (maps (a–d) respectively) climate scenarios. Negative values indicate a decrease in precipitation whereas positive values reflect an increase.*

4.2. Correlation between time series anomalies of NDVI, LST, precipitation and water reservoir changes

Time series anomalies have been previously employed for vegetation index time series analysis in relation to climatic variables [58,59] and hydrological parameters [48]. They provide an intuitive way to identify the intensity and duration of phenological and vegetation degradation processes, along with extreme climate variations. Correlations between NDVI and precipitation in the study area were found to be low, especially for the wetter Algar-Guadalest basin. It seems that vegetation phenology is not coupled with inter- and intra-annual precipitation patterns. We also reported this weak relationship between both time series for another study area in the province of Alicante [47].

Our previous research applied Fourier transform analysis to MODIS vegetation index and climate variables time series, and the results evidenced that vegetation phenology was not correlated with climatic variables for the harmonic analysis phase term, suggesting a delay between climatic variations and vegetation greenness [47]. It may be due to the semiarid and subhumid biomes' response to drought at long time scales caused by the physiological adaptions of Mediterranean vegetation to water stress periods [60]. Other authors also evidenced this low correlation between NDVI and rainfall, showing worse correlations in the wetter areas of the province of Alicante mountains (i.e., NDVI and precipitation correlations are not sufficient to assess and predict droughts) [61]. With respect to the LST, the correlation between NDVI and LST always produced negative values, thus indicating a reduction of vegetation greenness when LST rises. This kind of relation is characteristic of areas prone to droughts where water is ultimately the limiting factor for vegetation growth [27]. On the other hand, significant positive correlations among NDVI and surface water resources time series anomalies were obtained. These correlations suggest that an interannual relationship between NDVI and reservoir storage variability can be established. The importance of this observation lies in the fact that multi-temporal remote-sensing observations of certain environmental parameters could be used to monitor and predict the quantity of available water resources. The development of the vegetation causing an increase of NDVI, which showed an apparent contradiction between precipitations versus water storage, may be closely related to the soil moisture and a delayed response of plants after a rainfall event. Therefore, the response of vegetation after precipitation is closer to the process of storing water in reservoirs than the precipitation itself.

The z-score correlation images (Figure 4) were suitable to relate the variability of a point data time series (i.e., reservoir storage measured in a dam) with remotely-sensed spatial-temporal time series (like NDVI, LST, evaporation, etc.). The high positive values of the NDVI correlation image at the lower parts of Amadorio watershed evidence synchronization between vegetation (forest and seminatural vegetation and rainfed agriculture) and reservoir storage dynamics. This is reinforced by the results of the LST correlation image that highlighted a cluster of pixels with negative correlation values in the warmest sector of the Amadorio river basin. Its natural vegetation phenology and reservoir storage volume are controlled by LST temporal changes, because when LST rises (from spring to summer), vegetation greenness and surface water resources decline. This watershed is less suitable for cropping and water supply [37]. On the contrary, water resources (surface and groundwater) in the Algar-Guadalest basin are more intensively controlled by water management. A complex system of water transfer from the aquifers to the reservoir has been established to maintain steady water supply [37].

This water management system manages water demands from agriculture and tourism economic sectors, along with governmental (urban water supply) and environmental requirements. This situation greatly influences the magnitude of the correlation between Guadalest reservoir storage and climatic variables. Thus, remote sensing can play a critical role in the assessment of water demands. Another study in the province of Alicante confirmed the great utility of remote-sensing images to detect different water management practices in irrigated agricultural areas and nearby natural areas [62]. The information portrait in the land cover map (Figure 1) was compared with the NDVI correlation image (Figure 4). It reveals that permanent crops (i.e., fruit trees) are located where a large cluster of pixels with negative correlation is shown. Crops' productivity maintenance requires an adequate water supply even in drought years/seasons, thus explaining the negative correlation. In addition, negative correlations were observed in two sectors of the Guadalest basin. These areas are quite elevated, with predominantly very steep and rocky slopes, and with little or no vegetation (CORINE Land Cover classes 32 and 33). Leptosols over highly permeable calcites are found here. Mean NDVI values of those pixels were relatively low with respect to surrounding areas (Figure 2) due to the characteristics of these mountainous ecosystems. Both clusters of pixels are approximately located over the two most important aquifers (i.e., Beniardá and Algar) of the Marina Baja water supply system whose waters are employed for irrigation (through springs and irrigation channels), diverted for water supply to other areas or stored in the Guadalest reservoir. This may explain the weak relationship found between NDVI and reservoir storage in those aquifer recharge zones.The term low has been changed

4.3. Assessing water demands and usage with MODIS derived products

Our final analysis was focused on the exploration of possible future scenarios of water scarcity that may hamper human activities and environmental processes. This particularly concerns arid/semiarid areas that are the most sensitive ecosystems to climate impact [63]. Because correlation results between remote-sensing variables and precipitation time series were weak and inconclusive, we decided to explore the effects of spatial autocorrelation through spatial analysis techniques. Spatial autocorrelation is a property of random variables, taking values in pairs of locations at a certain distance apart that are more similar (positive autocorrelation) or less similar (negative autocorrelation) than expected for randomly associated pairs of observations [56]. We used spatial regression models because they are developed to deal with the fact that observations over geographical space are likely to be correlated with one another [64],

and spatial regression models can effectively resolve problems with correlated geographic data [65,66]. Our previous research in a nearby study area evidenced the importance of considering spatial autocorrelation effects by combining remote sensing and ancillary information [67]. [67]. In this sense, our spatial regression results (Table 2) suggest that LST and NDVI time series can be utilized as proxies to predict future scenarios of precipitation in an effort to improve land management practices. Positive trends of NDVI time series in semiarid regions could be associated with less dramatic precipitation changes, whereas an increase of LST values may negatively impact the water cycle in this kind of Mediterranean watershed.

Future carbon sequestration will also be at risk predominantly in southern Europe [68]. Especially lower precipitation is expected in the more elevated areas of the watersheds that are extremely important for groundwater recharge and the efficient functioning of the entire water supply system. Therefore, it is recommended that the knowledge gained through remote sensing in this work (the spatial-temporal influence of NDVI and LST time series on available water resources) be used to promote an alert system that allows integrating water and land management. Future scenarios of climate change will pose a challenge for the maintenance of our socio-economic activities and the conservation of ecosystems. In this sense, the best source of information available is most likely remote sensing, given that it is capable of providing information about land, atmosphere and water, in their spatial and temporal dimensions. Additionally, in the context of the study area, spatial autocorrelation effects seem to be highly relevant and have to be considered to properly extract information from the remote-sensing data sources.

5. Conclusions

This study assessed the interdependency between vegetation spectral indices (NDVI), LST, precipitation (current and future), and surface water resources in a semiarid area (two watersheds in southeastern Spain with serious difficulties in meeting water demands). NDVI and LST images were obtained from MODIS and allowed for the identification of relevant responses to current climate variability (from 2001 to 2014). Correlations between NDVI and precipitation time series were not very strong, probably because vegetation phenology is not perfectly coupled with inter- and intra-annual precipitation patterns (semiarid and subhumid biomes may respond to droughts of long time scales due to the ability of vegetation to withstand periodic droughts). Additionally, correlations between NDVI and LST always produced negative values, thus indicating a reduction of vegetation greenness when LST rises. The relationships among NDVI and climate variables evidenced the importance of water as a relevant limiting factor for vegetation growth.

The temporal correspondence between reservoir storage and remote-sensing time series was very remarkable, thus suggesting a great potential of NDVI and LST to improve the monitoring and management of water resources in the study area. In this sense, correlation maps allowed for the identification of areas where natural vegetation phenology and reservoir storage volume is controlled by LST temporal changes (Amadorio basin). Additionally, negative NDVI correlations were found at different sectors of the Algar-Guadalest basin. They are associated with areas of irrigated crops with high water demands and forest and seminatural areas located over aquifers intensely exploited for agriculture and water supply. Of great concern should be the fact that the best correlation with reservoir storage coincides with areas where significant decreases in precipitation are expected, which correspond with the two most important aquifers of the study area . These results evidence the capability of optical remote-sensing data (MODIS, Landsat, Sentinel-2) to detect different water management practices related to the transfer of water from the main aquifers to the Guadalest reservoir. Spatial regression models evidence the importance of taking into account spatial autocorrelation effects in the statistical analyses along with the potential use of NDVI and LST time series to predict future scenarios of precipitation under climate change constrains.

The enormous competition for available water in the study area (i.e., urban water supply, agriculture and maintenance of ecosystems) may be exacerbated in the future. Climate change will most likely trigger a change in Mediterranean arid and semi-arid regions to lower rainfall scenarios. A comparison of current precipitation and future precipitation conditions obtained from global climate models reinforces this statement and evidences that the most dramatic precipitation reductions will be associated with the higher elevation areas in both basins. This observation concerns areas that are very important for groundwater storage and surface runoff that critically contribute to reservoir storage variations. The future impact of climate change on water resources needs adaptive strategies based on accurate and updated spatial-temporal information. For this reason, the use of Earth Observation technologies to monitor and predict land cover changes, soil-vegetation degradation processes, and available water resources is a scientific and social priority.

Author Contributions: G.M.-D.S. and I.M.-P. have a major contribution in the experimental development and the other authors in the experimental design. All of the authors contributed equally for the rest of the work.

Funding: This research received no external funding.

Acknowledgments: We express our gratitude to the NASA's MODIS project for providing NDVI satellite imagery free of charge. We acknowledge the Spanish Meteorological Agency (AEMET) and the Agroclimatic Information System for Irrigation (SIAR) for providing meteorological information. We are also grateful to the European Environmental Agency for the public access of the CORINE land cover cartography.

Conflicts of Interest: The authors declare no conflict of interest.

References

1. Vicente-Serrano, S.M. Evaluating the Impact of Drought Using Remote Sensing in a Mediterranean, Semi-arid Region. Nat. Hazards 2007, 40, 173–208, doi:10.1007/s11069-006-0009-7.
2. Giorgi, F.; Lionello, P. Climate change projections for the Mediterranean region. Glob. Planet. Chang. 2008, 63, 90–104, doi:10.1016/j.gloplacha.2007.09.005.
3. Vera-Rebollo, J.F. Cambio climático y política turística en España: Diagnóstico del litoral mediterráneo español. Cuadernos de Turismo 2016, 38, 323–359, doi:10.6018/turismo.38.271471.
4. Verheye, W.H. Dry Lands and Desertification. In Encyclopedia of Land Use, Land Cover Soil Sciences; Verheye, W.H., Ed.; United Nations Educational, Scientific and Cultural Organization (UNESCO) and Encyclopedia of Life Support Systems (EOLSS): Paris, France, 2009; pp. 1–40.
5. Olcina Cantos, J. Cambio climático y riesgos climáticos en España. Investigaciones Geográficas 2009, 197–220, doi:10.14198/INGEO2009.49.10.
6. Ostendorf, B. Overview: Spatial information and indicators for sustainable management of natural resources. Ecol. Indic. 2011, 11, 97–102, doi:10.1016/j.ecolind.2010.10.003.
7. De Araujo Barbosa, C.C.; Atkinson, P.M.; Dearing, J.A. Remote sensing of ecosystem services: A systematic review. Ecol. Indic. 2015, 52, 430–443, doi:10.1016/j.ecolind.2015.01.007.
8. IPCC. Part A: Global and Sectoral Aspects. Contribution of Working Group II to the Fifth Assessment Report of the Intergovernmental Panel on Climate Change. In ClimateChange 2014: Impacts, Adaptation, Vulnerability; Field, C.B., Barros, V.R., Dokken, D.J., Mach, K.J., Mastrandrea, M.D., Bilir, T.E., Chatterjee, M., Ebi, K.L., Estrada, Y.O., Genova, R.C., *et al.,* Eds.; Cambridge University Press: Cambridge, UK; New York, NY, USA, 2014; ISBN 978-1-107-64165-5.
9. World Water Assessment Programme. The United Nations World Water Development. Report 3: Water in a Changing World; United Nations Educational, Scientific and Cultural Organization (UNESCO)/Earthscan: Paris, France; London, UK, 2009; p. 429; ISBN 978-9-23104-095-5.

10. Consorcio de Aguas de la Marina Baja. Available online: https://www.diarioinformacion.com/especiales/dia-mundial-agua/2018/03/consorcio-aguas-marina-baja-mejor-gestion-integral-recursos-n1433_1_42849.html (accessed on 04/06/2019).
11. Lehner, B.; Liermann, C.R.; Revenga, C.; Vörömsmarty, C.; Fekete, B.; Crouzet, P.; Döll, P.; Endejan, M.; Frenken, K.; Magome, J.; *et al.* High-resolution mapping of the world's reservoirs and dams for sustainable river-flow management. Front. Ecol. Environ. 2011, 9, 494–502, doi:10.1890/100125.
12. IPCC-TGICA. General Guidelines on the Use of Scenario Data for Climate Impact Adaptation Assessment, 2nd ed.; Intergovernmental Panel on Climate Change (IPCC)-Task Group on Data and Scenario Support for Impact and Climate Assessment (TGICA): Geneva, Switzerland, 2007; p. 66.
13. García-Ruiz, J.M.; López-Moreno, J.I.; Vicente-Serrano, S.M.; Lasanta, T.; Beguería, S. Mediterranean water resources in a global change scenario. Earth-Sci. Rev.2011, 105, 121–139, doi:10.1016/j.earscirev.2011.01.006.
14. Mereu, S.; Sušnik, J.; Trabucco, A.; Daccache, A.; Vamvakeridou-Lyroudia, L.; Renoldi, S.; Virdis, A.; Savić, D.; Assimacopoulos, D. Operational resilience of reservoirs to climate change, agricultural demand, and tourism: A case study from Sardinia. Sci. Total Environ. 2016, 543, 1028–1038, doi:10.1016/J.SCITOTENV.2015.04.066.
15. Mühlbauer, S.; Costa, A.C.; Caetano, M. A spatiotemporal analysis of droughts and the influence of North Atlantic Oscillation in the Iberian Peninsula based on MODIS imagery. Theor. Appl. Climatol. 2016, 124, 703–721, doi:10.1007/s00704-015-1451-9.
16. Nilsson, C. Reservoirs. Encycl. Inland Waters 2009, 625–633, doi:10.1016/B978-012370626-3.00039-9.
17. Nemani, R.; Running, S. Land Cover characterization using multitemporal RED, NEAR-IR, and THERMAL-IR data from NOAA/AVHRR. Ecol. Appl. 1997, 7, 79–90, doi:10.1890/1051-0761(1997)007[0079:LCCUMR]2.0.CO;2.
18. Zhan, Z.; Qin, Q.; Wang, X. The application of LST/NDVI index for monitoring land surface moisture in semiarid area. In Proceedings of the International Geoscience Remote Sensing Symposium (IGARSS), Anchorage, AK, USA, 27 December 2004; Volume 3, pp. 1551–1554.
19. Leroux, L.; Baron, C.; Zoungrana, B.; Traore, S.B.; Lo Seen, D.; Begue, A. Crop Monitoring Using Vegetation and Thermal Indices for Yield Estimates: Case Study of a Rainfed Cereal in Semi-Arid West Africa. IEEE J. Sel. Top. Appl. Earth Obs. Remote Sens. 2016, 9, 347–362.
20. Colliander, A.; Fisher, J.B.; Halverson, G.; Merlin, O.; Misra, S.; Bindlish, R.; Jackson, T.J.; Yueh, S. Spatial Downscaling of SMAP Soil Moisture Using MODIS Land Surface Temperature and NDVI during SMAPVEX15. IEEE Geosci. Remote Sens. Lett. 2017, 14, 2107–2111.
21. Tran, H.T.; Campbell, J.B.; Tran, T.D.; Tran, H.T. Monitoring drought vulnerability using multispectral indices observed from sequential remote sensing (Case Study: Tuy Phong, Binh Thuan, Vietnam). GIScience Remote Sens. 2017, 54, 167–184.

22. Wang, P.; Li, X.; Gong, J.; Song, C. Vegetation temperature condition index and its application for drought monitoring. In Proceedings of the International Geoscience Remote Sensing Symposium (IGARSS), Sydney, Australia, 9–13 July 2001; Volume 1, pp. 141–143.
23. Wan, Z.; Wang, P.; Li, X. Using MODIS Land Surface Temperature and Normalized Difference Vegetation Index products for monitoring drought in the southern Great Plains, USA. Int. J. Remote Sens. 2004, 25, 61–72.
24. Cunha, A.P.M.; Alvalá, R.C.; Nobre, C.A.; Carvalho, M.A. Monitoring vegetative drought dynamics in the Brazilian semiarid region. Agric. For. Meteorol. 2015, 214, 494–505.
25. Sánchez, N.; González-Zamora, A.; Piles, M.; Martínez-Fernández, J. A new Soil Moisture Agricultural Drought Index (SMADI) integrating MODIS and SMOS products: A case of study over the Iberian Peninsula. Remote Sens. 2016, 8, 287.
26. Patel, N.R. Investigating relations between satellite derived land surface parameters and meteorological variables. Geocarto Int. 2006, 21, 47–53.
27. Karnieli, A.; Agam, N.; Pinker, R.T.; Anderson, M.; Imhoff, M.L.; Gutman, G.G.; Panov, N.; Goldberg, A. Use of NDVI and land surface temperature for drought assessment: Merits and limitations. J. Clim. 2010, 23, 618–633.
28. You, N.; Meng, J.; Zhu, L. Sensitivity and resilience of ecosystems to climate variability in the semi-arid to hyper-arid areas of Northern China: A case study in the Heihe River Basin. Ecol. Res. 2018, 33, 161–174.
29. IGME-SGE. Geología de España; Vera, J.A., Ed.; Geological Survey of Spain (IGME) and Spanish Geological Society (SGE): Madrid, Spain, 2004; p. 884, ISBN 84-7840-546-1.
30. Generalitat Valenciana. Informe del Sector Agrario Valenciano 2016; Available online: http://www.agroambient.gva.es/es/informes-del-sector-agrario-valenciano (accessed on 12 June 2018).
31. IUSS Working Group WRB. World Reference Base for Soil Resources 2014. Update 2015. World Soil Resources Report No. 106; Food and Agriculture Organization of the United Nations (FAO): Rome, Italy, 2015; p. 203, ISBN 978-92-5-108369-7.
32. European Commission. Soil Atlas of Europe. European Soil Bureau Network European Commision; Office for Official Publications of the European Communities: Luxembourg, 2005; p. 128, ISBN 92-894-8120-X.
33. AEMET-IMP. Iberian Climate Atlas. Air Temperature Precipitation (1971–2000); Spanish Meteorological Agency (AEMET) and Portuguese Institute of Meteorology (IMP): Madrid, Spain; Lisbon, Portugal, 2011; p. 80, ISBN 978-84-7837-079-5.
34. Zaragozí, B.; Navarro, J.T.; Ramón, A.; Rodríguez-Sala, J.J. A Study of Drivers for Agricultural Land Abandonment Using GIS and Data Mining Techniques. In Proceedings of the Eighth International Conference on Ecosystems and Sustainable Development, Alicant, Spain, 13–15 April 2011; Volume 144, pp. 363–374.
35. Martí, T.T. Use competition and water exchange in Marina Baja district, Alicante, Spain. Water Sci. Technol. Water Supply2005, 5, 265–272.

36. Rico-Amoros, A.M.; Sauri, D.; Olcina-Cantos, J.; Vera-Rebollo, J.F. Beyond Megaprojects? Water Alternatives for Mass Tourism in Coastal Mediterranean Spain. Water Resour. Manag. 2013, 27, 553–565.
37. Castaño, S.; Murillo, J.M.; Hernández, L.R. Alternatives in water resources management in Marina Baja district (Alicante province, Spain). In Proceedings of the 3rd International Conference on Future Groundwater Resources at Risk-FGR'01; Ribeiro, L., Ed. CVRM-Instituto Superior Técnico[I2] ; Lisbon, Portugal, 2001; pp. 479–486.
38. Rouse, J.W.; Hass, R.H.; Schell, J.A.; Deering, D.W. Monitoring Vegetation Systems in the Great Plains with ERTS. In Proceedings of the Third Earth Resources Technology Satellite-1 Symposium, Washington, DC, USA, 1 January 1974; pp. 3010–3017.
39. Huete, A.; Justice, C.; Van Leeuwen, W. MODIS Vegetation Index (MOD 13). Algorithm Theoretical Basis Document. Version 3; NASA Goddard Space Flight Center: Greenbelt, MD, USA, 1999; pp. 129.
40. Pastor, F.; Gómez, I.; Estrela, M.J. Numerical study of the October 2007 flash flood in the Valencia region (Eastern Spain): The role of orography. Nat. Hazards Earth Syst. Sci. 2010, 10, 1331–1345, doi:10.5194/nhess-10-1331-2010.
41. Akaike, H. A New Look at the Statistical Model Identification. IEEE Trans. Automat. Contr. 1974, 19, 716–723, doi:10.1109/TAC.1974.1100705.
42. O'brien, R.M. A Caution Regarding Rules of Thumb for Variance Inflation Factors. Qual. Quant. 2007, 41, 673–690, doi:10.1007/s11135-006-9018-6.
43. R Core Team. R: A Language and Environment for Statistical Computing; R Foundation for Statistical Computing: Vienna, Austria, 2018.
44. Hijmans, R.J.; Cameron, S.E.; Parra, J.L.; Jones, P.G.; Jarvis, A. Very high resolution interpolated climate surfaces for global land areas. Int. J. Climatol. 2005, 25, 1965–1978, doi:10.1002/joc.1276.
45. Schmidt, G.A.; Ruedy, R.; Hansen, J.E.; Aleinov, I.; Bell, N.; Bauer, M.; Bauer, S.; Cairns, B.; Canuto, V.; Cheng, Y.; *et al.* Present-Day Atmospheric Simulations Using GISS ModelE: Comparison to *In Situ*, Satellite, and Reanalysis Data. J. Clim. 2006, 19, 153–192, doi:10.1175/JCLI3612.1.
46. Schmidt, G.A.; Kelley, M.; Nazarenko, L.; Ruedy, R.; Russell, G.L.; Aleinov, I.; Bauer, M.; Bauer, S.E.; Bhat, M.K.; Bleck, R.; *et al.* Configuration and assessment of the GISS ModelE2 contributions to the CMIP5 archive. J. Adv. Model. Earth Syst. 2014, 6, 141–184, doi:10.1002/2013MS000265.
47. Melendez-Pastor, I.; Navarro-Pedreño, J.; Koch, M.; Gómez, I.; Hernández, E.I. Land-Cover Phenologies and Their Relation to Climatic Variables in an Anthropogenically Impacted Mediterranean Coastal Area. Remote Sens. 2010, 2, 697–716, doi:10.3390/rs2030697.
48. Melendez-Pastor, I.; Hernández, E.I.; Navarro-Pedreño, J.; Gómez, I.; Almendro-Candel, M.B. Influence of precipitation and land cover changes in a Mediterranean mountain watershed (Guadalaviar River, Spain). Eur. Water 2017, 57, 141–146.

49. Barbosa, H.A.; Huete, A.R.; Baethgen, W.E. A 20-year study of NDVI variability over the Northeast Region of Brazil. J. Arid Environ. 2006, 67, 288–307, doi:10.1016/j.jaridenv.2006.02.022.
50. Anselin, L.; McCann, M. OpenGeoDa, open source software for the exploration and visualization of geospatial data. In Proceedings of the ACM International Symposium on Advances in Geographic Information Systems, Tempe, AZ, USA, 4–9 November 2009; pp. 550–551.
51. Anselin, L.; Syabri, I.; Kho, Y. GeoDa: An Introduction to Spatial Data Analysis. Geogr. Anal. 2006, 38, 5–22, doi:10.1111/j.0016-7363.2005.00671.x.
52. Erol, A.; Randhir, T.O. Watershed ecosystem modeling of land-use impacts on water quality. Ecol. Modell. 2013, 270, 54–63, doi:10.1016/j.ecolmodel.2013.09.005.
53. Palazón, L.; Navas, A. Modeling sediment sources and yields in a Pyrenean catchment draining to a large reservoir (Ésera River, Ebro Basin). J. Soils Sediments 2014, 14, 1612–1625, doi:10.1007/s11368-014-0911-7.
54. Julien, Y.; Sobrino, J.A. The Yearly Land Cover Dynamics (YLCD) method: An analysis of global vegetation from NDVI and LST parameters. Remote Sens. Environ. 2009, 113, 329–334.
55. Khan, J.; Wang, P.; Xie, Y.; Wang, L.; Li, L. Mapping MODIS LST NDVI Imagery for Drought Monitoring in Punjab Pakistan. IEEE Access 2018, 6, 19898–19911.
56. Legendre, P. Spatial Autocorrelation : Trouble or New Paradigm? Ecology 1993, 74, 1659–1673.
57. Dutilleul, P. Spatial Heterogeneity and the Design of Ecological Field Experiments. Ecology 1993, 74, 1646–1658.
58. Anderson, L.O.; Malhi, Y.; Aragão, L.E.O.C.; Saatchi, S. Spatial patterns of the canopy stress during 2005 drought in Amazonia. In Proceedings of the 2007 IEEE International Geoscience and Remote Sensing Symposium, Barcelona, Spain, 23–28 July 2007; pp. 2294–2297.
59. González-Loyarte, M.M.; Menenti, M. Impact of rainfall anomalies on Fourier parameters of NDVI time series of northwestern Argentina. Int. J. Remote Sens. 2008, 29, 1125–1152, doi:10.1080/01431160701355223.
60. Vicente-serrano, S.M.; Gouveia, C.; Julio, J.; Beguería, S.; Trigo, R. Response of vegetation to drought time-scales across global land biomes. Proc. Natl. Acad. Sci. USA2012, 110, 52–57, doi:10.1073/pnas.1207068110.
61. Belda, F. Relationships between climatic parameters and forest vegetation: Application to burned area in Alicante (Spain). For. Ecol. Manag. 2000, 135, 195–204, doi:10.1016/S0378-1127(00)00310-8.
62. Melendez-Pastor, I.; Navarro-Pedreño, J.; Gómez, I.; Koch, M. Detecting drought induced environmental changes in a Mediterranean wetland by remote sensing. Appl. Geogr. 2010, 30, 254–262, doi:10.1016/j.apgeog.2009.05.006.

63. Roerink, G.J.; Menenti, M.; Soepboer, W.; Su, Z. Assessment of climate impact on vegetation dynamics by using remote sensing. Phys. Chem. Earth 2003, 28, 103–109, doi:10.1016/S1474-7065(03)00011-1.
64. Baltagi, B.H.; Heun Song, S.; Cheol Jung, B.; Koh, W. Testing for serial correlation, spatial autocorrelation and random effects using panel data. J. Econom. 2007, 140, 5–51.
65. Yang, X.; Jin, W. GIS-based spatial regression and prediction of water quality in river networks: A case study in Iowa. J. Environ. Manag. 2010, 91, 1943–1951.
66. Yin, C.; Yuan, M.; Lu, Y.; Huang, Y.; Liu, Y. Effects of urban form on the urban heat island effect based on spatial regression model. Sci. Total Environ.2018, 634, 696–704.
67. Melendez-Pastor, I.; Navarro-Pedreño, J.; Koch, M.; Gómez, I. Multi-resolution and temporal characterization of land use classes in a Mediterranean wetland with land cover fractions. Int. J. Remote Sens. 2010, 31, 5365–5389.
68. Van Oijen, M.; Balkovi, J.; Beer, C.; Cameron, D.R.; Ciais, P.; Cramer, W.; Kato, T.; Kuhnert, M.; Martin, R.; Myneni, R.; et al Impact of droughts on the carbon cycle in European vegetation: A probabilistic risk analysis using six vegetation models. Biogeosciences 2014, 11, 6357–6375, doi:10.5194/bg-11-6357-2014.

Ortofoto PNOA sobre el Embalse del Negratín, Granada.
Fuente: OrtoPNOA 2021 CC-BY 4.0

Marco Dos Santos, G., Meléndez-Pastor, I.. Navarro-Pedreño, J., , Gómez Lucas, I. (2021).

Using Landsat images to determine water storing capacity in Mediterranean environments.

Journal of Geographical Research, 4(4), 3780.

https://doi.org/10.30564/jgr.v4i4.3780

Abstract

Reservoirs play an important role in water management and are key elements for water supply. Monitoring is needed in order to guarantee the quantity and quality of stored water. However, this task is sometimes not easy. The objective of this study was to develop a procedure for predicting volume of stored water with remote sensing in water bodies under Mediterranean climate conditions. To achieve this objective, multispectral Landsat 7 and 8 images (NASA) were analyzed for the following five reservoirs: La Serena, La Pedrera, Beniarrés, Cubillas and Negratín (Spain). Reservoirs water surface was computed with the spectral angle mapper (SAM) algorithm. After that, cross-validation regression models were computed in order to assess the capability of water surface estimations to predict stored water in each of the reservoirs. The statistical models were trained with Landsat 7 images and were validated by using Landsat 8 images. Our results suggest a good capability of water volume prediction from free satellite imagery derived from surface water estimations. Combining free remote sensing images and open source GIS algorithms can be a very useful tool for water management and an integrated and efficient way to control water storage, especially in low accessible sites.

Keywords

Climate change; decision-making tools; GIS; reservoir; water storage

1. Introduction

Reservoirs are a very important tool for water management, especially in semi-arid areas [1]. They facilitate water supply in scarcity periods, flood control, hydroelectric power generation and other uses [2]. In arid and semi-arid areas, with water scarcity and irregular precipitation, an efficient use of water resources is one of the greatest challenges for managers [3], especially considering the climate change projections where a decrease in available water resources is expected [4,5]. In Spain, there has been a significant increase in water demand mainly to the growth in population, above all in the coastal areas due to tourism. Likewise, the irrigated area, mainly in the South, has increased in the past decades. Increased population, irrigation and energy generation are the main causes of the regulation of river flows. In fact, Spain is the EU country with the largest irrigated area [6]. Therefore, there is a water stress caused by a situation of lack of water resources and a high extraction rate [7]. As a result, most of the rivers are regulated by dams, which negatively affect fluvial dynamics such as sediment transport, alteration in the runoff balance, and aquifers recharge. Spain is the European country with the largest number of dams (more than 1,200 dams with total water stored capacity of 56,000 hm^3) [8] and with a large supply network. However, all of these infrastructures entail a very high maintenance cost. Despite this, according to a report carried out by SEOPAN (Spanish Association of Construction Companies and Concessionaires of Infrastructures), Spain is the country of the EU that less economic investment dedicates to the water infrastructures maintenance and improvement (nowadays, it is investing 60% less than in 2007) [9]. According to data from the Ministry for the Ecological Transition [10], in March 2019, the Spanish water reserve rose up to 58.1% of the total capacity, and in March of 2021 this was close to 63.1%. The sum of the consequences of climate change and the aging of infrastructures, can lead to an alarming situation with important losses of this valuable resource and the storage capacity.

There are different techniques to estimate the water reserve and the storing capacity. In Spain, the most commonly used equipment to measure the water level in reservoirs are pressure methods (hydrostatic collection, pneumatic capture, etc.), since they have high precision and stability[11] in addition to the traditional limnimetric method. However, the use of this type of sensors could suppose a cost in the maintenance and the time dedicated (i.e. inspections and technical visits), especially for smaller and/or dispersed reservoirs in the territory. Even more, one of the problems in the water reserve temporal series data is the deficiency of homogeneity in the values due to changes in the gauging stations over time [12]. In developing countries, it could be difficult the availability and the continue maintenance of these tools to measure the water stored.

Remote sensing is a tool that can be very useful to study the water quantity and quality over time, especially when direct observation or validation *in situ* is not possible [1,13]. It offers the possibility of assess current and monitor future water demands in order to better allocate limited water resources with integrated management systems [14]. Satellite images can provide us with an overview of the resource spatiotemporal dynamics and incorporate it into management measures [15,16]. Even more, the free availability of Landsat images can help to control and manage water and produce models to estimate the future scenarios of water storage and demand [17].

Despite the possibility of cloud cover [18,19] the images obtained from the Landsat ETM and ETM+ sensors present a medium spatial and temporal resolution [20] that allow to map variations of the surface of the dammed water. There are some researches who used different remote sensing products to assess, estimate and monitor, and develop methodologies in order to obtain data series [21-24] that help in the management of water resources, even in developing countries [25,26].

Considering the facilities of acquiring remote sensing images and the possibilities offered by free Geographic Information Systems (GIS) for modelling and predicting future sceneries, the combination of both could be useful for water management and decision makers [27-31].

The purpose of this study was to assess the potential use of remote sensing images to estimate storage capacity in different reservoirs by using open source tools and establishing a quick method to estimate the volume of water stored, that can be integrated into an automatic or semiautomatic management system.

2. Materials and Methods

Five reservoirs with different sizes (and water storing capacity) were selected in this study (Figure 1) combining Landsat images and hydrological studies [32]. These reservoirs are located in the climatic Mediterranean area of Spain: La Pedrera and Beniarrés, both in the province of Alicante, Cubillas and Negratín in the province of Granada and La Serena in the province of Badajoz. The annual average rainfall of all areas is between 300-500 mm and the annual average temperature range from 14ºC to 16°C [33].

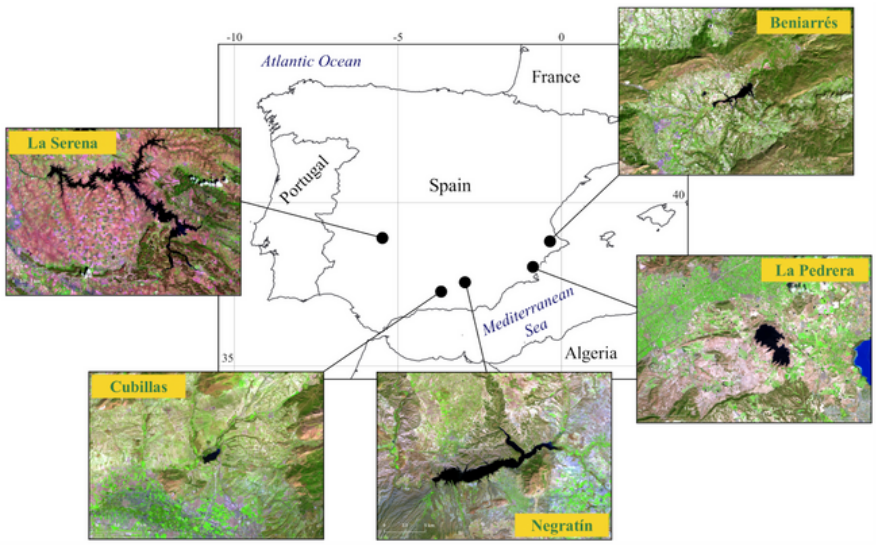

Figure 1. *Location of the studied reservoirs. False color composites of each study area are shown (source: Landsat 8 OLI RGB:5.6.2).*

Characteristics of each reservoir, such as surface and maximum capacity are summarized in Table 1. La Serena reservoir (38°55'49.4"N 5°13'36.1"W) is located at the confluence of the Zújar river and the Guadalemar river in the Guadiana river basin. It was built in 1990 over a large part of the old Zújar Reservoir. Annual average precipitation values are around 550.40 mm, and frequent droughts periods during summer months. The main uses are mainly irrigation, but also water supply and hydroelectric power generation [34].

La Pedrera reservoir (38°01'05.9"N 0°51'56.9"W) was built to use it as a regulator in the distribution of water from the Tajo-Segura transfer to the Campo de Cartagena in 1985. It is located on the Rambla de Alcoriza, in the Segura watershed. This area is characterized by low and irregular rainfall (around 300 mm, mainly in April and October), and high temperature. La Pedrera reservoir is a key element which is part of a natural and man-made environment cataloged as a Protected Landscape of Sierra Escalona and its surroundings. Moreover, this area is classified as a Special Protection Area (SPA) for Birds and Site of Community Importance (SCI) [35,36].

Beniarrés reservoir (38°48'21.2"N 0°21'52.2"W) is located on the Serpis river and it was built in 1958 mainly for agricultural irrigation, but fishing is also allowed. Annual average precipitation is about 650 mm.

The reservoir is surrounded by two SCI's: Sierra de la Safor and Valls de la Marina, both with a great endemic vegetation representation [37,38].

Cubillas reservoir (37°16'37.0"N 3°40'13.6"W) was built in 1956 on the Cubillas river and it is not only used for irrigation but also as a bathing area. The Cubillas watershed average rainfall values are around 600 mm, with dry hot summers. It is located close to Sierra de Huétor Natural Park [39].

Negratín reservoir (37°17'19.03"N 3°39'44.66" W) was built in December of 1984 on the Guadiana Menor river and currently is the third biggest reservoir in Andalusia (Spain). The main uses are irrigation and electric generation, but also has a great social component for sailing, fishing or bathing [40]. It is situated 100 kilometers northeast of the Cubillas reservoir.

Table 1. *Main characteristics of the study reservoirs. Source: Spanish Yearbook of the Water Gauging Information System [40].*

Reservoir	Surface (ha)	Maximum storage capacity (hm^3)
La Serena	13,708.3	3,219
La Pedrera	1,226.9	246
Beniarrés	224.3	27
Cubillas	184.6	21
Negratín	2,016.8	567

To describe material and methods employed in this research, a flowchart with the sequence of data sources and analyses is provided (Figure 2).

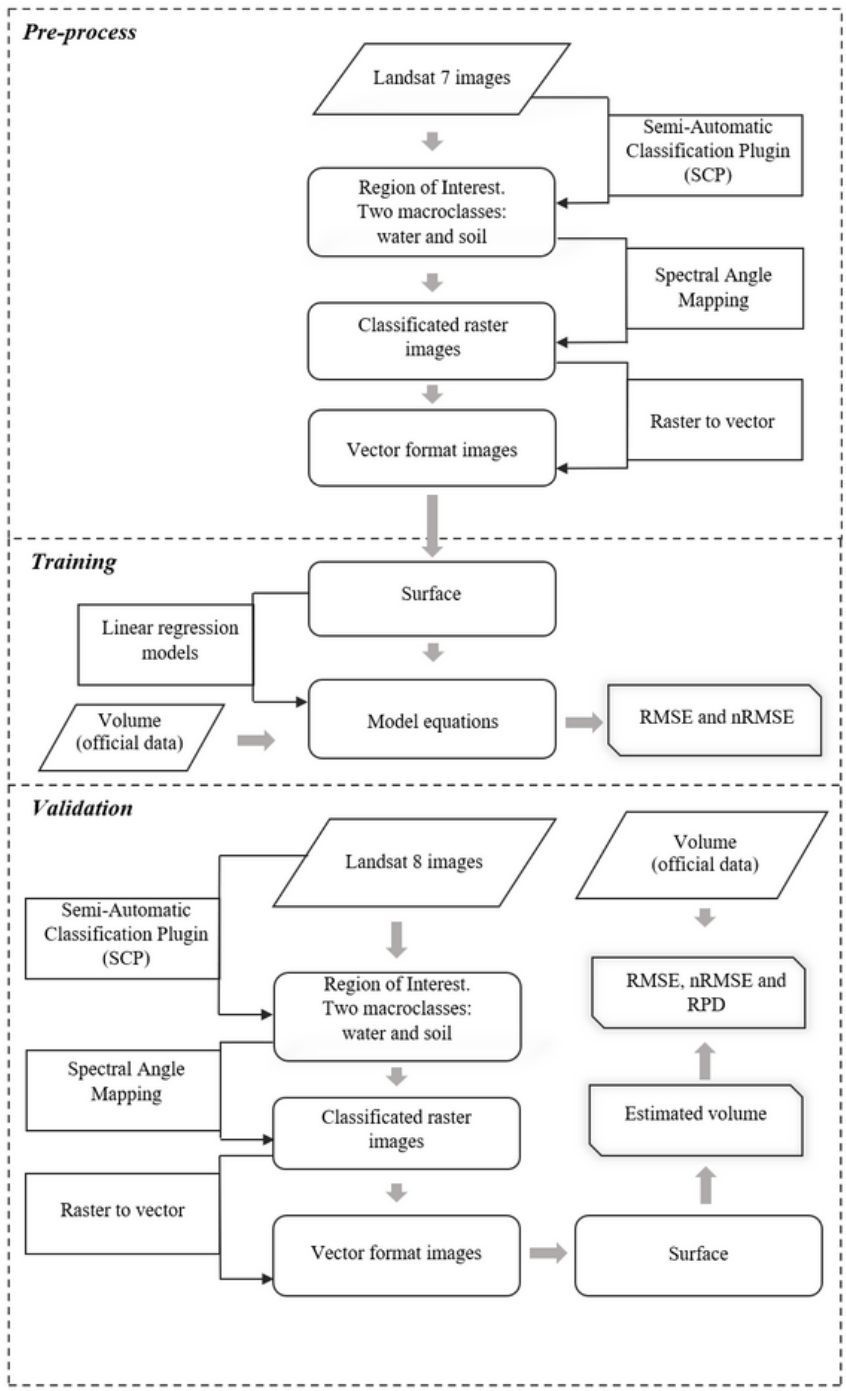

Figure 2. *Flow chart of the process: 1) Pre-processing of Landsat 7 images with QGIS and the SCP plugin, 2) Training model, 3) Validation process with Landsat 8.*

2.1. Hydrological data

Water storage data proceeded from the web tool State Monitoring Networks and Hydrological Information [41] owned firstly by the Ministry of Agriculture and Fisheries, Food and Environment (MAPAMA), nowadays by the Ministry of Ecological Transition and Demographic Challenge (MITECO), with information about outlet flow, reservoir water level, and water storage.

Daily values of water level variation for each reservoir were obtained from the monitoring control stations network. These data do not consider evaporation losses. Reservoir water volume data used for each reservoir were from the same dates when the remote sensing images were obtained. This information is publicly available and facilitated the production of water storage time series.

The Official Gauging Stations Network has been in operation since the hydrological year 1911-1912, so there may be some variations in the data homogeneity, due to changes and improvements in the measurement systems used over the years. Gauging stations are part of the continental water masses monitoring program.

2.2. Remote sensing data

Multispectral Landsat images were processes in this study (336 images). Landsat 7 ETM+ (Level-2) images acquired from the U.S. Geological Survey-Earth Explorer Geodatabase [42], corresponding with dates between October 1999 and May 2003, were employed in the first stage of this study. Although the main limitation was cloud cover, the number of cloud free (under 10%) images used for each dam were the following: 28 images for La Serena, 85 for La Pedrera, 43 for Beniarrés, 35 for Cubillas and 62 for Negratín.

Additionally, a set of images acquired between April 2013 and December 2015 by the Landsat 8 Operational Land Imager (OLI) (Level-2) were use in the second stage of the study. A total of 17 images for La Serena, 14 for La Pedrera, 16 for Beniarrés, 15 for Cubillas and 21 for Negratín were used.

Landsat images have been widely used in numerous studies around the world for the observation and monitoring changes and processes in water masses, mainly due to the image's availability from the 1970s to the present day.

2.3. Image processing

Firstly, the images were bounded by using a buffer created from the geographical data files (shapefiles) of the reservoirs (maximum surface). This geographical database was obtained from the open source spatial data infrastructure of the different Hydrographic Confederations of the rivers: Guadiana [34], Segura [35], Júcar [37] and Guadalquivir [39].

A supervised classification approach was employed to calculate the water surface of each Landsat image [43]. For each one, the algorithm was trained with sets of pixels belonging to the following categories “water” or “upland”. In this study, we focused on delimiting the area corresponding to the water surface, associated with the thematic class “water”. The Spectral Angle Mapper algorithm (SAM) [44,45] was employed for mapping surface water extent. The algorithm calculates the similarities between the spectral signatures of the training image and the spectral signatures of the pixels of the image as vectors in an equal dimension to the number of bands (bands 1, 2, 3, 4, 5, 7 for Landsat 7 and bands 2, 3, 4, 5, 6, 7 for Landsat 8). The SAM equation is the following (Equation 1):

$$(x, y) = \cos^{-1}\left(\frac{\sum_{i=1}^{n} x_i y_i}{\left(\sqrt{\sum_{i=1}^{n} x_i^2}\right)^{\frac{1}{2}}\left(\sqrt{\sum_{i=1}^{n} y_i^2}\right)^{\frac{1}{2}}}\right) \quad (1)$$

where *n* is the number of bands in the image, *x* is the spectral signature vector of a pixel image, *y* is the spectral signature vector of the training area. Therefore, a pixel belongs to the class having the lower angle (Equation 2):

$$x \in C_k \Leftrightarrow \theta(x, y_k) < \theta(x, y_j) \forall k \neq j \quad (2)$$

where *Ck* is the *k* coverage class, *yk* is the *k* class spectral signature, and *yj* is the *j* class spectral signature.

Digital image processing analyses were performed with the QGIS vs. 3.4 “Madeira” open source Geographical Information System [46] and the Semi-Automatic Classification Plugin (SCP) [47].

2.4. Statistical analyses

Descriptive statistics of estimated surface water and officially registered water volume were compared for each reservoir. After that, a statistical modeling approach for predicting water volume from remote sensing surface water estimation was done.

Least square regression models were computed to predict water volume from the obtained surface water maps. In order to develop a cross-validation modeling approach, Landsat 7 images were used for training and Landsat 8 images were for independent validation. In this sense, 75% of the images were employed for training and 25% for independent validation.

The training stage implied the development of regression models between surface water estimations and official water volume. Then, regression coefficients were used to compute the estimated water volume in the validation stage and compared with measured water volume. A set of statistical measurement were used to assess the accuracy of both modeling stages. Firstly, Pearson correlation coefficient (R2) was calculated to explain how much variation in the dependent variable y (volume) is explained by x (surface) variable. Then, the adjustment of the estimation model was evaluated by using the Root Mean Square Error (RMSE) and Normalized Root Mean Square (nRMSE) [48,49]. RMSE compares a predicted value and an observed value (Equation 3).

$$RMSE = \sqrt{\frac{\sum(M-E)^2}{n}} \tag{3}$$

where M = measure value, E = estimated value, and n = number of samples used for prediction. The smaller a RMSE value is, the closer the predicted and observed values are. Due to reservoirs have different dimensions, the nRMSE was calculated in order to provide a practical comparison among regression models for reservoirs with different spatial scales. This measurement was computed as a normalization of the RMSE respect to the range of the response variable (Equation 4).

$$nRMSE\ (\%) = \frac{RMSE}{range} \cdot 100 \tag{4}$$

Finally, the robustness of the predictions in the validation stage were evaluated with the Residual Predictive Deviation (RPD) that is computed as the standard deviation (σ) of

observed values divided by the Root Mean Square Error or Prediction (RMSEP) as shown in Equation 5.

$$RPD = \frac{\sigma}{RMSEP} \quad (5)$$

To interpret the results of the RPD statistics, Cheng *et al.* [50] proposed that successful models should have RPD values higher that 2, moderately successful models have RPD values in the range 1.4 to 2, and unsuccessful models have lower values. All statistical analyses were developed with the R programming language [51] in the RStudio (https://www.rstudio.com/) integrated development environment.

3. Results

During all the studied period, reservoirs exhibited large stored water fluctuations. Average water volume of La Serena was 2369.9 hm^3 (74% of its maximum capacity), 83.9 hm^3 for la Pedrera (34% of its maximum capacity), 11.1 hm^3 for Beniarrés (41% of its maximum capacity), 15.8 hm^3 for Cubillas (75% of its maximum capacity) and 388.1 hm^3 for Negratín (68% of its maximum capacity). Those water bodies with a lower value than the maximum capacity correspond to reservoirs with greater seasonal variability, measured by their coefficient of variation. In fact, significant negative correlation between both variables ($R=-0.94$; $p\text{-value}<0.05$) was obtained. It denotes the high variability of the water surface, especially in drier Southeast of Spain.

Training stage implied the development of regression models among the estimated water surface of each reservoir from Landsat 7 images and the officially measured stored water data (Figure 3). In these five cases, we reported R^2 values over 0.9.

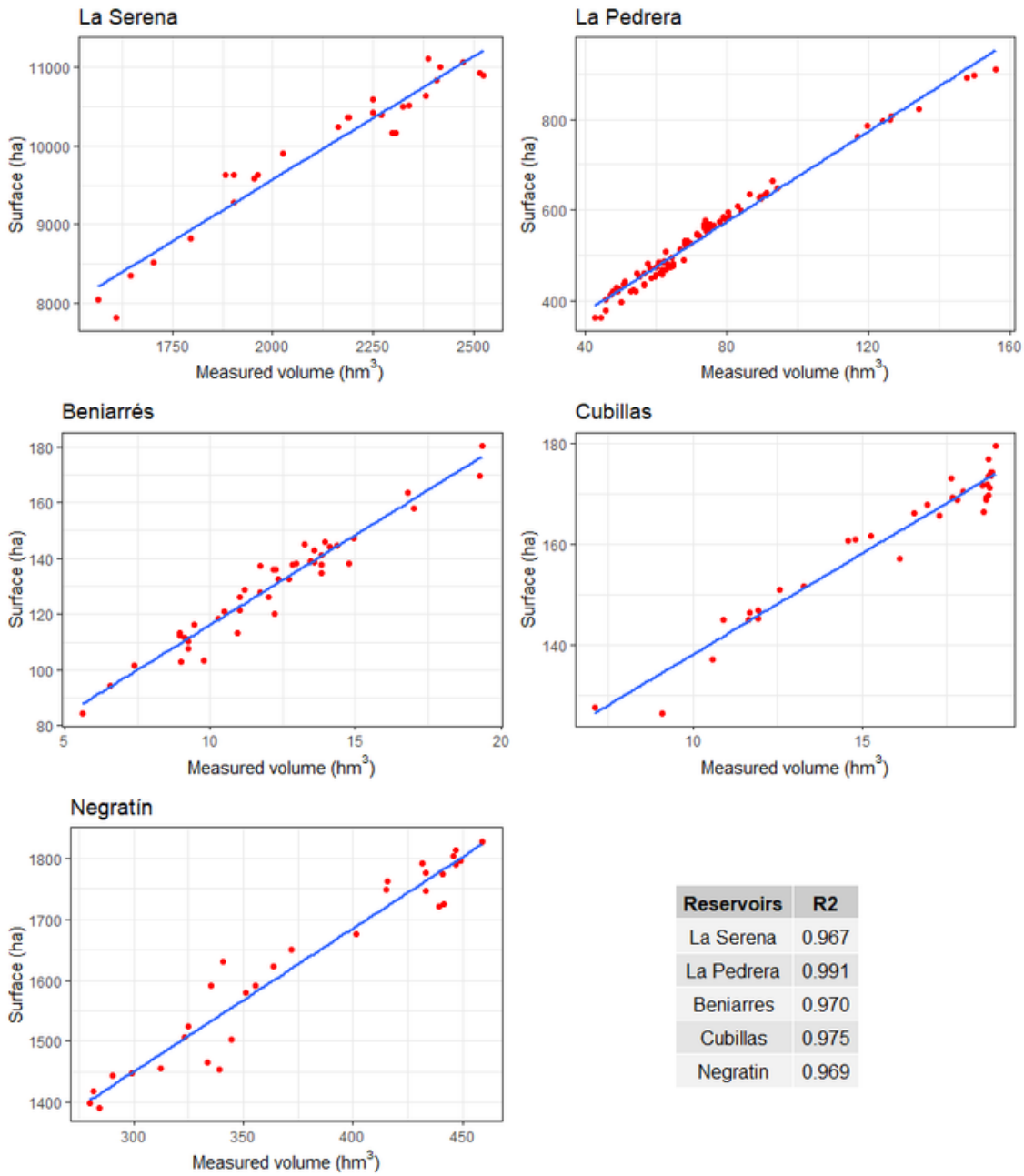

Reservoirs	R2
La Serena	0.967
La Pedrera	0.991
Beniarres	0.970
Cubillas	0.975
Negratin	0.969

Figure 3. *Linear regression between water surface and water storage in the five reservoirs (note: R2 means R^2).*

In order to increase the knowledge about the performance of the regression models, RMSE and nRMSE were computed along with the Pearson correlation coefficient (Table 2). Lower RMSE values indicate a better fit of the models, and the lower values were obtained for Beniarrés (RMSE = 0.713) and Cubillas (RMSE = 0.742) reservoirs. These results should be analysed carefully because this statistic is scale-dependent. To avoid this problem, RMSE was normalized with the range of the predicted variable, thus obtaining the nRMSE. A more coherent comparison of the model was possible with the nRMSE and its values were about 20-25% except for La Pedrera, that was notably lower (nRMSE = 13.4%). All of them show adequate results of the model adjustment [50].

Table 2. *Cross-validation results. Estimation of water volume from remote sensing surface water.*

	Training			Validation			
Reservoir	**R^2**	**RMSE**	**nRMSE**	**R^2**	**RMSE**	**nRMSE**	**RPD**
La Serena	0.967	72.352	25.0%	0.939	37.408	33.2%	3.01
La Pedrera	0.991	3.288	13.4%	0.991	3.926	12.7%	7.90
Beniarrés	0.970	0.713	24.0%	0.973	1.018	22.3%	4.49
Cubillas	0.975	0.742	21.7%	0.990	0.378	13.7%	7.32
Negratín	0.969	14.721	24.2%	0.930	11.644	35.8%	2.79

Validation of the previous regression models was developed with an independent Landsat 8 repository of images. Coefficients of the training stage were employed to predict water volume from estimated water surface. Then, water storage predictions were compared with officially measured water volume [52].

4. Discussion

Our results suggest that this methodology used for estimating surface water was robust enough (Table 2 and Figure 4), even at highly variable water bodies (human consumption, irrigation…) such as our studied reservoirs. Pearson correlation coefficients were always high ($R^2 > 0.9$) and RMSE and nRMSE were similar to those obtained in the training stage. La Pedrera (nRMSE = 12.7%) and Cubillas (nRMSE = 13.7%) reservoirs reported the better results for those statistics.

The predictive capability of regression models was evaluated with the residual predictive deviation (RPD) statistics. All the models reported RPD values higher than 2, that is a threshold commonly employed to identify model that could bring successful predictions of selected variables.

The use of temporal series of images to study and monitoring hydrologic dynamics in arid and semi-arid areas is becoming of great interest due to the increasing pressure on the water resources [53,54]. In addition, predictions of climate change cause growing concern about the efficiently management of resources.

In this study, according to the results obtained, the relationship between the water surface of the reservoirs and the stored water presents a good adjustment although some values of nRMSE were relatively low. Values of RPD over 2 indicate a successful prediction with maximum values for La Pedrera and Cubillas.

The complex sinuosity of the shore of the reservoirs and the existence of vegetation that covers the borders could affect the delimitation of the water surface by using automatic classification tools.

Despite the usually clouds coverage presented in these areas, there are a large number of images available to obtain good prediction models for water storage. However, there may be changes in the storage capacity due to structural, operational level modifications or sedimentation processes [55,56]. Knowing these, managers could quickly re-estimate the available water and use this methodology efficiently.

The information provided from this study could be useful when trying to estimate the available volume mainly in those areas where reservoirs monitoring has a complex accessibility, cost and time-consuming [17,52]. This information could be integrated into semiautomatic or automatic decision-making tools and big data management and can help to study the effects of the climate change and predict future sceneries to determine water availability.

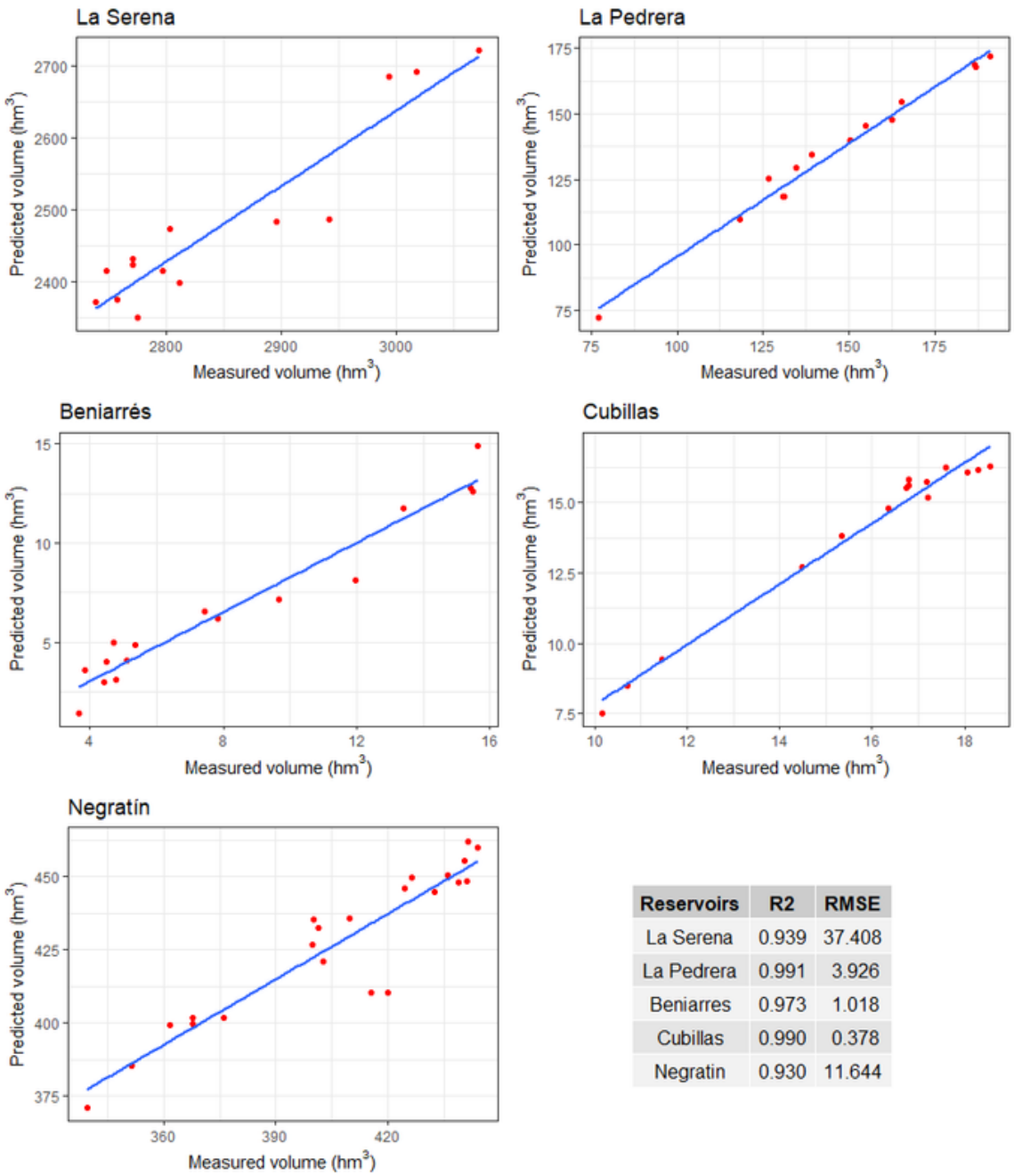

Reservoirs	R2	RMSE
La Serena	0.939	37.408
La Pedrera	0.991	3.926
Beniarres	0.973	1.018
Cubillas	0.990	0.378
Negratin	0.930	11.644

Figure 4. *Comparison between measured and predicted volume obtained from validation in Landsat 8 images (note: R2 means R^2).*

5. Conclusions

The relationship between area and water stored obtained in this study presents a good adjustment with high R2 values and great RCP values, mainly in two reservoirs: La Pedrera and Cubillas. The study indicates the possibility of incorporating this methodology into management systems as an auxiliary tool to control water reservoirs. One of the main advantages of using remote sensing is the availability of images to create temporal series with water storage data in a quickly and less costly way by using an open source Geographic Information System and free download images such as Landsat. This can help to take decisions and create strategies to predict different future scenarios.

This methodology has the aim of facilitating the implementation of an essay tool and method to manage water resources with a minimum cost, based on the use of free sources and open software.

Another advantage may be that this type of methodology can be easily automated. It is possible to create plugins and run personalize applications. For instance, using a programming language, a script can be created to automate the process of obtaining update images, processing and calculating the water surface. To manage and analyse large volumes of information, as well as adjust and customize the methodology, this type of tools is very efficient and suitable. In this sense, this would be the first step for an automated management of big data and control data of a wide variety of reservoirs in order to establish regional or national strategies for water supply, hydroelectrical energy production and irrigation water availability.

References

1. Sawunyama, T.; Senzanje, A.; Mhizha, A. (2006). Estimation of small reservoir storage capacities in Limpopo River Basin using geographical information systems (GIS) and remotely sensed surface areas: Case of Mzingwane catchment [C]. Physics and Chemistry of the Earth, 31, 15-16: 935-943. https://doi.org/10.1016/j.pce.2006.08.008
2. Loumagne, C.; Normand, M.; Riffard, M.; Weisse, A.; Quesney, A.; Lehégarat-Mascle, S.; Alem, F. (2001). Integration of remote sensing data into hydrological models for reservoir management [C]. Hydrological Sciences Journal, 46, 1: 89-102. http://doi.org/10.1080/02626660109492802
3. FAO. (2015). Towards a water and food secure future. Critical Perspectives for Policy-makers. Food and Agriculture Organization of the United Nations (Rome) and World Water Council (Marseille) [R]. Available online: http://www.fao.org/3/a-i4560e.pdf (accessed on 18/04/2019)

4. Vargas-Amelin, E.; Pindado, P. (2014). The challenge of climate change in Spain: Water resources, agriculture and land [C]. Journal of Hydrology, 518B: 243-249. https://doi.org/10.1016/j.jhydrol.2013.11.035
5. Jiménez Álvarez, C.; Mediero Orduña, A.; García Montañés, L. Review and selection of stadistical models to fit maximum annual peak flows distribution function in Spain [R]. CEDEX, Spain. Available online: http://www.cedex.es/NR/rdonlyres/96DF4741-0D23-4D67-9956-4BAF6DA5CD97/129082/CEH1174_v2.pdf (accessed on 15/04/2021)
6. Planas, L. La modernización de regadíos es clave para la sostenibilidad y el futuro de nuestra agricultura [N]. XIX Jornada Técnica de Fenacore. Ministry of Agriculture, Fisheries and Food, Spain. Available online: https://www.mapa.gob.es/es/prensa/ultimas-noticias/luis-planas-la-modernizaci%C3%B3n-de-regad%C3%ADos-es-clave-para-la-sostenibilidad-y-el-futuro-de-nuestra-agricultura/tcm:30-506649 (accessed on 23/04/2021)
7. Rovira, A.; Polo, M.J. (2015). Current and future challenges in water resources management in Spain [S]. Global Water Forum, IRTA-Aquatic Ecosystems; University of Cordoba. Available online: http://www.globalwaterforum.org/2015/04/20/current-and-future-challenges-in-water-resources-management-in-spain/ (accessed on 19/04/2021)
8. MITECO. Desarrollo, situación actual y perspectivas de futuro de las presas en España. Available online: https://www.miteco.gob.es/es/agua/temas/seguridad-de-presas-y-embalses/desarrollo/ (accessed on 28/04/2021)
9. P. Alarcos, A. (2018). Seopan: "La falta de inversión en infraestructuras pone en peligro la competividad de la economía" [N]. Available online: https://www.idealista.com/news/finanzas/inversion/2018/06/19/766177-seopan-alerta-la-falta-de-inversion-en-infraestructuras-pone-en-peligro-la-competividad (accessed on 19/04/2021)
10. Ministry for the Ecological Transition. (2021). Estado de los embalses [N]. Available online: https://www.miteco.gob.es/es/prensa/ultimas-noticias/la-reserva-h%C3%ADdrica-espa%C3%B1ola-se-encuentra-al-616-por-ciento-de-su-capacidad-/tcm:30-525179 (accessed on 20/04/2021)
11. González de la Aleja, S.M. (2006). Medida de nivel en embalses. Evolución, posibilidades y tratamiento actual [S]. CONAMA Foundation: SMAGUA Zaragoza, Spain. Available online: http://www.hidrosanco.com/pdf/Medida%20de%20niveles%20en%20embalses.pdf
12. MAPAMA. Anuario de aforos 2014-15. Available online: http://ceh-flumen64.cedex.es/anuarioaforos/AnuarioMemoria.pdf (accessed on 16/04/2021)
13. Peng, D.; Guo, S.; Liu, P.; Liu, T. (2006). Reservoir Storage Curve Estimation Based on Remote Sensing Data [C]. Journal of Hydrologic Engineering, 11, 2: 165–172. doi: 10.1061/(ASCE)1084-0699(2006)11:2(165)
14. Marco-Dos Santos, G.; Melendez-Pastor, I.; Navarro-Pedreño, J.; Koch, M. (2019). Assessing Water Availability in Mediterranean Regions Affected by Water Conflicts through MODIS Data Time Series Analysis [C]. Remote Sensing, 11, 11: 1355. https://doi.org/10.3390/rs11111355

15. Nkwonta, O.I.; Dzwairo, B.; Otieno, F.A.O.; Adeyemo, J.A. (2017). A review on water resources yield model [C]. South African Journal of Chemical Engineering, 23: 107-115. https://doi.org/10.1016/j.sajce.2017.04.002
16. Avisse, N.; Tilmant, A.; Müller, M.F.; Zhang, H. (2017). Monitoring small reservoirs' storage with satellite remote sensing in inaccessible areas [C]. Hydrology and Earth System Sciences, 21, 12: 6445–6459. doi: 10.5194/hess-21-6445-2017
17. E.A. Silva; M.M. Pedrosa; S.C. Azevedo; G.P. Cardim; F.P.S. Carvalho. (2016). Assessment of surface water at the Sobradinho reservoir under the effects of drought using multi-temporal Landsat images [C]. International Archives of the Photogrammetry, Remote Sensing and Spatial Information Sciences, XLI-B8, XXIII ISPRS Congress. doi:10.5194/isprsarchives-XLI-B8-387-2016
18. Pipitone, C.; Maltese, A.; Dardanelli, G.; Lo Brutto, M.; La Loggia, G. (2018). Monitoring water surface and level of a reservoir using different remote sensing approaches and comparison with dam displacements evaluated via GNSS [C]. Remote Sensing, 10, 1: 71. https://doi.org/10.3390/rs10010071
19. Melendez-Pastor, I.; Navarro-Pedreño, J.; Koch, M.; Gómez, I. (2010). Multi-resolution and temporal characterization of land-use classes in a mediterranean wetland with land-cover fractions [C]. International Journal of Remote Sensing, 31, 20: 5365-5389. doi: 10.1080/01431160903349065
20. Fang, H.-b.; Hu, T.-s.; Zeng, X.; Wu, F.-y. (2014). Simulation-optimization model of reservoir operation based on target storage curves [C]. Water Science and Engineering, 7,4: 433-445. doi: 10.3882/j.issn.1674-2370.2014.04.008
21. Soti, V.; Tran, A.; Bailly, J.S.; Puech, C. (2009). Assessing optical earth observation systems for mapping and monitoring temporary ponds in arid areas [C]. International Journal of Applied Earth Observation and Geoinformation, 11, 5: 344-351. https://doi.org/10.1016/j.jag.2009.05.005
22. Cai, X.; Feng, L.; Hou, X.; Chen. (2016). Remote Sensing of the Water Storage Dynamics of Large Lakes and Reservoirs in the Yangtze River Basin from 2000 to 2014 [C]. Scientific Reports, 6. https://doi.org/10.1038/srep36405
23. Lacaux, J. P.; Tourre, Y. M.; Vignolles, C.; Ndione, J. A.; Lafaye, M. (2007). Classification of ponds from high-spatial resolution remote sensing: Application to Rift Valley Fever epidemics in Senegal [C]. Remote Sensing of the Environment, 106, 1: 66–74. https://doi.org/10.1016/j.rse.2006.07.012
24. Y. Ma; N. Xu; J. Sun; X.H. Wang; F. Yang; S. Li. (2019). Estimating water levels and volumes of lakes dated back to the 1980s using Landsat imagery and photon-counting lidar datasets [C]. Remote Sensing of the Environment, 232: 111287. https://doi.org/10.1016/j.rse.2019.111287
25. R. Schaeffer, B.A.; Schaeffer, K.G.; Keith, D.; Lunetta, R.S.; Conmy, R.; W. Goild, (2013). Barriers to adopting satellite remote sensing for water quality management [C]. International Journal of Remote Sensing, 34, 21: 7534–7544. https://doi.org/10.1080/01431161.2013.823524

26. Venkatesan, V.; Balamurugan, R.; Krishnaveni, M. (2012). Establishing water surface area-storage capacity relationship of small tanks using SRTM and GPS [C]. Energy Procedia, 16, B: 1167–1173. https://doi.org/10.1016/j.egypro.2012.01.186
27. Abileah, R.; Vignudelli, S.; Scozzari, A. (2011). A completely Remote Sensing approach to monitoring reservoirs water volume [C]. Fifteenth International Water Technology Conference, IWTC 15. Available online: https://www.researchgate.net/publication/228517141_A_Completely_Remote_Sensing_Approach_To_Monitoring_Reservoirs_Water_Volume (accessed on 15/04/2021)
28. Martin, P.H.; LeBoeuf, E.J.; Dobbins, J.P.; Daniel, E.B.; Abkowitz, M.D. (2005). Interfacing GIS with water resource models: a state-of-the-art review [C]. Journal of the American Water Resources Association (Jawra), 41, 6: 1471-1487. https://doi.org/10.1111/j.1752-1688.2005.tb03813.x.
29. Valjarević, A.; Filipović, D.; Valjarević, D.; Milanovic, M.; Milosevic, S.; Zivic, N., Lukic, T. (2020) GIS and remote sensing techniques for the estimation of dew volume in the Republic of Serbia [C]. Meteorological Applications, 27, 3: e1930. https://doi.org/10.1002/met.1930.
30. Valjarević, A.; Milanović, M.; Valjarević, D.; Basarin, B.; Gribb, W.; Lukic, T. (2021). Geographical information systems and remote sensing methods in the estimation of potential dew volume and its utilization in the United Arab Emirates [C]. Arabian Journal Geosciences 14, 1430. https://doi.org/10.1007/s12517-021-07771-3
31. Martin, P.H.; LeBoeuf, E.J.; Daniel, E. B.; Dobbins, J.P.; Abkowitz, M.D. (2004). Development of a GIS-based Spill Management Information System [C]. Journal of Hazardous Materials, 112, 3: 239-252, https://doi.org/10.1016/j.jhazmat.2004.05.014
32. Ogilvie, A.; Belaud, G.; Massuel, S.; Mulligan, M.; Le Goulven, P.; Malaterre P.-O.; Calvez, R. (2018). Combining Landsat observations with hydrological modelling for improved surface water monitoring of small lakes [C]. Journal of Hydrology, 566: 109-121. https://doi.org/10.1016/j.jhydrol.2018.08.076
33. AEMET-IMP. (2011). Iberian Climate Atlas. Air temperature and precipitation (1971-2000) [M]. Spanish Meteorological Agency (AEMET) and Portuguese Institute of Meteorology (IMP): Madrid, Spain and Lisbon, Portugal. ISBN 978-84-7837-079-5.
34. Guadiana Hydrographic Confederation. Ministry for the Ecological Transition. Available online: https://www.chguadiana.es/ (accessed on 01/03/2021)
35. Segura Hydrographic Confederation. Ministry for the Ecological Transition. Available online: https://www.chsegura.es/chs/index.html (accessed on 01/03/2021)
36. Ministry of Agriculture, Rural Development, Climate Emergency and Ecological Transition. Natural Protected Areas. Available online: https://agroambient.gva.es/es/web/espacios-naturales-protegidos/serra-escalona-presentacio (accessed on 22/10/2021)
37. Júcar Hydrographic Confederation. Ministry for the Ecological Transition. Available online: https://www.chj.es/es-es/Organismo/Paginas/Organismo.aspx (accessed on 01/03/2021)

38. Ministry of Agriculture, Rural Development, Climate Emergency and Ecological Transition. Natura 2000 Areas Network. Available online: https://agroambient.gva.es/es/web/red-natura-2000/listado-lic (accessed on 22/10/2021)
39. Guadalquivir Hydrographic Confederation. Ministry for the Ecological Transition. Available online: https://www.chguadalquivir.es/inicio (accessed on 01/03/2021)
40. MAPAMA. Spanish Yearbook of the Water Gauging Information System. Available online: https://sig.mapama.gob.es/redes-seguimiento/ (accessed on 01/03/2021)
41. Ministry for the Ecological Transition. State Monitoring Networks and Hydrological Information. Available online: https://sig.mapama.gob.es/redes-seguimiento/ (accessed on 02/03/2021)
42. U.S. Department of the Interior. U.S. Geological Survey-Earth Explorer. Available online: https://earthexplorer.usgs.gov/ (accessed on 01/03/2021)
43. Magome, J.; Ishidaira, H.; Takeuchi, K. (2003). Method for satellite monitoring of water storage in reservoirs for efficient regional water management [C]. Hydrological Risk, Management and Development (Proceedings of symposium HS02b held during IUOG2003 at Sapporo, July 2003). IAHS Publ. no. 281 Water Resources Systems, 2: 303–310. Available online:http://hydrologie.org/redbooks/a281/iahs_281_303.pdf (accessed on 12/04/2021)
44. Rashmi, S.; Addamani, S.; Venkat; Ravikiran, S. (2014). Spectal Angle Mapper Algorithm for remote Sensing Image Classification [C]. International Journal of Innovative Science, Engineering & Technology, 1, 4: 201–205. ISSN 2348 – 7968
45. Lobo, F. D. L.; Márcia, E. M.; Faria, C.C.; Soares, L. (2012). Reference spectra to classify Amazon water types [C]. International Journal of Remote Sensing, 33, 11: 37–41. http://dx.doi.org/10.1080/01431161.2011.627391
46. QGIS Development Team. QGIS Geographic Information System. 2018. Available online: https://qgis.org/es/site/
47. Congedo, L. (2016). Semi-Automatic Classification Plugin Documentation [S]. Release 6.0.1.1. doi: 10.13140/RG.2.2.29474.02242/1
48. Gao, H.; Birkett, C.; Lettenmaier, D.P. (2012). Global monitoring of large reservoir storage from satellite remote sensing [C]. Water Resources Research, 48, 9 https://doi.org/10.1029/2012WR012063
49. Budak, M.; Gunal, H. (2016). Visible and Near Infrared Spectroscopy Techniques for Determination of Some Physical and Chemical Properties in Kazova Watershed [C]. Advances in Environmental Biology, 10, 5: 61–72. ISSN-1995-0756
50. Cheng-Wen, C.; Laird, D.; Mausbach, M.J.; Hurburgh Jr., C.R. (2001). Near-Infrared Reflectance Spectroscopy–Principal Components Regression Analyses of Soil Properties [C]. Soil Science Society of America Journal, 65, 2: 480-490. https://doi.org/10.2136/sssaj2001.652480x
51. R Core Team. (2018). R: A Language and Environment for Statistical Computing [S]. RFoundation for Statititstical Computing: Vienna, Austria.

52. S. Lu; N. Ouyang; B. Wu; Y. Wei; Z. Tesemma. (2013). Lake water volume calculation with time series remote-sensing images [C]. International Journal of Remote Sensing, 34, 22: 7962-7973. https://doi.org/10.1080/01431161.2013.827814
53. Marco Dos Santos, G.; Meléndez Pastor, I.; Navarro Pedreño, J.; Gómez Lucas, I. (2018). Water Management in Irrigation Systems by Using Satellite Information [M]. In Satellite Information Classification and Interpretation; Rustam, B.R.; InTech, United Kingdom. doi: 10.5772/intechopen.82368
54. W. Zhu; J. Yan; S. Jia. (2017). Monitoring Recent Fluctuations of the Southern Pool of Lake Chad Using Multiple Remote Sensing Data: Implications for Water Balance Analysis [C]. Remote Sensing, 9, 10: 1032; https://doi.org/10.3390/rs9101032
55. R. Cobo. (2008). Los sedimentos de los embalses españoles [J]. Ingeniería del Agua, 15,4: 231-241. https://doi.org/10.4995/ia.2008.2937
56. Duane Nellis, M.; Harrington, J.A.; Jaiping Wu, Jr. (1998). Remote sensing of temporal and spatial variations in pool size, suspended sediment, turbidity, and Secchi depth in Tuttle Creek Reservoir, Kansas: 1993 [C]. Geomorphology, 21, 3-4: 281-293. https://doi.org/10.1016/S0169-555X(97)00067-6

Parque Natural de El Hondo, Elche-Crevillente.
Fotografía: Gema Marco Dos Santos

Marco Dos Santos, G., Navarro-Pedreño, J., Meléndez-Pastor, I., , Gómez Lucas, I., Almendro Candel, M.A., Zorpas, A.A. (2021).

Agricultural drainage water characterization to determine the desalination possibilities for irrigation in a semiarid environment.

Desalination and Water Treatment, 227(2021), 34-41.

https://doi.org/10.5004/dwt.2021.27301

Abstract

Agriculture drainage water (ADW) can be desalinized and could provide water resources for irrigation. The major concern is the excess of soluble salts in ADW. In this sense, it is possible to use reverse osmosis (RO) system plants to reduce salinity and provide irrigation water of high quality. Several parameters such as pH, electrical conductivity (EC), total suspended solids, etc., should be taken into consideration before planning the installation of a reverse osmosis system. In this study, the water quality of an ancient drainage system of the SE of Spain was evaluated. The final results are directly applicable to help decision-makers and engineers to take an adequate decision, in order to select which of the drainage canals is the best option to produce desalinized water at low cost.

Keywords

Agriculture; Climate change; Electrical conductivity; Water flow; Water reuse

1. Introduction

Water scarcity is considered as one of the most vital and significant environmental issues globally with climate change impacts to follow in the framework of agricultural sector demand [1,2]. In response to the growing world population and economic growth, water withdrawals for human consumption will be intensified, increasing the competition for freshwater between urban, industrial, agricultural, environmental, and recreational desires [3]. The highest water demand activity in the agri-sector [4], will lead to a rise in evapotranspiration rates, thereby increasing crop water demand across Europe [5] and globally [6]. Under this background, the reuse of water as well as wastewater [7–10] for agricultural purposes is a necessary target for land sus¬tainability and food supply [11].

Traditional irrigation systems of the South of the Alicante province (Spain), which have more than a thousand kilometers of drainage canals, can offer water for desalination in better conditions, than that coming from the Mediterranean Sea, because of the lower salinity comparing with seawater. However, it must be considered that feed water quality is influenced by seasonal variation (i.e., irrigation necessities, floods, drought, and climatic impact) [12]. For these reasons, it is important to study the water quality and the available flow to maintain a desalination plant active. In the South of Alicante, drainage water is commonly reused for irrigation several times (two or three times) along a complex agricultural system developed three centuries ago. This system, based on an ancient water network, reveals a real example of water resources optimization looking for maximum use of the resource in a low and irregular rainfall area of the Spanish peninsular Southeast [13]. As a result of the water reutilization, water is becoming more and more saline after each use, so it is highly common in these areas the cultivation of salt-tolerant crops such as pomegranates or palm trees. However, drainage water reuse on increasingly salt-tolerant crops concentrates dissolved solutes and reduces its volume [14], mainly due to evapotranspiration.

Among the options for enhancing freshwater resources is the desalination of salty groundwater, brackish drainage water, and seawater [15]. Zarzo *et al.* [16] provide a novel and additional water resource for agriculture and irrigation. Moreover, treatment and utilization of agriculture drainage water (ADW) is mandatory for development needs in arid and semi-arid zones [17] where the scarcity of this resource is critical to keep agricultural productivity. Drainage canals, which recover excess water from agricultural irrigation and subsurface waters, can be a good alternative and a possible source for irrigation water after adequate treatment and management. ADW is a complex mixture of dissolved and suspended chemical species and may contain a wide variety of microorganisms [18]. Opportunities for recovering significant amounts of water depending on the availability of large quantities of ADW [19].

ADW frequently has a great amount of soluble salts that makes it difficult for direct use for irrigation, especially considering non-tolerant crops to salinity. The salt content of the collected subsurface drainage water mainly reflects the salinity characteristics of soil solution, which in turn is influenced by soil parent material, the salinity of the shallow groundwa¬ter, and salts brought into the soil with irrigation water [3]. The direct reuse of this ADW for irrigation may result in salinization and reduces agricultural yield [20]. Moreover, saline water application not only reduces agricultural production but also causes soil destruction [21–23] and greater salt damage caused by long-term irrigation [24].

Similar processes with seawater desalination is been applied to the drainage water. From the economic point of view, an appropriate selection of the desalting scheme as well as on the operational features are needed [25]. For instance, in the case of low flows from agricultural drainage systems, although several technical options can be considered, small to medium volume reverse osmosis (RO) system plants could be used [26]. In addition, nowadays these plants can be supplied by solar energy to treat saline water [27] and provide water for irrigation as a sustainable alternative with a low carbon footprint [28]. The structure of these RO systems would be similar to that presented in Fig. 1. First, it is necessary to pre-treat the drainage water, so it reaches adequate physical and chemical conditions, to avoid membrane saturation. The pre-treatment process may include sand, carbon, and nanofiltration [17], but these technologies should focus on relatively low-cost systems [19] making them affordable by farmers and should be joined to irrigation efficient systems. After the extraction of the water from the RO system, water flow is split into two streams: one has no (or limited) salinity and the other has high salinity (Fig. 1). The low salinity stream is known as “permeate or product water” while the high salinity stream is known as “concentrate, brine, or reject” [29]. The management of the brine is one of the major concerns.

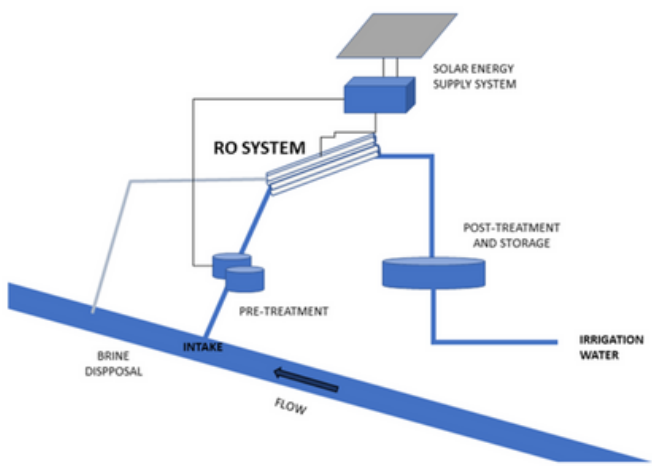

Figure 1. *Location of the studied reservoirs. False color composites of each study area are shown (source: Landsat 8 OLI RGB:5.6.2).*

There are many factors that affect a desalination plant, including the substantial operation costs, recovery efficiency, membrane fouling level, energy consumption as well as the production, and the disposal of the end product (i.e., brine) [30]. Among several parameters (i.e., total suspended solids, pH, etc.), the relevant desalination costs may be related to also to electrical conductivity and total dissolved solids (TDS) [31]. Desalting subsurface drainage water is costly due to the increasing salinity and the potential for scaling and fouling of RO membranes [32]. As consequence, the service life of the membranes becomes shorter and the cost increases accordingly [33], a low saline ADW is preferable to reduce cost. Energy will be increased when ADW salinity is high. In the case of ADW, the feasibility of effective desalination with high-performance low-pressure RO membranes has been demonstrated [17]. Even more, less cost per cubic meter of product water and the excellent tolerance to salinity changes of RO has been proven [26].

In water consumption sectors, that is, agriculture, low-cost desalination methods are vital [34,35] and several small plants feeding with solar energy have been developed for commercial use. Furthermore, it is part of the 4th strategies from the European Green Deal, Circular Economy Strategy, and UNSDG [36–38] aimed at reducing greenhouse gas emissions to mitigate climate change. A good example of low-cost treatment for a brackish aquifer (with electrical conductivity values above 6,000 µS/cm) is given by Aparicio *et al.* [39] for the small desalination plant situated at the University of Alicante in San Vicente del Raspeig (Alicante, Spain). Due to the continual increase of the drainage water suitability for reuse in irrigation purposes, must be intensively assessed [40]. One of the most important KPI to assess the desalination units is the EC [41]. However, it is important to determine the availability of a permanent flow of water supply to maintain the system working [18] and provide enough water for irrigation.

Regarding this, the main objective of this paper was to study the water quality of the drainage system in the counties of La Vega Baja and the Baix Vinalopó (Alicante, Spain), in order to determine which of the canals has adequate charac-teristics, enough flow, and water quality (salinity) that can favor the desalination by using a RO system.

2. Materials and Methods

The study was conducted in the Elche Depression and lower Segura river basin, located in the Eastern sector of the Betic Ranges in the South of the Alicante province (Spain). The selected area is mainly agricultural, with flat topography, situated at the end of the

rivers Segura and Vinalopó. It is developed on three main types of soils: Fluvisols, Solonchacks, and Gleysols [42], transformed along the last century by agriculture.

The origin of this area is an ancient coastal lagoon and marshes, transformed from centuries by farmers. The drainage system, formed by numerous canals, was the main conductor of this transformation, created to reduce the shallow groundwater level and drain the area. Since the 18th century, the establishment of agriculture and the foundation of new rural settlements were favored [43]. The old Elche lagoon (Albufera de Elche) was formed by a coastal sand barrier during the late Holocene [44,45] at which time marine conditions would have extended 19 km inland from the present coast and persisted until at least the bronze age [46], was dried.
Drainage canals were analyzed to recover the water from a dense network of minor agriculture canals and were divided into two groups, depending on the mouth of the two main rivers where the canals finally flow and discharge their waters to the sea: Vinalopó River and Segura River (Fig. 2). A total amount of 13 drainage canals (Table 1) were analyzed between 2016 and 2018 (12 sampling periods from September-16 to July-18, taking four subsamples per canal), and monitored for a sufficient length of time due to possible seasonal changes [14]. Samples were taken at the end of the drainage canal but far enough from the coast to avoid influences from seawater (sample points presented in Fig. 2). Most of these canals are open-air canals, ground edges along their path, and cemented in some sections to maintain the shores. Because the subsurface passage of water through the bed and aquifer material provides several natural treatment processes [47], it is important to keep the ground banks, such a natural riverside, improving the quality of the agricultural drainage waters.

Salinity was analyzed by determining the electrical conductivity at 25°C as well as the water pH. TSS was determined by filtration (glass microfiber filters 1.2 μm) and the major anion and cation related to salinity (chloride and sodium), were analyzed following the Standard Methods for Examination of Water and Wastewater [48,49]. Additionally, the flow of the canals was estimated in a rectangular-shaped section, following the methodology based on the float method [50], to know which of them could provide enough water to maintain a stream for a small or medium-size RO system plant.

Statistical descriptive analysis (maximum, minimum, mean, standard deviation (SD)) and the ANOVA F-test were used to determine the statistical significance and differences between the means.

3. Results and discussion

The main characteristics of the drainage water determined in each of the canals are presented in Tables 2 and 3. The results showed no significant differences, regarding the pH, but differences have been detected in the rest of the parameters. According to the pH, waters can be considered moderately alkaline and the pH range allows the reuse for irrigation purposes [51].

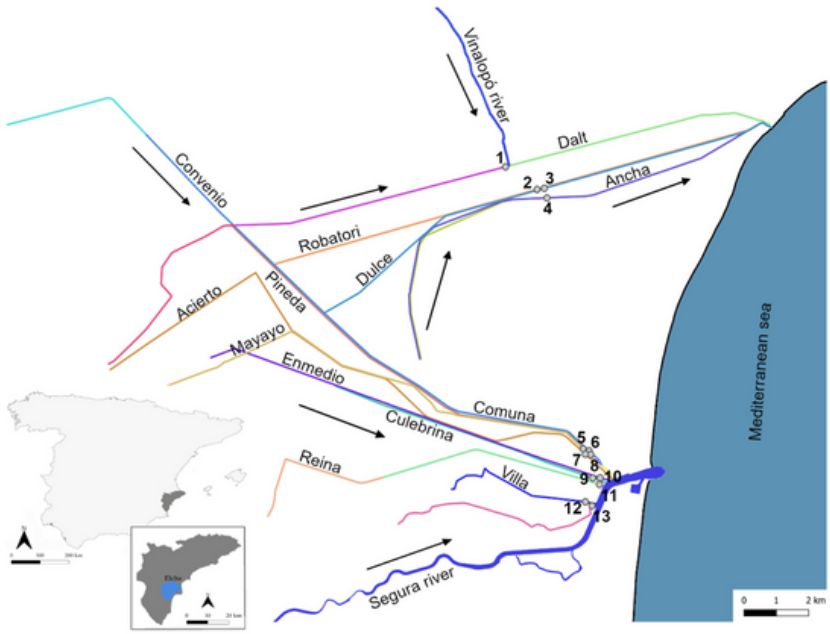

Figure 2. *Drainage canals and sampling points. Arrows indicate the direction of the flow of the drainage water.*

Area of discharge	Drainage canal	Sample point
Mouth of Vinalopó river	Azarbe de Dalt Azarbe del Robatori Azarbe Dulce Azarbe Ancha	1 2 3 4
Mouth of Segura River	Azarbe del Convenio Azarbe de Pineda Azarbe Mayayo Azarbe del Acierto Azarbe de Enmedio Azarbe Culebrina Azarbe de la Reina Azarbe de la Villa Azarbe de la Comuna	5 6 7 8 9 10 11 12 13

Table 1. *Cross-validation results. Estimation of water volume from remote sensing surface water.*

In general, according to the salinity, determined by the electrical conductivity, drainage waters from the canals associated with the Segura river are generally less saline than those associated with the Vinalopó river. Mean EC range between 3.1 and 15.5 mS/cm, indicates a high degree of salinity (for agricultural purposes) and specifies a high amount of dissolved substances in water [52], but in all of the cases under the salinity estimated for the seawater [53]. The feed water, based on its quality can be processed into RO plants similar to those used to brackish water (BWRO) where the salinity ranges from 500 mg/l to mg/l. In contrast to the seawater RO plants (SWRO) where the salinity is around 30,000 mg/l [54].
Additionally, BWRO is further sub-grouped into low salinity BRWO that process feed water with salinity between 500 and 2,500 mg/l, and high salinity BRWO plants that process water with salinity between 2,500 and 10,000 mg/l [54]. This difference is critical for the energy cost. The mean EC value of most of the canals indicates that ADW belongs to the second subgroup, and ADW should be treated by high salinity BRWO plants.

Following Scherer and Meehan [55], EC is a proxy measurement to determine the TDS in water. Using the conversion factor given by these authors, the TDS varied approximately between 2,300 and 12,700 mg/l, while most of the canals have from 3,000 to 6,000 mg/l approximately. The acceptable TDS concentration for irrigation purposes is about 750 mg/l [15], so it is important to consider that reducing EC, makes it easy to achieve the desired value for TDS in the treated water due to the direct relation between EC and TDS.

EC (salinity) follows the same pattern that those found for chloride and sodium (Table 3), as it was expected. Most of the soils are formed on an ancient saltmarsh area, they have been irrigated for centuries with medium or low-quality water and soil salinity may be determined by the presence of dissolved salts. Considering the chloride concentration, the degree of restriction for reuse directly the drainage waters is severe because it is over 355 mg/l [51].

The flow rate was very different for each canal and should be considered to determine which can supply enough water for a small or medium RO system. The mean water flow results in a wider range, between 0.001 and 4.18 m^3/s, from extremely low flow to an important mean value over 4 m^3/s. In this sense, a constant flow of about 0.5–1 m^3/s could provide enough water for a small or medium RO plant. Considering a high-efficiency RO plant and low energy consumption, the selection, in this case, maybe determined by the percentage of desired desalinized water/brine ratio. Low saline waters

may facilitate selecting a high water/brine ratio.

TSS was also determined because the pre-treatments should reduce the TSS to avoid problems in the membranes, reducing these associated with suspended particulates, which could serve as seeds for promoting surface crystal nucleation [56]. It is important to consider the presence of suspended solids but also other floating objects that can be presented in the drainage canals due to mismanagement of people and, in such case, the pre-treatment should include screening systems to remove these elements prior to desalination treatment. As it might seem from Table 2, great variability of TSS was determined. However, most of the mean values are under 70 mg/l of TSS, reducing the risk in the ADW treatment, excepting the Pineda drainage canal which can be discarded for a lower cost RO system.

To implement a desalination treatment, EC and flow should be determined and help for the process optimization (low salinity and availability of enough feed water). It is necessary to maintain the flow [14] to optimize the performance of the water treatment plant. Analyzing the water quality of all the canals, El Convenio and La Reina, have a higher mean flow close or over 1 m^3/s, which can be enough to supply a small RO plant. When feed water supply is guaranteed, electrical conductivity is the main parameter to be considered.

Table 2. *Characteristics of the drainage water (mean value, standard deviation SD, maximum value Max, minimum value Min, and ANOVA F test *** $p \leq 0.001$; ** $p \leq 0.01$; * $p \leq 0.05$; ns = not significant).*

Drainage canal	pH				EC (mS/cm)			
	Mean	SD	Max.	Min	Mean	SD	Max.	Min
Dalt	7.8	0.2	8.2	7.6	12.8	3.4	16.2	9.3
Robatori	7.8	0.2	8.2	7.5	9.1	3.2	12.3	5.9
Dulce	8.0	0.2	8.2	7.7	3.1	0.5	3.6	2.6
Ancha	7.8	0.2	8.0	7.6	11.0	2.0	13.0	9.0
Convenio	7.8	0.2	8.0	7.7	10.8	1.1	12.0	9.7
Pineda	7.9	0.2	8.1	7.8	7.1	2.2	9.3	4.9
Mayayo	8.0	0.2	8.2	7.7	6.2	2.8	9.0	3.4
Acierto	7.8	0.2	8.3	7.7	5.7	1.6	7.3	4.1
Enmedio	8.0	0.2	8.3	7.8	4.8	1.1	5.8	3.7
Culebrina	7.9	0.2	8.2	7.7	4.7	1.0	5.6	3.7
Reina	8.1	0.2	8.4	7.8	3.7	0.8	4.5	3.0
Villa	7.9	0.2	8.3	7.8	4.0	0.9	4.9	3.0
Comuna	7.9	0.2	8.3	7.7	3.8	0.9	4.7	2.9
ANOVA F-test	ns				***			

Drainage canal	Flow (m^3/s)				TSS (mg/L)			
	Mean	SD	Max.	Min	Mean	SD	Max.	Min
Dalt	0.303	0.171	0.686	0.178	35	19	68	13
Robatori	0.311	0.182	0.483	0.000	48	33	75	9
Dulce	0.003	0.004	0.003	0.000	35	42	137	7
Ancha	0.193	0.102	0.253	0.000	34	14	57	12
Convenio	1.468	1.219	4.180	0.564	46	28	120	15
Pineda	0.523	0.409	0.690	0.000	104	57	198	42
Mayayo	0.164	0.117	0.378	0.000	62	107	399	4
Acierto	0.810	0.715	0.945	0.152	39	14	57	19
Enmedio	0.137	0.121	0.270	0.000	46	18	85	21
Culebrina	0.182	0.109	0.270	0.000	37	19	60	16
Reina	0.967	0.796	2.179	0.100	32	25	103	8
Villa	0.050	0.092	0.200	0.000	29	15	66	12
Comuna	0.050	0.092	0.200	0.000	24	18	78	9
ANOVA F test	***				***			

However, changes in flow rate due to seasonality can affect the desalination treatment and vary the amount of salts. If the concentration of the inlet to the desalination unit is low, the final volume of the permeate could be maximized by blending the permeate with the inlet water, thereby decreasing the unit cost of irrigation water [57]. Nevertheless, low salinity feedwater types require less applied pressure than high salinity feedwater types for desalination [58], reducing the energy cost. For both canals, El Convenio and La Reina, a great difference in mean values of EC were obtained, favoring the selection of the La Reina canal. Representing both parameters, mean electrical conductivity expressed in mS/cm and average flow expressed in m^3/s, a previous approach to understand which is the preferable ADW and as a consequence, the drainage canal, to install a desalination plant. As a result of representing both parameters (Fig. 3), the La Reina canal could be used for desalination purposes.

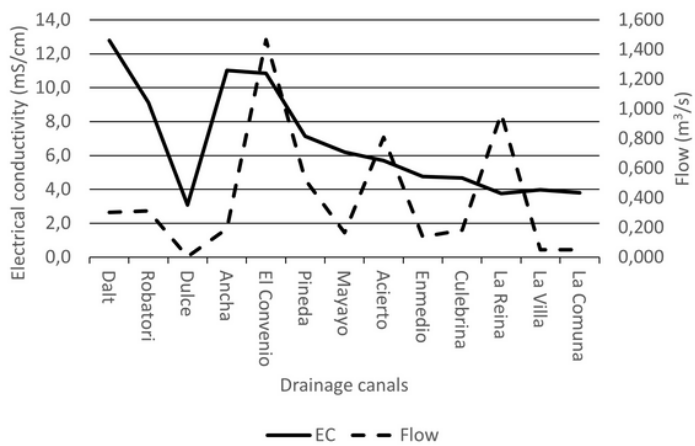

Figure 3. *Electrical conductivity and flow of each drainage canal.*

Table 3. *Chloride and sodium measure in drainage canal (mean value, standard deviation SD, maximum value Max, minimum value Min, and ANOVA F test *** p ≤ 0.001 ; ** p ≤ 0.01 ; * p ≤ 0.05 ; ns = not significant).*

Drainage canal	Cl (mg/L)				Na (mg/L)			
	Mean	SD	Max.	Min	Mean	SD	Max.	Min
Dalt	2,996	966	3,962	2,030	1,858	579	2,437	1,279
Robatori	1,952	815	2,767	1,137	1,261	533	1,794	728
Dulce	647	173	820	473	394	104	498	290
Ancha	2,520	559	3,079	1,960	1,552	342	1,894	1,209
Convenio	2,484	315	2,799	2,169	1,539	180	1,718	1,359
Pineda	1,485	595	2,080	890	913	325	1,238	588
Mayayo	1,276	757	2,033	519	785	436	1,221	349
Acierto	1,059	336	1,395	723	688	258	946	430
Enmedio	874	277	1,151	597	551	165	716	385
Culebrina	831	239	1,070	592	524	144	668	381
Reina	633	160	793	472	396	93	489	303
Villa	669	185	855	484	424	114	538	310
Comuna	648	200	848	447	410	124	534	286
ANOVA F test	***				***			

The effectiveness of a desalination plant would be asso¬ciated with a compromise between salinity (EC, TDS) and availability of water (flow). For instance, the Dulce drain¬age canal gave the minimum value for salinity (3.1 mS/ cm); however, the mean water flow was 0.003 m^3/s. On the other side, El Convenio has the highest mean water flow of 1.468 m^3/s, but salinity was almost three times the salinity of La Reina.

After these considerations, RO is proposed because of its reliability and comparatively low energy consumption in which leads to a significant reduction of energy cost [59]. The unit product cost was the lowest RO ($0.3–0.7/$m^3$) comparing with other treatments [60]. The management of brine disposal is a fundamental issue [61] that should be considered in the early planning stage [19]. The brine has two options if a plant is installed: (i) gone with the drainage water to the sea following the flow direction after the catchment of feed water to the RO system from the canal (Fig. 1), or (ii) construct a parallel canal or pipe for the brine to discharge this into the sea (open sea waters). The volume of brine produced is determined at each individual (operational) desalination plant [58] and, low salinity feedwater favors the reduction of brine volume. Therefore, the situation of the treatment plant, close to the end of the drainage system (La Reina, sampling point 11), facilitates the brine disposal to the sea and can be discharged by using the same drainage canal because water is not going to be re-used for irrigation after that point. Nevertheless, brine can lead to the pollution of coastal waters, damage

to sensitive marine life that will ultimately threaten the food chain [62,63] and this should be considered for a future and sustainable design. For instance, nitrates must be considered to avoid coastal eutrophication and several solutions can be applied as those given by Álvarez-Rogel *et al.* [64], by using woodchips bioreactors or constructed wetlands.

4. Conclusions

Water physicochemical characterization is considered vital for the selection of the operational factors of a desalination treatment plant. In our case, and considering a RO scheme, an approach based on easy measurable parameters, EC, estimation of the flow, TSS, could give us, a quick method to understand which is the best option (canal), to install a desalination treatment plant. These parameters can be considered for the optimization of the process and the design of the plant as well. The targets, are to determine salinity and availability of enough water flow, in order to choose the better RO system and reduce the relevant cost, minimize the consumption of energy during operation and extend the membrane life. In this study, La Reina canal the EC is 3.7 mS/cm and the flow rate is 0.967 m^3/s, which indicates that a small unit must be applied. In fact, the project will be centered in a solar desalination plant, that could be extended to other canals of the ancient drainage system in order to get new resources of water, with high quality, that can be used for high-value crops (non-tolerant to salinity) and be a support of farmers income and diversification of agricultural production under water scarcity scenery. Furthermore, future water scarcity may reduce the possibilities for sustainable development, as well as, to retain or create new adequate jobs [65], ensuring at the same time water quality according to the Water Framework Directive. In this line, several projects like DESEACROP LIFE 16 ENV/ES/000341 try to give solutions, increasing the possible sources for irrigated agriculture by using salty waters, which is in the line of this article.

Acknowledgments

This research was supported by the Conselleria de Agricultura, Medio Ambiente, Cambio Climático y Desarrollo Rural of the Valencian Goverment (Spain).

References

1. FAO, Climate change, water and food security, FAO water reports 36, Rome, 2011.
2. D. Bilalis, P.E. Kamariari, A. Karkanis, A. Efthimiadou, A.A. Zorpas and I. Kakabouki., Energy inputs, output and productivity in organic and conventional maize and tomato production, under Mediterranean conditions, Notulae Botanicae Horti Agrobotanici Cluj-Napoca, 41(1) (2013) 1-5.
3. K.K. Tanji and N.C. Kielen, Agricultural drainage water management in arid and semi-arid areas, FAO Irrigation and Drainage Paper 61, FAO, Rome, 2002.
4. B.J. Hipólito-Valencia, F. W. Mosqueda-Jiménez, J. Barajas-Fernández and J.M. Ponce-Ortega, Incorporating a seawater desalination scheme in the optimal water use in agricultural activities, Agric. Water Manage. 244 (2021) 106552.
5. EEA, Crop water demand, Ed. European Environment Agency, Copenhagen, 2016.
6. B.E. Jiménez Cisneros, T. Oki, N.W. Arnell, G. Benito, J.G. Cogley, P. Döll, T. Jiang, and S.S. Mwakalila, In: C.B. Field, V.R. Barros, D.J. Dokken, K.J. Mach, M.D. Mastrandrea, T.E. Bilir, M. Chatterjee, K.L. Ebi, Y.O. Estrada, R.C. Genova, B. Girma, E.S. Kissel, A.N. Levy, S. MacCracken, P.R. Mastrandrea, and L.L.White, Impacts, Adaptation, and Vulnerability. Part A: Global and Sectoral Aspects, Cambridge University Press, Cambridge 2014, pp. 229-269.
7. M. Tsangas, I. Gavriel, M. Doula, F. Xeni and A.A. Zorpas, Life cycle analysis in the framework of agricultural strategic development planning in the Balkan region, Sustainability 12 (2020) 1813.
8. A.A. Zorpas, M. Drtil, K. Chryso, I. Voukkali and P. Samaras, Operation description and physicochemical characteristics of influent, effluent and the tertiary treatment from a sewage treatment plant of the Eastern Region of Cyprus under warm climates conditions. A seven-year project, Desalin. Water Treat. 22 (2010) 244-257.
9. A.A. Zorpas, C. Coumi, M. Drtil and I. Voukkali, Municipal Sewage Sludge Characteristics and Waste Water Treatment Plant Effectiveness Under Warm Climate conditions, Desalin. Water Treat. 36 (2011) 319-333.
10. A. A. Zorpas, I. Voukkali and P. Loizia, Proposed treatment applicable scenario for the treatment of domestic sewage sludge which is produced from a sewage treatment plant under warm climates conditions, Desalin. Water Treat. 51 (2013) 3081-3089.
11. M. Hallack-Alegría and D.J. Watkins, Annual and warm season drought intensity-duration-frequency analysis for Sonora, Mexico, J. Climate, 20 (2006) 1897-1909.
12. N.K. Khanzada, S. Jamal Khan and P.A. Davies, Performance evaluation of reverse osmosis (RO) pre-treatment technologies for in-land brackish water treatment, Desalination 406 (2017) 44-50.
13. A. Trapote, J.F. Roca, and J. Melgarejo, Azudes y acueductos del sistema de riego tradicional de la Vega Baja del Segura (Alicante, España), Investigaciones Geográficas 63 (2015) 143-160.
14. J.D. Oster and S.R. Grattan, Drainage water reuse, Irrig. Drain. Syst. 16 (2002) 297-310.

15. FAO, Water desalination for agricultural applications, Land and water discussion paper 5, Rome, 2006.
16. D. Zarzo, E. Campos, and P. Terrero, Spanish experience in desalination for agri-culture, Desal. Water Treat. iFirst (2012) 1–14.
17. H.A. Talaat and S.R. Ahmed, Treatment of agricultural drainage water: technological schemes and financial indicators, Desalination 204 (2007) 102-112.
18. R.W. Lee, J. Glater, Y. Cohen, C. Martin, K. Kovac, M.N. Milobar and D.W. Bartel, Low-pressure RO membrane desalination of agricultural drainage water, Desalination 155 (2003) 109-120.
19. M.H. Sorour, N.M.H. El Defrawy and H.F. Shaalan, Treatment of agricultural drainage water via lagoon/reverse osmosis system, Desalination 152 (2002) 359-366.
20. W. Suwaileh, D. Johnson and N. Hilal, Membrane desalination and water re-use for agriculture: State of the art and future oulook, Desalination 49 (2020) 114559.
21. I.P. Abrol, J.S.P. Yadav and F.I. Massud, Salt-affected soils and their management, FAO Soils Bulletin 39, Rome, 1988.
22. F. Sheng and C. Xiuling, Using shallow saline groundwater for irrigation and regulating for soil salt-water regime, Irrig. Drain. Syst. 11 (1997) 1-14.
23. J.J. Escolano, J. Navarro Pedreño, I. Gómez Lucas, M. B. Almendro Candel and A.A. Zorpas. Decreased organic carbon associated with land management in Mediterranean environments. In: Soil Management and Climate Change: Effects on organic carbon, nitrogen dynamics and greenhouse gas emissions, Eds: María Ángeles Muñoz and Raúl Zornoza, Elsevier, 16-29, http://dx.doi.org/10.1016/B978-0-12-812128-3.0001-x
24. Z. Liu, D. Zhang, J. Ping, Y. Han and Q. Cai, Applicability evaluation of groundwater in the People's Victory Canal Irrigation Area, China, Desalin. Water Treat. 168 (2019): 207-215.
25. M.H. Sorour, A.G. Abulnour and H.A. Tallat, Desalination of agricultural drainage water, Desalination 86 (1992) 63-75.
26. A.G. Abulnour, M.H. Sorour and H.A. Talaat, Comparative economics for desalting of agricultural drainage water (ADW), Desalination 152 (2002) 353-357.
27. L.T.A. Salama and K.Z. Addalla, Design and analysis of a solar photovoltaic powered seawater reverse osmosis plant in the southern region of the Gaza Strip, Desalin. Water Treat. 143 (2019) 96-101.
28. A. Tal, Addresing Desalination's Carbon Footprint: The Israeli Experience, Water 10 (2018) 197.
29. S.G. Salinas-Rodríguez, J.C. Schippers and M.D. Kennedy (2016), In: S. Burn S. and S. Gray, Efficient desalination by reverse osmosis. A guide to RO practice, IWA, London 2016, pp. 5-25.
30. N.C. Darre and G.S. Toor, Desalination of Water: a Review, Curr. Pollut. Rep. 4 (2018) 104-111.
31. J.A. Medina, Desalación de aguas salobres y de mar. Osmosis inversa, Mundi-Prensa, Madrid, 2000.

32. B.E. Smith, Desalting and ground water management in the San Joaquin Valley, California, Desalination 87 (1992) 151-174.
33. E. Guler, E. Onkal, M. Clen and E. Sari, Cost analysis of seawater desalination using an integrated reverse osmosis system on a cruise ship, Global NEST J. 1(2) (2015) 389-396.
34. A. Aghakhani, S.F. Mousavi, B. Mostafazadeh-Fard, R. Rostamian and M. Seraji, Application of some combined adsorbents to remove salinity parameters from drainage water, Desalination 275 (2011) 217-223.
35. A.F. Mashaly, A.A. Alazba, A.M. Al-Awaadh and M.A. Mattarb, Area determination of solar desalination system for irrigating crops in greenhouses using different quality feed water, Agri. Water Manage. 154 (2015) 1-10.
36. A.A. Zorpas, Strategy Development in the Framework of Waste Management, Sci. Total Environ. 716 (2020) 137088.
37. P. Loizia, N. Neofytou and A.A. Zorpas, The concept of circular economy in food waste management for the optimization of energy production through UASB reactor, Environ. Sci. Pollut. Res. 26 (2019) 14766–14773.
38. P. Loizia, I. Voukkali, A.A. Zorpas, J. Navarro-Pedreño, G. Chatziparaskeva, V.J. Inglezakis and I. Vardopoulos, Measuring Environmental Performance in the Framework of Waste Strategy Development, Sci. Total Environ. 753 (2021), 141974.
39. J. Aparicio, L. Candela and O. Alfranca, Social and private cots of water for irrigation: The small desalination plant in San Vicente del raspeig, Spain, Desalination 439 (2018) 102-107.
40. M. Nasr and H. Zahran, Using of pH as a tool to predict salinity of groundwater for irrigation purpose using artificial neural network, Egypt. J. Aquat. Res. 40 (2014) 111-115.
41. R. Hashimoto, Improved conductivity analysis in desalination processes, Water & Wastewater Asia Jan/Feb (2015) 40-42.
42. IUSS Working Group WRB, World Reference Base for Soil Resources 2014, update 2015 International soil classification system for naming soils and relating legends for soil maps, World Soil Resources Reports 106, Rome, 2015.
43. A. Gil and G. Canales, Consolidación de dominios en las Pías Fundaciones del cardenal Belluga (Bajo Segura), Investigaciones Geográficas 5 (1987) 7-26.
44. K. Fleming, P. Johnston, D. Zwartz, Y. Yokoyama, K. Lambeck, and J. Chapell, Refining the eustatic sea-level curve since the Last Glacial Maximum using far and intermediated-fieldsites, Earth Plan. Sci. Let. 163 (1998) 327–342.
45. J.E. Tent-Manclús, Cambio de la línea de costa en el Bajo Segura (Sur de Alicante) en los últimos 15000 años, Estudios Geográficos 74(275) (2013) 683-702.
46. A.M. Blázquez, and J. Usera, Palaeoenvironments and Quaternary foraminifera in the Elx coastal lagoon (Alicante,Spain), Quat. Int. 221 (2010) 68-90.
47. K. Ghodeif, T. Grischelk, R. Bartak, R. Wahaab and J. Herlitzius, Potential of river bank filtration (RBF) in Egypt, Environ. Earth Sci. 75 (2016) 671.

48. APHA, AWWA and WEF, Standard methods for the examination of water and wastewater, 21st ed., American Public Health Association, Washington D.C., 2005.
49. A. G. Vlyssides, M. Loizidou and A.A Zorpas, Characteristics of solid residues from olive oil processing as a bulking material for co-composting with industrial wastewater, J. Environ. Sci. Heal. A, Vol. 34(3) (1999) 737-748.
50. J.P. Michaud and M. Wierenga, Estimating discharge and stream flows. A guide for sand and gravel operators, Ecology Publication 05-10-070. Washington State Department of Ecology, 2005.
51. R. Ayers and D. Westcot, Water Quality for Agriculture, Irrigation and Drainage Paper 29. Rome, 1994.
52. M. Thompson, D. Brandes and A. Kney, Using electronic conductivity and hardness data for rapid assessment of stream water quality, J. Environ. Manage. 104 (2012) 152-157.
53. R.H. Tyler, T.P. Boyer, T. Minami, M.M. Zweng and J.R. Reagan, Electrical conductivity of the global ocean. Earth Plan. Space 69 (2017) 156.
54. M. Qasim, M. Bdrelzaman, N.D. Darwish and N.A. Darwish, Reverse osmosis desalination: A state-of-the-art review, Desalination 459 (2019) 59-104.
55. T. Scherer and M. Meehan, Using electrical conductivity and total dissolved solids meters to field test water quality, WQ1923, North Dakota State University, Fargo N.D., 2019.
56. J. Thompson J., A. Rahardianto, H. Gu, M. Uchymiak, A. Bartman, M. Hedrick, D. Lara, J. Cooper, J. Faria, P.D. Christofides and Y. Cohen, Rapid field assessment of RO desalination of brackish agricultural drainage water, Water Res. 47 (2013) 2649-2660.
57. R.A.O. Barron, G. Hodgson, D. Smith, E. Qureshi, D. McFarlane, E. Campos and D. Zarzo, Feasibility assessment of desalination application in Australian traditional agriculture, Desalination 364 (2015) 33–45.
58. E. Jones, M. Qadir, M.T.H. van Vliet, V. Smakhtin and S. Kang, The state of desalination and brine production: A global outlook, Sci. Total Environ. 657 (2019) 1343-1356.
59. N.A. Ahmad, P.S. Goh, L.T. Yogarathinam, A.K. Zulhairun and A.F. Ismail, Current advances in membrane technologies for produced water desalination, Desalination 493 (2020) 114643.
60. S. Bhojwani, K. Topolski, R. Mukherjee, D Sengupta and M.M. El-Halgawi, Technology review and data analisys for cost assessment of water treatment systems, Sci. Total Environ. 651 (2019) 2749-2761.
61. A. Loya-Fernández, L.M. Ferrero-Vicente, C. Marco-Méndez, E. Martínez-García, J. Zubcoff and J.L. Sánchez-Lizaso, Comparing four mixing zone models with brine discharge measurements from a reverse osmosis desalination plant in Spain, Desalination 286 (2012) 217-224.
62. U. Caldera and C. Breyer, Assessing the potential for renewable energy powered desalination for the global irrigation sector, Sci. Total Environ. 694 (2019) 133598.

63. K Elsaid, M. Kamil, E.T. Sayed, M.A. Addelkareem, T. Wilberforce and A. Olabi, Environmental impact of desalination technologies: A review, Sci. Total Environ. 748 (2020) 141528.
64. N. Nabbou, M. Belhachemi, M. Boumelik, T. Merzougui, D. Lahcene, Y. Harek, A.A. Zorpas and M. Jeguirim, Removal of fluoride from groundwater using natural clay (kaolinite): optimization of adsorption conditions, CR Chim. 22 (2019) 105-112.

Agradecimientos

Parece que cuando se escriben los agradecimientos es cuando te das cuenta realmente de que el doctorado está llegando a su fin y, como en cualquier proyecto largo, hay una mezcla de alegría, emoción y nervios. Aunque había momentos en los que parecía que "no veía la luz", con un último empujoncito finalmente he conseguido acabar esta tesis.

Desde luego ha sido un gran trabajo en quipo.

Sé que con unas breves frases no es suficiente para agradeceros todo lo que me habéis ayudado, pero confío en que la gente que me conoce sabe que soy más bien escasa en palabras.

Empiezo con Jose Navarro, mi director de tesis, que si no fuera por él es muy probable que ni me hubiese planteado llevar a cabo una tesis doctoral. Gracias Jose por tu confianza y por guiarme en el mundillo de la teledetección desde mi TFG hasta ahora.

Quiero dar las gracias también a mi codirector de tesis, Ignacio Meléndez, por enseñar para comprender y cuestionar. Gracias por demostrarme la importancia de tener claro los objetivos en todo momento para no perdernos en la información. Ahora siempre están en mi mente el "¿por qué?" y "¿para qué?".

Ana y Mª Belén gracias a vosotras por reconciliarme con el laboratorio y sobre todo, por enseñarme a saber estar en él. De vosotras me llevo una infinidad de consejos, valores, risas y buenos momentos. Gracias por todo a las dos.

Quiero agradecer a Ignacio Gómez por contar conmigo y darme el empujoncito hacia la vida profesional. María José, gracias a ti por tus palabras de ánimo y amabilidad.

De esta experiencia no solo me llevo las enseñanzas de un gran equipo de profesionales, sino también a buenos amigos y amigas, ¡gracias!

Gracias en general al departamento, cada vez que voy me siento como en casa. También agradecer a mis compañeros de doctorado por su compañerismo y acogida cuando fui delegada de nuestro programa. Enhorabuena a los que ya han finalizado y mucho ánimo a los que quedan.

Gracias a mis compañeros y compañeras de trabajo por vuestras palabras de apoyo: Pedro, Loli, Fran, Patricia e Isabel.

Dar las gracias a mi madre en una frase sí que se me va a quedar infinitamente escaso. Eres quien me ha dado la vida y está siempre al pie del cañón, con uñas dientes o lo que haga falta. Eres mi guerrera de referencia. Gracias por ayudarme y formar parte de quien soy hoy. Ah y no me puedo olvidar las comidas de la mami, que siempre serán las mejores.

Elena, mi hermana, que con lo que cuida de mí ya no sé cuál de las dos es la mayor y cuál la pequeña. Tú ya sabes lo mucho que te adoro, gracias mei-mei por existir.

Alba, mi mejor amiga, gracias por todos estos años, por nuestros paseos terapeúticos, por escucharme cuando lo he necesitado y, simplemente, por ser tú y estar a mi lado siempre.

Jose David gracias por apoyarme desde el principio, por animarme, hacerme reír e infundirme valor. No puedo sentirme más afortunada por haberte conocido. Es nuestra serendipia.

A mi abuela que ha cuidado tanto de nosotras.

¡Os quiero muchísimo!

El agua es un recurso esencial para el mantenimiento de los ecosistemas naturales, la regulación del clima y el desarrollo de la humanidad. La creciente presión sobre este recurso en las últimas décadas y los cambios en el clima hacen prioritario evaluar y proteger nuestros recursos naturales de manera cooperativa, hacia unos mismos objetivos. Por ello, la legislación y el impulso de la administración resultan fundamentales para llevar a cabo diferentes estrategias para poner en marcha proyectos que favorecen el uso coordinado, equitativo y sostenible de los recursos hídricos y alcanzar los objetivos de la planificación hidrológica.

Sobre esta base, la finalidad de esta tesis es destacar la capacidad de la teledetección y los Sistemas de Información Geográfica (SIG) en la planificación hidrológica, no solo como herramienta de diagnóstico del estado actual de los recursos, sino también para incorporarlo al proceso de toma de decisiones en los sistemas de control en tiempo real. La teledetección nos proporciona una gran cantidad de información complementaria a la obtenida in situ a la que, además, se pueden incluir otro tipo de parámetros ambientales como indicadores de los efectos producidos por el cambio climático.

En los artículos que comprenden esta tesis se realiza una evaluación de los recursos hídricos a partir de metodologías sencillas con imágenes de satélite y formulación de modelos que permitan prever la disponibilidad de agua bajo diversos escenarios de escasez hídrica. Al mismo tiempo, se apunta hacia una de las estrategias de reutilización y de obtención de recursos como es la desalinización.

UNIVERSITAS Miguel Hernández

PROGRAMA DE DOCTORADO EN
MEDIO AMBIENTE Y SOSTENIBILIDAD